



ARCHITECTURE & ENGINEERING

Volume 7
Issue 4
December, 2022



By Architects. For Architects.
By Engineers. For Engineers.

Architecture
Civil and Structural Engineering
Mechanics of Materials
Building and Construction
Urban Planning and Development
Transportation Issues in Construction
Geotechnical Engineering and Engineering Geology
Designing, Operation and Service
of Construction Site Engines

eISSN: 2500-0055
<http://aej.spbgasu.ru/>

Architecture and Engineering

Volume 7 Issue 4 (2022)

ISSN: 2500-0055

Editorial Board:

Prof. Askar Akaev (Kyrgyzstan)
Prof. Emeritus Demos Angelides (Greece)
Mohammad Arif Kamal (India)
Prof. Stefano Bertocci (Italy)
Prof. Tigran Dadayan (Armenia)
Prof. Milton Demosthenous (Cyprus)
Prof. Josef Eberhardsteiner (Austria)
Prof. Sergei Evtukov (Russia)
Prof. Georgiy Esaulov (Russia)
Prof. Andrew Gale (UK)
Prof. Theodoros Hatzigogos (Greece)
Prof. Santiago Huerta Fernandez (Spain)
Yoshinori Iwasaki (Japan)
Prof. Jilin Qi (China)
Prof. Nina Kazhar (Poland)
Prof. Gela Kipiani (Georgia)
Prof. Darja Kubečková (Czech Republic)
Prof. Hoe I. Ling (USA)
Prof. Evangelia Loukogeorgaki (Greece)
Prof. Jose Matos (Portugal)
Prof. Dietmar Mähner (Germany)
Prof. Saverio Mecca (Italy)
Prof. Menghong Wang (China)
Stergios Mitoulis (UK)
Prof. Valerii Morozov (Russia)
Prof. Aristotelis Naniopoulos (Greece)
Sandro Parrinello (Italy)
Prof. Paolo Puma (Italy)
Prof. Jaroslaw Rajczyk (Poland)
Prof. Marlena Rajczyk (Poland)
Prof. Sergey Sementsov (Russia)
Anastasios Sextos (Greece)
Eugene Shesterov (Russia)
Prof. Alexander Shkarovskiy (Poland)
Prof. Emeritus Tadatsugu Tanaka (Japan)
Prof. Sergo Tepnadze (Georgia)
Sargis Tovmasyan (Armenia)
Marios Theofanous (UK)
Georgia Thermou (UK)
Prof. Yeghiazar Vardanyan (Armenia)
Ikujiro Wakai (Japan)
Vardges Yedoyan (Armenia)
Prof. Askar Zhusupbekov (Kazakhstan)



Editor in Chief:

Professor Evgeny Korolev (Russia)

Executive Editor:

Anastasia Sidorova (Russia)



CONTENTS

Architecture

- 3 **Jorge Gallego Sánchez-Torija, María Antonia Fernández Nieto, Jesús García Herrero**

Rehabilitating J. L. Romany's Social Housing in the 21st Century

Urban Planning and Development

- 17 **Asmaaa M. Hassan, Naglaa A. Megahed**
Improving Urban Energy Resilience with an Integrative Framework Based on Machine Learning Methods

Civil Engineering

- 36 **Carlos Rosa-Jiménez, Carlos Prados-Gomez**
Smart multi-functional micro-hub for neighborhoods: sustainable mobility and environmental restoration in high-density social neighborhoods
- 49 **Yuri Dmitriev**
Analysis of cooling system efficiency
- 60 **Valentin Ushkov, Ruslan Ibragimov, Oleg Figovsky, Svetlana Samchenko**
Repair mortars obtained by plasma modification and vortex activation
- 70 **Artem Tiraturyan, Evgeniya Uglova, Vladimir Akulov**
Determining viscoelastic characteristics of the elements of multi-layer structures based on energy dissipation analysis

Architecture and Engineering

peer-reviewed scientific journal

Start date: 2016/03

4 issues per year

Founder, Publisher:

Saint Petersburg State University
of Architecture and Civil Engineering

Indexing:

Scopus, EBSCO, Russian Science Citation Index, Directory of Open Access Journals (DOAJ), Google Scholar, Index Copernicus, Ulrich's Periodicals Directory, WorldCat, Bielefeld Academic Search Engine (BASE), Library of University of Cambridge and CyberLeninka

Corresponding address:

4 Vtoraya Krasnoarmejskaja Str.,
St. Petersburg, 190005, Russia

Website: <http://aej.spbgasu.ru/>

Phone: +7(812)316-48-49

Email: aejeditorialoffice@gmail.com

Date of issue: 29.12.2022

The Journal was re-registered by the Federal Service for Supervision of Communications, Information Technologies and Mass Communications (Roskomnadzor) on May 31, 2017; registration certificate of media organization EI No. FS77-70026

REHABILITATING J. L. ROMANY'S SOCIAL HOUSING IN THE 21ST CENTURY

Jorge Gallego Sánchez-Torija¹, María Antonia Fernández Nieto², Jesús García Herrero*¹

¹ Polytechnic University of Madrid
Avda. Juan de Herrera 4, 28040 Madrid, Spain

² Polytechnic School, Architecture. Francisco de Vitoria University
Carretera Pozuelo a Majadahonda, Km 1.800, 28223, Madrid, Spain

*Corresponding author: jesus.garciah@upm.es

Abstract

Introduction: The modern heritage of 20th century Spanish architecture, particularly in the city of Madrid, includes an extensive range of high-quality social housing that, due to its peripheral location and economic restrictions, can be lost without public policies to preserve it. Updating this housing to meet the current habitability requirements, as well as enhancing and transforming it into high-quality 21st century residential buildings, is a task that cannot be postponed. **Purpose of the study:** The issues of energy efficiency, habitability and accessibility are very salient today, so it seems pertinent to recover relevant examples of 20th century architecture and investigate to what extent the parameters with which they were designed are still valid. **Methods:** This paper reviews housing case studies in two neighborhoods, Poblado Dirigido de Fuencarral and Colonia Juan XXIII de Carabanchel, comprehensively analyzing the original buildings and their current rehabilitation. This includes comparing the buildings' energy efficiency before and after the intervention carried out. **Approach:** This study verified that in both cases, an attempt was made to recover several elements of the original design during rehabilitation. **Results:** We found that both projects were originally committed to creating an open, pedestrian-friendly city with abundant vegetation, which is still a valid value today. Despite the economic restrictions at the time of construction, both projects used advanced energy strategies, such as the passive design offered by cross ventilation, the unusual thermal insulation envelope, or the efficient district heating. **Novelty:** In addition, this paper aims to incorporate the heritage of the great mid-20th century architect José Luis Romany, author of both projects, into modern Spanish architecture.

Keywords

modern heritage; Madrid social housing; residential rehabilitation; energy efficiency; Poblado Dirigido de Fuencarral; Colonia Juan XXIII.

Introduction

Social housing in the mid-20th century was one of the main experimental revival areas after the Spanish Civil War. Even though there were a few attempts to make something different from the official architecture during the late 1940s (Obra Sindical del Hogar, mainly by Cabrero and Aburto), it was during the second half of the 1950s that social housing truly emerged. Many of the architects who are currently considered masters started their professional activity during those years, joining what Baldellou aptly defined as a "furious investigation" (Baldellou, 1998).

In Madrid, it was the public sector that dominated social housing construction until the arrival of the Housing Ministry in 1957 allowed for supporting and promoting private initiatives. That said, charities and non-profit associations also contributed to

residential construction during those years, following the contemporary low-income housing rules. One such organization is the Constructora Benéfica del Hogar del Empleado (CBHE). Its Technical Office gathered a group of young architects who would subsequently play a major role in the development of the Poblados Dirigidos de Renta Limitada, or neighborhoods for limited-income residents (1956–1957). The neighborhood of Entrevías was designed by Oiza and Sierra together with Alvear. Whereas Cubillo and Romany were in charge of Canillas and Fuencarral respectively. They won first place in the Experimental Houses Competition organized by the Housing Ministry in 1956.

Another active team consisted of Vázquez de Castro, Iñiguez de Onzoño, Leoz and Ruiz Hervás. After designing the Poblado de Absorción de San

Fermín, the architects received the order to create the famous neighborhood of Poblado Dirigido de Caño Roto. Leoz and Ruiz Hervás were assigned to Orcasitas. The Bretón de los Herreros team — Corrales, Molezún, and García de Paredes, together with Carvajal — designed the Poblado Dirigido de Almendrales. Corrales and Molezún collaborated with Cano Lasso, under Gutierrez Sotos' direction, in section G of Gran San Blas (Gutierrez Sotos').

These high-quality interventions in the social housing environment continued during the 1960s. Romany continued to collaborate with the CBHE. Carlos Ferrán and Eduardo Mangada joined the group as well.

The Unidad Vecinal de Absorción de Hortaleza (UVA) neighborhood, built in 1963, was recognized by Le Corbusier and Louis Kahn as the most human-friendly design among the 2300 worldwide projects presented at the X Congress of the UIA (Industrial Union of Argentina) in Buenos Aires in 1969 (Araujo Armero and Seco, 1994). The neighborhood was the work of Espinosa, Higuera, Cabrera, Miró, Weber and Crespi.

Some of the members of this generation of professionals even lived in the neighborhoods that they had designed, to demonstrate their personal

involvement. Vazquez de Castro lived in the Poblado Dirigido de Caño Roto, while Oíza and Romany hosted their first promotion of the Covadonga Colony in the Hogar del Empleado. Lucho Miquel, another member of Romany's, lived in a house of his own design as well.

Despite the unquestionable quality of the projects, many of the architects listed in this quick summary (for photos of the architects, see Fig. 1) fell into the obscurity. One of them is José Luis Romany, eclipsed by the renown of Oíza. The two architects shared the National Architecture Prize for designing the Chapel in the Camino de Santiago neighborhood, in collaboration with the sculptor Jorge Oteiza.

A humble architect without a media presence, Romany knew how to mix his extraordinary sensitivity with a remarkable rigor in his construction projects during the time we are studying.

The problem to be addressed is of a dual nature.

On the one hand, we want to assess whether the quality of José Luis Romany's work deserves this lack of attention, or whether, on the contrary, he is just as remarkable as some of his better-known colleagues.

In addition to this, we must face another problem. We want to determine if social housing, built more



Fig. 1. Photograph of some of the architects who designed social housing in Madrid in the mid-20th century (Baldellou, 1995)

than 50 years ago, may be considered architectural heritage that can be both preserved and adapted to the modern times through enhancing the original work's strengths, which will make it habitable for another half-century. In the current context, where the issues of energy efficiency, habitability and accessibility are becoming relevant, it seems pertinent to investigate what measures can be taken to ensure that the original project corresponds to society's new demands. The incorporation of energy efficiency parameters into existing social housing is far from simple (Trebilcock, 2011).

Materials and methods

In order to highlight José Luis Romany's work, we will analyze two of his most significant projects: Poblado Dirigido de Fuencarral and Colonia Juan XXIII, both located in Madrid.

These are two examples of social housing designed by the same architect, the first on his own and the second in collaboration with other two architects. These projects were also created at roughly the same time. They date back to the mid-20th century, with less than six years between them.

Firstly, we shall study the most relevant data from both projects, as well as the context in which they emerged. Subsequently, we shall analyze both cases at different levels: the neighborhood level, the building level, and the housing level.

We shall examine two interventions in multi-family residential buildings in order to see if social housing of the mid-20th century can be adapted to today and whether the original values need enhancing:

- Poblado Dirigido de Fuencarral by b102 arquitectura (b102arquitectura, 2022).
- Colonia Juan XXIII by g+f arquitectos (g+f arquitectos, 2022).

Finally, we shall compare the energy efficiency of the original and the refurbished state. The purpose of this study was to assess the difficulty of adapting Jose Luis Romany's work to present needs. The software used, CE3, is officially authorized in Spain to obtain energy certification for buildings.

Results

1 Poblado Dirigido de Fuencarral and Colonia Juan XXIII

As mentioned before, we chose Poblado Dirigido of Fuencarral and Colonia Juan XXIII for this case study. The data for both projects is provided in Table 1.

In the middle of the 20th century there was a pressing issue on Madrid's periphery: the growth of shanty towns (Esteban Maluenda, 1999). The 1950s saw a huge migration from the countryside to the city, quantified at an average of 229,000 people per year over the course of the decade (Oteiza et al., 2018). The existing residences in Madrid could not meet the demand for housing, which caused an uncontrolled spread of self-constructed settlements. The projects

selected for this study were part of various efforts to curb the situation.

The neighborhood of Fuencarral (see Fig. 2 for its aerial photograph) was targeted by a series of unusually innovative projects, known as "Poblados Dirigidos", promoted by the Urban Planning Station of Madrid under the guidance of Julián Laguna (Fernández-Galiano et al., 1989). As many as 10,925 homes were built during the project's first stage, between 1959 and 1962 (Guillem González-Blanch, 2013).

Colonia Juan XXIII (Fig. 3 shows the neighborhood's model) was promoted by a non-profit organization, Hogar del Empleado, created to support young workers who would come to the city and start new families there. From 1952 to 1966, 6000 homes were built (Fernández Nieto, 2006).

Romany divided his days between working in a shed at Fuencarral in the mornings and then joining his crew of architects from Hogar del Empleado at his studio home in Colonia Covadonga, one of the first neighborhoods established by the association, in the evenings (Fernández-Galiano et al., 1989).

2 Neighborhood level

At a time of frenetic construction activity, issues of such magnitude called for urgent solutions. When land was expropriated, housing was built quickly. The legalization of urban planning could wait (Betrán Abadía, 2002).

This way, the architect would get assigned to create not just a residential building, but an entire neighborhood or settlement. In just one project the

Table 1. Data for the projects selected

	Fuencarral	Juan XXIII
Architects	José Luis Romany	José Luis Romany, Eduardo Mangada and Carlos Ferrán
Project date	1956	1962
Implementation date	1959–1960	1963–1966



Fig. 2. Aerial photograph of Poblado Dirigido in the neighborhood of Fuencarral (Fernández-Galiano et al., 1989)

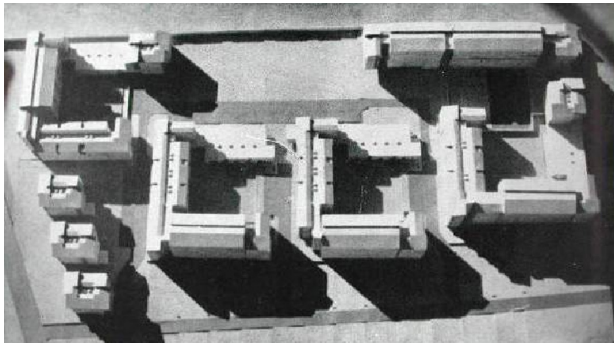


Fig. 3. Model of Colonia Juan XXIII (Fernández Nieto, 2006)

architect had to consider the neighborhood as a whole, including traffic circulation, free spaces, infrastructure and links to the rest of the city, block scaling and groupings, and the orientation and size of living spaces. The architect approached the assignments with coherence, complexity, experimentation, and boldness. The principal urban parameters for both projects are demonstrated in Table 2.

The Fuencarral area borders the coastal road in the south, the Poblado de Absorción Fuencarral A in the east, the now defunct Unidad Vecinal de Absorción of Fuencarral in the north, and the railway in the west (Moya González et al., 2017a). Linear blocks and rows of one-family homes are built with north-south and east-west orientation. The buildings, as observed in Fig. 4, are organized around a one-way road encircling the settlement.

A line of buildings is positioned along the outer perimeter of the road, while the rest are grouped within the inner perimeter. Access to the inner buildings is provided by little branching paths with no way out (Guillem González-Blanch, 2013). As the traffic only moves in one direction, this bars the road from being used by non-residents and prevents vehicles from reaching high speeds. This layout is very pedestrian-friendly. The inner public space

Table 2. Urban parameters of both projects (COAM, 1964; Fernández Nieto, 2006; Instituto Nacional de Estadística, 2016; Moya González, 1983)

	Fuencarral	Juan XXIII
No. of residential buildings	1839	502
Implementation area	20,758 ha	3230 ha
Construction density	89 blg/ha	155 blg/ha
Residential buildings	27%	29%
Non-residential buildings	3%	0%
Free private zones	6%	30%
Free public zones	59%	30%
Road traffic	5%	11%
Average income per household (AIH) (2016)	28,255 € 71% of AIH in Madrid	26,520 € 67% of AIH in Madrid

is made exclusively for pedestrians and features multiple green zones.

Free spaces between blocks are stacked into terraces adapted to the land topography. There is no pavement, except for the road and pedestrian paths. The abundant construction-free land is mostly covered with deciduous trees, hedges, and grass. In the center of the settlement are the non-residential buildings: a public school, a parish, and markets.

The Juan XXIII area is bordered by other residential development areas in the northwest and southeast. The southeast boundary was once a wall of a vast land plot occupied by the Marianistas' school, and before that, by Count de Campo Alange's retreat. Today, a street has been built here, with a housing block and a sport center on the other side, which has shrunk the school's outer land

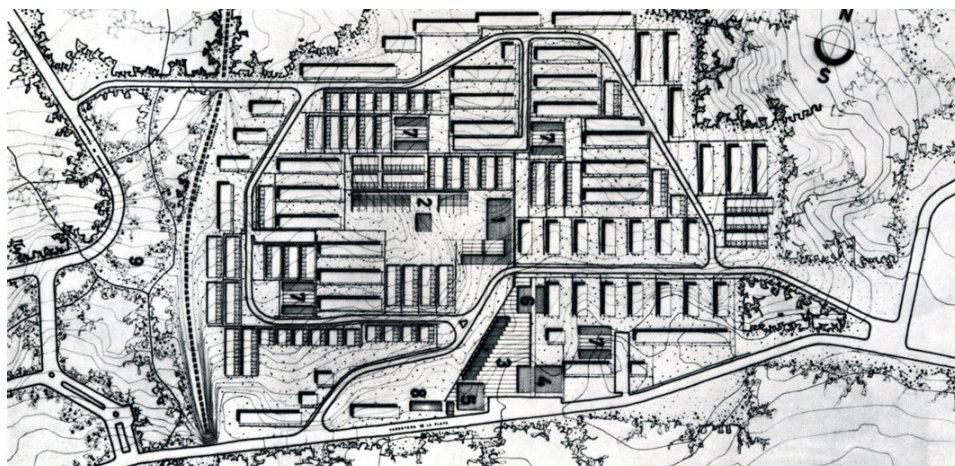


Fig. 4. Plan of Poblado Dirigido de Fuencarral (Fernández-Galiano et al., 1989)

plot. The northeast boundary is the neighborhood's only link to the city, through Joaquin Turina Street, formerly Camino de los Cuatro Vientos.

Four U-shaped blocks are placed along the perimeter. The first U-shaped block stretches from the approach to Joaquin Turina Street to the southeast boundary, leaving space for 3 rectangular blocks that offer greater connectivity with the city.

The rest of the U-shaped blocks are grouped close to the northeast boundary. The space near the southeast boundary is occupied by a linear block at the very end, leaving a vast free plot in the center, as seen in Fig. 5.

The traffic follows a U-shaped road. The road accesses, and exits into, San Deogracias Street, previously Antonio Bueno, running beyond the northeast section. The one-way traffic and the road's 90° turns reduce vehicle speed, prioritizing pedestrians against cars.

Large arcades are provided, where small shops are integrated into the residential buildings, all connecting with the large central free space, which could also function as a playground for the local children. Currently, this space has become a parking lot. On an intermediate scale, each U-shaped block has a central courtyard that is landscaped, as are the edges of the arcades. Notably, very little remains of this vegetation today.

There are no buildings with other uses, except for a small thermal power plant that produces heat for the whole neighborhood. Its sculpted chimney is an eye-catching landmark. The implementation of this solution, which is considered advanced from the energy efficiency standpoint, counts on a limited range of factors, some of which are as important

as the thermal power plant of the University City (Torroja, 1943).

3 Block level

In Fuencarral, residential buildings are arranged into 4- and 5-level linear blocks. At the core of each block, there is a staircase of minimal dimensions, without an elevator, giving access to two residences per level. This typology allows for cross-ventilation throughout the buildings.

As observed in Fig. 6, the blocks face each other and form groups between 2 and 6 blocks (in very few cases, they may stand alone). The block selected for this study is part of a group of 4 blocks, with 40 residences in total. Half of these residences have 4 bedrooms each, while the other half have 3 bedrooms each. The shape factor is 0.21 m^{-1} .

The load-bearing structure, as shown in Fig. 7, is formed by walls perpendicular to the façade, opening up the living room and much of the kitchen. The principal façade forms a one-meter enclosure with glass terrace railings. This creates a lightweight sensation, more common of the Nordic architecture. At the time, it was difficult to build reinforced concrete portico structures, and therefore, the structural solutions for load-bearing walls were becoming more intelligent and efficient. The most common material was brick, although in the case of Fuencarral, the supply of the unusually light-colored brick chosen by Romany eventually ran out, which was why in some buildings, including the one reviewed here, the load-bearing walls were instead made of concrete blocks lined with ceramic tiles.

The back façade, where the bedrooms are, features landscape-format openings, 50 cm in height and practically as wide as the entire room (García

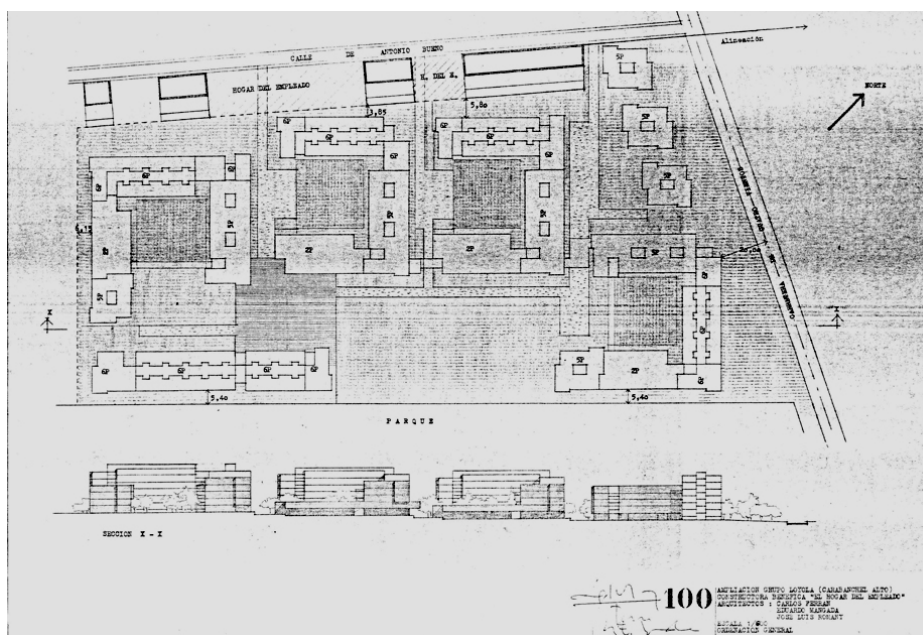


Fig. 5. Plan of Colonia Juan XXIII (Fernández Nieto, 2006)



Fig. 6. View of a group of blocks in Fuencarral (Fernández-Galiano et al., 1989)

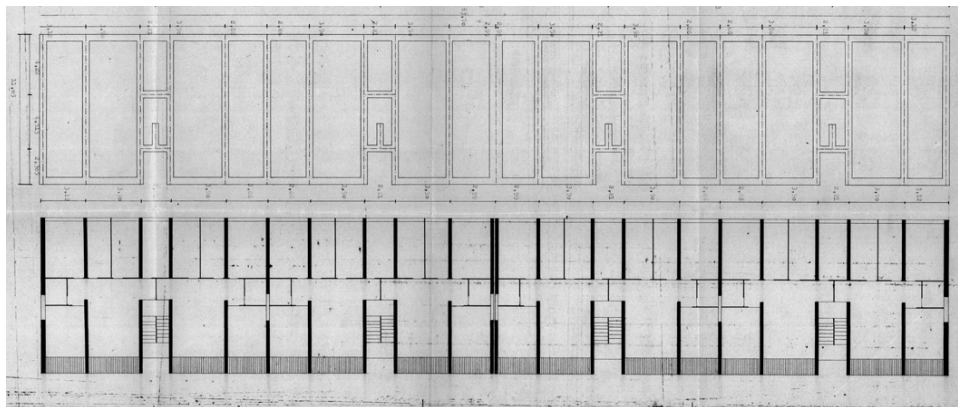


Fig. 7. Block layout in Fuencarral (Romany, 1957)

Herrero, 2013). Despite the fact that it is a more blind enclosure, the existence of continuous gaps affirms that it is not a load-bearing element.

In the Juan XXIII neighborhood, the residences are arranged into three types of blocks. The type of block selected for our case study is the most recurring. It is a U-shaped block with a central courtyard. As seen in Fig. 8, one side of the U-shape has two height levels. The ground floor opens to several porticoes, from where residents can access 5 commercial stores. The residences themselves are located on the first floor. This block's low height allows the sunlight to reach the community courtyard and the other sides of the building.

Starting from the second floor, the blocks form an L-shape with southeast and southwest "arms", ensuring appropriate sunlight exposure. One of the "arms" has 5 floors, while the other has 6. The block comprises 83 residences of 6 different types, with two, three or four bedrooms. The blocks are isolated, as shown in Fig. 9, although the commercial porticoes do create some continuity within the street layout. The shape factor is 0.18 m^{-1} .

The block we are studying in the Juan XXIII neighborhood is 15% more compact than its Fuencarral counterpart, due to its large size and height.

The depth of the block in this case exceeds 12 m, which is the standard dimension of the Spanish dwelling with two orientations. This is achieved through introducing interior galleries that change the section of the block and the residences.

A single elevator provides access to most of the residences through spacious galleries. Some of the residences have windows along a single façade, while others open into two opposite façades. These are the residences located at the end and in the middle of the galleries. This typology, called the "scissors maisonette", has been imported from the London County Council (London County Council, 1962).

In this section, one house goes above the central gallery while the adjoining house goes below it. This creates a scissor-like layout, as seen in Fig. 10. This way, only one gallery is needed at every two floors, and one elevator is sufficient.

The load-bearing structure consists of walls parallel to the façade, allowing the different interior



Fig. 8. View of the group of blocks in the Juan XXIII neighborhood (González Amezqueta, 1973)

levels of the residences to pass through the central gallery. This constructive solution creates a "blind wall" appearance. The front is widened to avoid contact with the load-bearing walls of the façade, as well as to allow for window openings and spacious terraces that connect to the lounge and the kitchen.

The large exposed brick panels were inspired by the English residential architecture of the time, including, for example, the Ham Common apartments of Stirling and Gowan, where brick is featured both outside and inside the block (Arnell and Bickford, 1993), as well as by Ridolfi's neo-realist buildings in Italy (Benévolo, 1974).

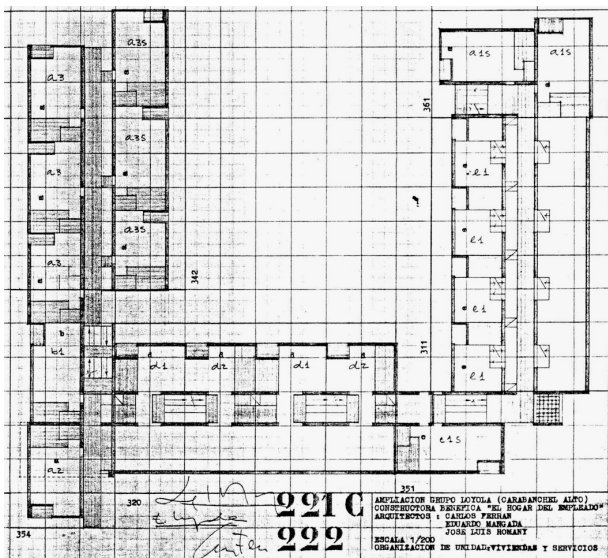


Fig. 9. Juan XXIII block structure (Fernández Nieto, 2006)

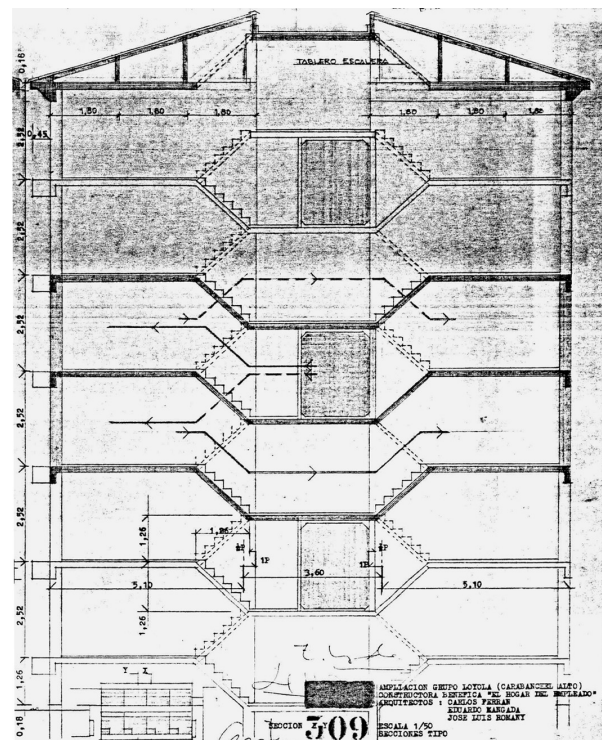


Fig. 10. Cross section of a block in the Juan XXIII neighborhood (Fernández Nieto, 2006)

4. Housing level

In each of the projects, we chose to review a four-bedroom apartment. These apartments were rehabilitated at a later time.

In the residence in Fuencarral (see floor plan in Fig. 11), the bedrooms face north, while the living room and the kitchen face south. It is a middle-

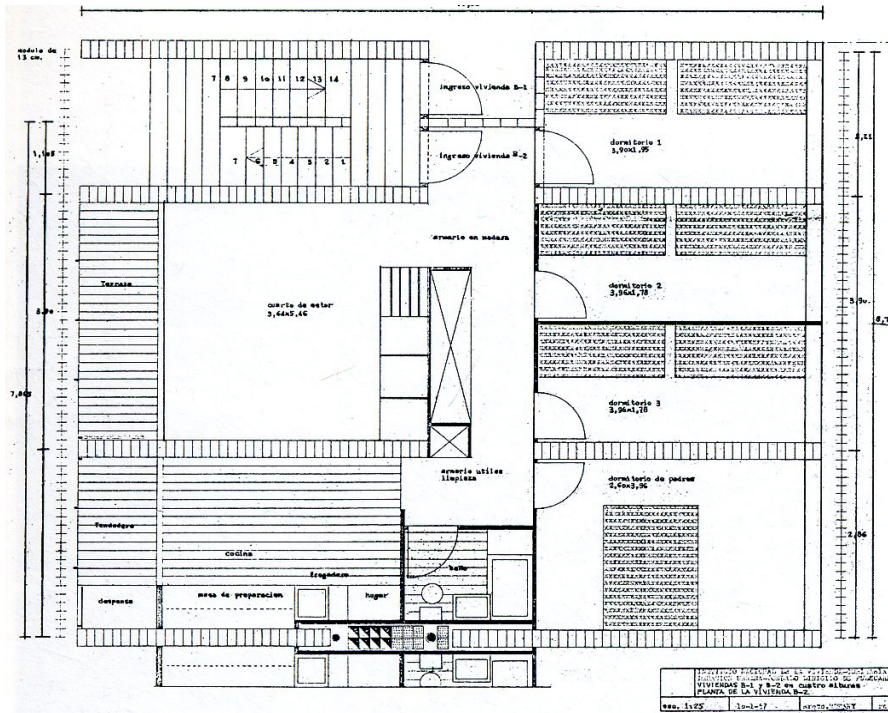


Fig. 11. Fuencarral apartment floor plan (Fernández-Galiano et al., 1989)

floor apartment, with three 11.05 m long corridors perpendicular to the façade. The first corridor, 2.21 m long, leads to the bedroom and the vestibule, and can be accessed from the core of the staircase. The second corridor, 3.90 m long, connects to two more bedrooms, the central area, and the living room. The third corridor, 2.86 m long, leads to the master bedroom, the kitchen, and the bathroom (without a gap in the façade). The total width of the façade is 8.97 m. The residence we shall examine in the Juan XXIII neighborhood is a through apartment located on the top floor, which consists of three corridors parallel to the 7.20 m front façade. The outer corridors are 5.10 m wide, while the central corridor is 3.60 m wide, resulting in a total width of 13.80 m.

The residence has several different levels. The hall, which is not represented in Fig. 12 where the rest of the floor can be seen, is at the same level as the gallery that provides access to the different residences. To reach the living room and the kitchen, which are oriented to the southeast and open onto the terrace, one has to go up half a floor. By moving half a floor in the opposite direction, one enters the access gallery. This level contains the bathrooms, which are ventilated by a shaft, and a bedroom that opens into the northeast, this being the first apartment in the gallery. Finally, going down half a floor will take one to the remaining three northwest-facing bedrooms.

Table 3 illustrates the usable space size in each room and the total size of each residence. According to Moya’s classification (Moya González et al., 2017b), these residences can be classified as large. In Moya’s time, only 9% of all social housing fit that category.

The constructive features of the thermal envelope are shown in Table 4. It is remarkable that the residences in Poblado Dirigido de Fuencarral have thermal insulation despite the limited budget and the absence of regulations that would have called for it (the first such regulations would not be set up until 23 years later).

5. 21st century rehabilitation

It has now been 50 years, and the context has changed. The once peripheral neighborhoods are now inside the city. In the early 21st century, Madrid implemented new urban intervention programs, or Programas de Intervención Urbanística (PAU), following a very different scenario. Today’s streets have been taken over by private vehicles. This urban layout means that residential development has broken apart into autonomous plots, which are closed around the perimeter, at the cost of the city’s permeability (Fernández Nieto, 2012).

At the beginning of the 21st century, two architectural studios discovered the potential offered by Romany’s achievements in the mid-20th century. They began to refurbish one apartment each, trying both to respect the legacy and focus on energy efficiency and habitability.

Utilizing the one-use city concept, they take on the challenge of the modern lifestyle, with each of the studios refurbishing the respective apartment for personal use. Table 5 lists basic information on these rehabilitation projects.

These teams are similar in many ways. They share an appreciation for the urban and architectural qualities of these 20th century heritage sites, have

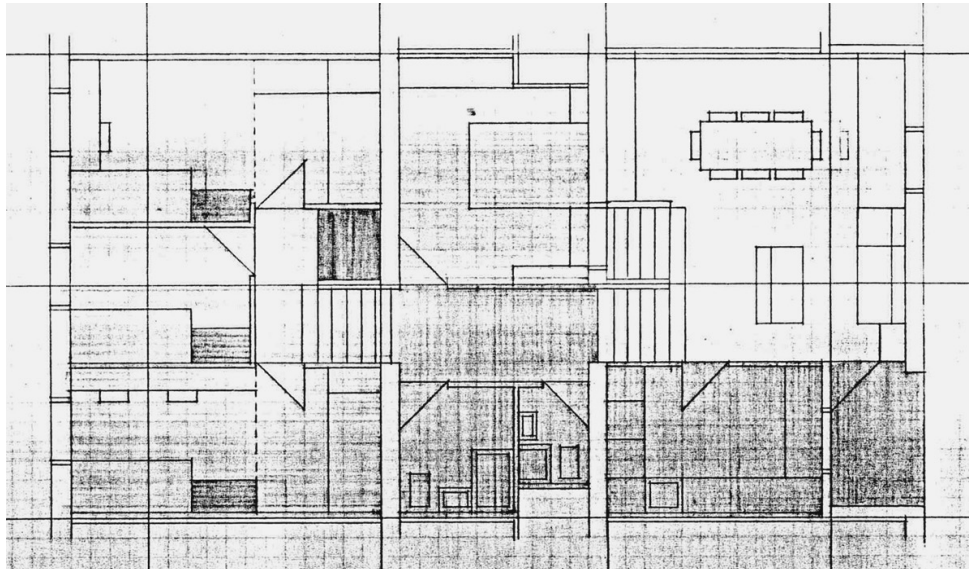


Fig. 12. Juan XXIII apartment floor plan (Fernández Nieto, 2006)

refurbished the residences for themselves to live in, and show the same enthusiasm towards Romany's work. The intervention projects' respect for the original concept has earned them two COAM awards: g+f arquitectos' work in Colonia Juan XXIII received the award in 2019 (COAM, 2019) and a similar project by b102 arquitectura in Poblado Dirigido de Fuencarral, in 2016 (Fundación arquitectura COAM, 2017).

During the rehabilitation of the Fuencarral residence, an attempt was made to return to the previously modified elements of the original project. The closed-off terrace and kitchen terrace were restored, and their glass elements were recreated according to the original model, as can be seen in Fig. 13.

With regard to the layout, Fig. 14 shows that the two bedrooms in the center were joined to create a study area that opens onto the living room, while the

bathroom was divided into two parts, allowing for an additional toilet.

The wardrobe between the living room and the hall did not originally reach the ceiling, thus a second wardrobe was created above it. A door was installed between the living room and the hall. Both elements were demolished, restoring the original status with

Table 3. Usable space and total space

	Fuencarral	Juan XXIII
Hall	14.7 m ²	19.9 m ²
Kitchen	8.8 m ²	7.8 m ²
Bedroom 1	10.3 m ²	12.1 m ²
Bedroom 2	7.7 m ²	11.0 m ²
Bedroom 3	7.0 m ²	10.0 m ²
Bedroom 4	7.0 m ²	5.6 m ²
Bathroom 1	3.0 m ²	4.2 m ²
Bathroom 2	-	2.2 m ²
Lobby	1.7 m ²	3.7 m ²
Corridor	7.3 m ²	7.7 m ²
Stairs	-	4.2 m ²
Terraces	3.8 m ² / 2.8 m ²	3.3 m ²
Total usable space	74.1 m ²	91.7 m ²
Total space	87.3 m ²	103.7 m ²

Table 4. Constructive features of the thermal envelope

	Fuencarral	Juan XXIII
Façade	2 cm brick panel 8 cm double-cavity brick 3 cm glass wool Air chamber 4 cm single-cavity brick	11.5 cm exposed brick Air chamber 8 cm double-cavity brick
Roof	Fiber-cement board 2 cm insulation Concrete slab False ceiling plaster	Flat tile Double brick board Brick wall Concrete slab
Window frame	White painted wood	Steel with prefabricated concrete frame
Window glass	Simple 3 mm	Simple 3 mm
Sun protection	Folding wooden shutters in the living room	Unprotected

Table 5. Rehabilitation project overview

	Fuencarral	Juan XXIII
Architects	b102 arquitectura: Jesús García Herrero and Inés Patiño Mejide	g+f arquitectos: Jorge Gallego Sánchez Torija and M ^a Antonia Fernández Nieto
Year	2005	2018



Fig. 13. Living room in the rehabilitated residence in Fuencarral



PLANTA VIVIENDA

Fig. 14. Plan of the rehabilitated residence in Fuencarral

visual continuity between the hall and the entrance. The space was also filled with more light.

In the bedrooms, interior blinds were chosen to regulate sunlight, while in the living room and kitchen, exterior sun-screen blinds were installed, flush with the façade. The original shutters of the living room were not recovered. Instead, the architects opted for glazing the entire front of the room. This returned it to its original recess position, a solution that was also applied to the kitchen.

As part of rehabilitating the residence in the Juan XXIII neighborhood, the terrace was enlarged to give it bigger dimensions and to add space to the living room, while slightly downsizing the kitchen, as can be seen in Fig. 15.

To achieve spatial continuity between the residence’s two opposite façades, as shown in Fig. 16, the external partition of the central bedroom was demolished to create a study area incorporated into the central space. The partition closing off the bedroom next to the bathrooms was demolished as well. In order to maintain the bedroom’s use for its intended purpose, it was closed off with glass for visual continuity and opaque fabric for privacy and dimming the light.

For energy efficiency purposes, the improvements reflected in Table 6 were incorporated into the thermal envelope.

Table 7 shows the residences’ thermal transmittance values, as well as their energy consumption, before and after their rehabilitation.

Measurements were made with the CE3 software.

6. Energy features

In its original state, the Juan XXIII residence had a 33% higher energy consumption rate per square meter than the Fuencarral residence. Although the Juan XXIII residence has more compact proportions

Table 6. Improvements incorporated into the thermal envelope

	Fuencarral	Juan XXIII
Façade	–	4 cm expanded polystyrene 1 cm laminated plaster
Roof	–	4 cm mineral wool
Window frame	Black aluminum without a thermal bridge break (TBB) on the north façade Black aluminum with a TBB on the south façade	White aluminum with a TBB in the living room, kitchen and bathrooms Unchanged
Window glass	Low-emission double glazing 4/8/6 on the south façade	Double glazing 4/16/6
Sun protection	Sun screen exterior blind on the south façade	Thermal aluminum blind



Figure 15. Living room, with terrace and kitchen at the back, in the rehabilitated residence in the Juan XXIII neighborhood

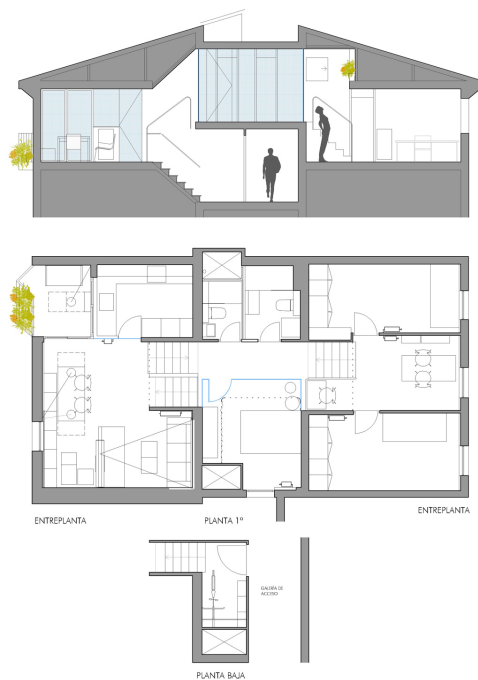


Fig. 16. Section plan of the rehabilitated residence in the Juan XXIII neighborhood

(façade: 1, depth: 1.9) than its Fuencarral counterpart (façade: 1, depth: 1.2), their façade surface area is similar due to the presence of the terrace and the lateral façade in the Juan XXIII residence, which is located at the corner of the U-shaped block.

On the other hand, the proportions of the façade openings are not similar. They take up 44% in the Fuencarral residence and merely 26% in the Juan XXIII residence. The presence of thermal insulation in the Fuencarral residence reduces the thermal transmittance of the walls by 50% and that of the roof, by 20%. The woodwork in the Fuencarral residence also falls 6% behind the Juan XIII residence steelwork in terms of thermal transmittance.

The greater opening size in the Fuencarral residence is compensated for by the enhanced

Table 7. Thermal transmittance and energy consumption values before and after rehabilitation

	Fuencarral	Juan XXIII
Façade	0.91/0.91 W/m ² K	1.72/0.60 W/m ² K
Roof	0.92/0.92 W/m ² K	1.14/0.54 W/m ² K
Windows	5.35/3.14 N; 2.39 S W/m ² K	5.70/2.95 NO; 2.75 SE W/m ² K
Energy use	131.4/106.9 kWh/m ²	198.7/168.8 kWh/m ²

properties of the enclosure. Therefore, difference in energy consumption can mainly be attributed to the fact that the Juan XXIII residence is located on the top floor of its building. If this residence was on one of the middle floors (as is the case with the Fuencarral residence), it would have consumed 6% less energy.

During the Fuencarral residence rehabilitation, work on the thermal enclosure was limited to replacing the woodwork. Even though the façade was designed in 1956, its transmittance values comply with those required by both the NBE-CT-1979 and the CTE-2006 standard. The renovation has reduced the residence energy consumption by 19%.

In the case of the Juan XXIII residence, the entire thermal envelope was affected by the rehabilitation process. The façade is now insulated, achieving a 30% lower transmittance compared to the Fuencarral residence. The roof is also insulated, and its properties slightly exceed those required by the CTE-2006. Likewise, the woodwork has been renewed in some spots and replaced with glass throughout the rest of the residence. This rehabilitation has reduced the residence energy consumption by 15%.

The consumption drop is more modest than in the other residence due to the large size of the roof surface area compared to the rest of the envelope. As the wall original condition was worse, renovating this element has saved more energy than improving the roof. If the Juan XXIII residence was located on the middle floor, its renovation would have reduced energy consumption by 25%.

The Juan XXIII residence is more compact and has a lower opening proportion, which means that its energy performance could have been better if it were not for the thermal load on the roof, which requires extra energy to compensate for.

Since this residence is located underneath the roof, energy consumption was 34% higher before the renovation and is 37% higher now.

Discussion

The interventions studied in this paper took place in socio-economically disadvantaged neighborhoods, where incomes are currently about 30% below the city average.

The two interventions differ notably in terms of approach. The Fuencarral project, which was publicly promoted, managed to achieve density parameters that are currently considered sufficient for escaping

a diffused, overcrowded cityscape (Rueda, 2000). At the same time, 90% of the area's free spaces are intended for public use.

The Juan XXIII project, by contrast, was promoted by a private organization, and the neighborhood density not only exceeds reasonable values, but is, in fact, fairly high, which is compensated for by the Las Cruces Park, a vital part of the area. The free spaces, located in each block, are divided equally between those for public use and those for private use.

In both cases, it is remarkable how little space is taken up by road traffic. Priority is given to pedestrian routes on the neighborhood level, while transport infrastructure is implemented on the district and city level.

The blocks prioritize a comfortable layout, although this is not a mandate. Some flexibility is granted in the interests of building a better neighborhood. Some blocks or certain parts of them are reduced in favor of configuring unique exterior spaces and laying down streets with an open block typology, which can become diluted on a larger city scale.

With all costs taken into consideration, cross ventilation in residences is the favored method. At a time when air conditioning was not available, this passive strategy was fundamental in maintaining comfortable conditions in Madrid's summer climate. Sometimes it was achieved through ingenious typology, like the "scissors masonettes" in the Juan XXIII neighborhood. This type of housing also addresses the low economic profitability of placing an elevator in a linear block to serve two apartments per floor (Guajardo, 2017). A single elevator serves 88 apartments.

The houses' design is set apart by its simplicity, clarity and rounded corners. It was quite advanced for the time period, especially thanks to incorporating thermal insulation in the Fuencarral neighborhood. In the case of the Juan XXIII neighborhood, what made the design innovative was the heating installation that served the needs of the whole area.

The rehabilitation projects carried out by different teams of architects have a few traits in common: their respect for, and enhancement of, the original project's values, combined with creating more open spaces, which is possible due to the smaller number of people living in the houses today.

Conclusions

We have studied two brilliant works of architecture exemplifying mid-20th century social housing in Madrid. Despite the projects' urgency and the scarce resources available, the two works

go beyond expectations in the context where they were produced.

Their recognition, however, leaves much to be desired. The Poblado Dirigido project in the Fuencarral neighborhood is, perhaps, better known, as there were other projects, the Poblados de Absorción (Absorption Towns), previously carried out in Fuencarral by Sota and Oíza, two well-known architects. In addition, there were a number of important studies made regarding the Poblados Dirigidos housing for limited-income families.

This is not true of the Colonia Juan XXIII neighborhood, which is less-studied, despite the uniqueness of its housing type and the fact that it was publicized in magazines of the time (Ferrán et al., 1973; González Amezcua, 1973). To date, José Luis Romany has not been given the recognition he deserves, like so many other architects who introduced modern concepts in Spain.

While other renowned architects of the time focused on building luxury residences with a surface area of over 300 m² (Carbajal-Ballell, 2017), Romany contributed to two outstanding social housing projects that contain important values.

Both projects are committed to creating an open city, with abundant vegetation and a pedestrian-friendly street layout. These are values that today's cities would benefit from, as they seek to become healthier by integrating vegetation and turning the streets more walkable.

Both projects use advanced energy strategies: passive design with cross ventilation, incorporation of thermal insulation into enclosure at a time when thermal regulations did not exist, and efficient heating for the whole neighborhood.

In Spanish, there is a saying, "dar gato por liebre", "pass off a cat as a hare", used for talking about fraudsters that try to sell a low-value object under the guise of something precious. But as Alejandro de la Sota notes, architects are the only ones capable of doing the reverse, of passing off a valuable hare as a modest cat (De La Sota, 2002). This is quite evident in both projects.

In the 21st century, four architects have made a personal commitment. In the face of the new, recently built atomized city, they choose to re-inhabit modernity.

The prizes awarded to the rehabilitation projects by the Association of Architects can serve as roundabout way of acknowledging the architect to whom we owe these buildings, José Luis Romany. Let this text serve as a tribute to him.

References

- Araujo Armero, R. and Seco, E. (1994). *Construir con acero. Arquitectura en España*. Madrid: Publicaciones Ensidesa, 477 p..
- Arnell, P. and Bickford, T. (1993). *James Stirling: buildings and projects*. New York: Rizzoli, 342 p.
- b102 arquitectura (2022). [online] Available at: <http://www.b102arquitectura.com> [Date accessed November 1, 2022].
- Baldellou, M. Á. (1995). Neorrealismo y arquitectura. El “problema de la vivienda” en Madrid, 1954-1966. *Arquitectura*, No. 301, pp. 20–51.
- Baldellou, M. A. (1998). *Madrid moderno 1950/1965. La furiosa investigación*. Proceedings of the International Congress “De Roma a Nueva York: itinerarios de la nueva arquitectura española 1950-1965”. Pamplona: T6 Ediciones, pp. 59–65.
- Benévolo, L. (1974) *Historia de la arquitectura moderna*. 2nd edition. Barcelona: Gustavo Gili, 944 p.
- Betrán Abadía, R. (2002). De aquellos barro, estos lodos: la política de vivienda en la España franquista y postfranquista. *Acciones e Investigaciones Sociales*, No. 16, pp. 25–67.
- Carbajal-Ballell, R. (2017). Luis Gutiérrez Soto en Sevilla. 1954-1965. *Informes de la Construcción*, Vol. 69, No. 548, e226. DOI: 10.3989/ic.16.046.
- COAM (1964). Poblados de actuación oficial de Madrid. *Arquitectura*, No. 62, pp. 40–48.
- COAM (2019). *Premios COAM y Premio Luis M. Mansilla 2019*. [online] Available at: <https://www.coam.org/es/servicios/concursos/concursos-ocam/premios-coam-y-premios-luis-m-mansilla-2019> [Date accessed November 1, 2022].
- De La Sota, A. (2002). *Escritos, conversaciones, conferencias*. Barcelona: Gustavo Gili, 216 p.
- Esteban Maluenda, A. (1999). La vivienda social española en la década de los 50: Un paseo por los poblados dirigidos de Madrid. *Cuaderno de Notas*, No. 7, pp. 55–80.
- Fernández-Galiano, L., Isasi, J. F., and Lopera, A. (1989). *La quimera moderna: los poblados dirigidos de Madrid en la arquitectura de los 50*. Madrid: Hermann Blume, 207 p.
- Fernández Nieto, M. A. (2006). *Las colonias del hogar del empleado: la periferia como ciudad*. PhD Thesis in Architecture.
- Fernández Nieto, M. A. (2012). *La ciudad reutilizada. Repensar el espacio público de la periferia*. In: García Carbonero, M. (ed.). *i making HETEROTOPÍAS laboratorio de estrategias urbanas*. Madrid: Universidad Francisco de Vitoria, pp. 101–115.
- Ferrán, C., Mangada, E., and Romany, J. L. (1973). Aproximación a un análisis tipológico del grupo de viviendas Juan XXIII. *Nueva Forma*, No. 93, p. 36.
- Fundación Arquitectura COAM (2017). *2005/2016 Premio COAM. Arquitectura contemporánea de Madrid*. Madrid: Fundación Arquitectura COAM, 960 p.
- g+f arquitectos (2022). [online] Available at: <https://gmasfarquitectos.wordpress.com> [Date accessed November 1, 2022].
- García Herrero, J. (2013). *Intervenciones en el poblado dirigido de Fuencarral*. In: Jornadas internacionales de investigación en construcción: vivienda: pasado, presente y futuro: resúmenes y actas. Madrid: Instituto Ciencias de la Construcción Eduardo Torroja, p. 141.
- González Amezqueta, A. (1973). El grupo Juan XXIII. *Hogar y Arquitectura*, No. 68, pp. 12–33.
- Guajardo, A. (2017). Análisis tipológico de bloques lineales de vivienda social: España 1950-1983. El caso de Andalucía occidental. *Informes de la Construcción*, Vol. 69 (545), e185. DOI: 10.3989/ic.16.055.
- Guillem González-Blanch, M. D. P. (2013). *Tipología de vivienda en los poblados dirigidos de renta limitada: Madrid 1956-1959*. PhD Thesis in Architecture.
- Instituto Nacional de Estadística (2016). *Atlas de Distribución de Renta de los Hogares*. [online] Available at: <http://www.ine.es/experimental/experimental.htm> [Date accessed November 1, 2022].
- London County Council (1962). London's “scissors” maisonettes. *Architects' Journal*, No. 9, pp. 453–460.
- Moya González, L. (1983). *Barrios de promoción oficial Madrid 1939-1976: la política de promoción pública de vivienda*. Madrid: COAM, 257 p.
- Moya González, L., Díez de Pablo, A., and Monjo Carrió, J. (2017a). La arquitectura ordinaria del siglo XX como patrimonio cultural: tres barrios de promoción oficial de Madrid. *EURE (Santiago)*, Vol. 43, No. 130, pp. 269–293. DOI: 10.4067/s0250-71612017000300269.
- Moya González, L., Fernández Salgado, C., and Escamilla Valencia, F. (2017b). Evolución del tamaño de la vivienda de promoción pública y su comparación con el resto del parque residencial construido en Madrid entre 1940-2010. *Informes de la Construcción*, Vol. 69, No. 545, pp. 30–38. DOI: 10.3989/ic.16.040.

Oteiza, I., Alonso, C., Martín-Consuegra, F., Monjo, J., González Moya, M., and Buldón, A. (2018). *La envolvente energética de la vivienda social. El caso de Madrid en el periodo 1939-1979*. Madrid: Consejo Superior de Investigaciones Científicas, 123 p.

Romany, J. L. (1957). *Poblado Dirigido de Fuencarral. Viviendas en bloque*. Archivo Servicio Histórico COAM.

Rueda, S. (2000). Modelos e indicadores para ciudades más sostenibles. In: *Economía, ecología y sostenibilidad en la sociedad actual*. Segovia: Fundación Universidad de Verano de Castilla y León, pp. 115–154.

Torroja, E. (1943). La calefacción a distancia. de la ciudad universitaria de Madrid. *Revista de Obras Públicas*, No. 2744, pp. 535–542.

Trebilcock, M. (2011). Perception of barriers to the inclusion of energy efficiency criteria in buildings. *Revista de la construcción*, Vol. 10, No. 1, pp. 4–14. DOI: 10.4067/S0718-915X2011000100002.

Urban Planning and Development

DOI: 10.23968/2500-0055-2022-7-4-17-35

IMPROVING URBAN ENERGY RESILIENCE WITH AN INTEGRATIVE FRAMEWORK BASED ON MACHINE LEARNING METHODS

Asmaaa M. Hassan*, Naglaa A. Megahed

Port Said University
Port Said, 42526, Egypt

*Corresponding author: assmaa.mohamed@eng.psu.edu.eg

Abstract

Introduction: Climate change and global warming are among the greatest challenges facing the world today. A new concept, known as urban resilience, has been developed in response. There are various approaches to urban resilience. Among them, is the urban energy resilience (UER) approach, which poses a considerable challenge. Machine learning (ML), as an application of artificial intelligence (AI), provides powerful and affordable computing resources, large-scale data mining, advanced algorithms, and real-time monitoring. However, very few studies have investigated how such aspects can be integrated into urban resilience in general, and UER in particular. **Purpose of the study:** The study develops an integrative framework that can improve UER, based on ML methods. **Methodology:** We carried out a bibliometric analysis and a systematic review of UER in accordance with AI concepts, models, and applications. **Results:** The findings of this study were used to create an integrative framework, based on three hierarchical phases, which effectively addressed the main capabilities of UER, identified its priorities, and shed light on how ML can benefit UER as a whole. **Novelty:** The framework developed in this study also offers insights in integrating ML methods into UER as strategically as possible, especially in the context of climate change and urban energy systems. This framework can serve as reference for specialists and decision-makers aiming to expand AI and ML applications to optimize UER.

Keywords

urban energy resilience; artificial intelligence; machine learning; climate change; energy systems; demand response.

Introduction

The 21st century has been referred to as the “century of the city”, since more than half of the world’s population currently resides in cities and urban areas (Nik et al., 2021; Ragheb et al., 2017). However, such areas are complex dynamic systems that face various social, economic, and environmental threats, all of which challenge their resilience and/or expose their vulnerabilities (Elzeni et al., 2022; Gültekin, 2021). Thus, the urban energy resilience (UER) concept is seeing increasing application in the fields of climate change, sustainability, and natural disaster risk analysis. Meanwhile, climate change and global warming present numerous challenges to energy resources in cities and urban areas (Ismail et al., 2022b; EL-Mokadem et al., 2016b; Noaman et al., 2022; Perera et al., 2021; Sharifi and Yamagata, 2014a). In fact, 60 to 80% of global energy is consumed in urban areas (Hassan et al., 2020a, 2020b; Olazabal et al., 2012; Sharifi, 2019; Sharifi and Yamagata, 2016a), which can lead to negative consequences, for instance an increase in blackouts and grid failures (Erker et al., 2017; Sharifi and Yamagata, 2016a). With regard

to meeting future demand and climate targets, Perera et al. (2021) highlighted the importance of promoting energy generation through sustainable approaches, including a significant transformation in the energy infrastructure to utilize renewable energy technologies. In response, researchers and policymakers have made noticeable shifts in mitigation and adaptation strategies, taking the effects of both past and present emissions into consideration (Sharifi and Yamagata, 2014a). In this context, the concepts of resilience in general, and UER in particular, have been applied to effectively prepare for, combat, absorb, adapt to, and recover from adverse disruptions (Eslamlou et al., 2022; Francis and Bekera, 2014; Gültekin, 2021; Masnavi et al., 2018; Hunter, 2021; Kapucu et al., 2021; Olazabal et al., 2012; Tumini et al., 2017). Tien et al. (2022) considered the resilience-focused approach to energy systems to be multifaceted, having found that many studies only focused on energy supply network faults on a spatial scale larger than a single city, while ignoring the complications specific to urban environments. In this context, Erker et al. (2017) demonstrated that an energy-resilient system

can successfully manage and rapidly recover from energy-related disruptions, while continuing to deliver affordable energy services. Currently, cities are characterized by a high energy demand and use, with adverse implications for energy availability, accessibility, and affordability (Perera et al., 2021). Under such circumstances, an effective demand response can create a cost-effective energy system that is both flexible and reliable (Antonopoulos et al., 2020). Wide-scale responses to energy challenges have increasingly incorporated machine learning (ML) and artificial intelligence (AI) applications, which have been used for site selection, parameter assessment, operation and maintenance optimization, planning, feasibility analysis, discharge forecasts, energy generation projections, and maintenance (Kumar and Saini, 2021).

Although the application of ML methods to UER has been gaining popularity, the topic has yet to be sufficiently investigated in light of recent climate change developments. This also indicates a growing need for an integrative framework that can bridge the gap in previous research and enhance UER as a whole (Bosisio et al., 2021; Du et al., 2014; Xie et al., 2020). Therefore, the present study creates an integrative framework that can integrate ML into UER in an acceptable and affordable manner.

We have arranged our study as follows. The research methodology is discussed in the next section, followed by a systematic review and bibliometric analysis of related works. Moreover, the relationships between climate change, the United Nations' (UN) Sustainability Development Goals (SDGs), and multiple dimensions of urban resilience are described, and urban energy systems resilience in more detail are discussed. Furthermore, AI technologies and applications with a detailed explanation of the proposed framework are identified. Finally, the conclusion is conducted.

Methodology

In order to create an integrative framework that can use ML methods to improve UER, we subjected the concept of UER to bibliometric analysis and a systematic review in accordance with AI concepts, models, and applications. First, we searched Scopus and Web of Science Core Collection for works with "resilience", "UER concept", "climate change", "urban energy systems", or "AI applications" in the title, abstract, or keywords. This was followed by a systematic review using the PRISMA method (preferred reporting items for systematic reviews and meta-analysis). The data extracted underwent bibliometric analysis in the VOSviewer software.

This keyword search yielded 3260 results. We applied "quick filters" to databases to sort results by broad categories such as document type (our study was limited to books, book chapters, journals, and conference proceedings), language (we focused on

studies written in English only), and publication date (between 2012 and 2023). As the first step, duplicate results were excluded from further investigation, and the initial results were reduced to 1138 documents. Then the titles, abstracts, and introduction of every publication were manually screened and assessed for relevance to the research topic. After irrelevant papers were excluded, the final dataset for this study was reduced to a total of 33 publications, as shown in Fig. 1. We carried out a bibliometric analysis to detect co-occurrence and co-authorship of related studies.

Literature Review

Previous studies have revealed various approaches to blending the UER concept and ML applications. As shown in the bibliometric analysis carried out in VOSviewer (Fig. 2), we have identified two major clusters: ML methods and resilience. However, limited studies have focused on the intersection of these clusters. Thus, the literature review below focuses on various concepts, starting with the concept of urban resilience in general, followed by the specific concepts of UER, AI applications, and ML methods (see Table 1).

Regarding the concept of urban resilience in general, several studies have emphasized its multidimensional nature, which encompasses infrastructure, climate, and social resilience, as well as resilience assessment (Carta et al., 2021; Francis and Bekera, 2014; Khalili et al., 2015; Krishnan et al., 2021; Sharifi, 2016). That said, the work of Woolf et al. (2016) stands out here, as it investigates resilience-related projects for localized infrastructure, specifically the pilot tests under the Kenya Slum Upgrading Program in Kibera, Nairobi.

In general, previous studies on the urban resilience concept have been based on theoretical frameworks that illustrate urban dynamics over time and show how the physical structure of cities can facilitate urban resilience (Olazabal et al., 2012; Sharifi, 2019; Sharifi and Yamagata, 2014a, 2018). However, more recent studies by Sharifi and Yamagata (2016b), Ohshita and Johnson (2017), Ragheb et al. (2017), and Nik et al. (2021) indicate how energy systems can be integrated into the infrastructure that fosters urban resilience. Moreover, Hasselqvist et al. (2022) provide a complex perspective of such resilience, by using households as a starting point. Conversely, several works focus on AI applications and their contributions to building urban systems, resilience in general, infrastructure resilience, and a sustainable urban environment (Abdul-Rahman et al., 2021; Bibri, 2021a; Haggag et al., 2021; Huang and Ling, 2019; Huang and Wang, 2020; Konila Sriram et al., 2019; Ladi et al., 2022; Ortiz et al., 2021; Rahimian et al., 2020; Tekouabou et al., 2021; Zhang et al., 2022). Regarding the relationship between AI applications and energy systems, Rahimian et al.

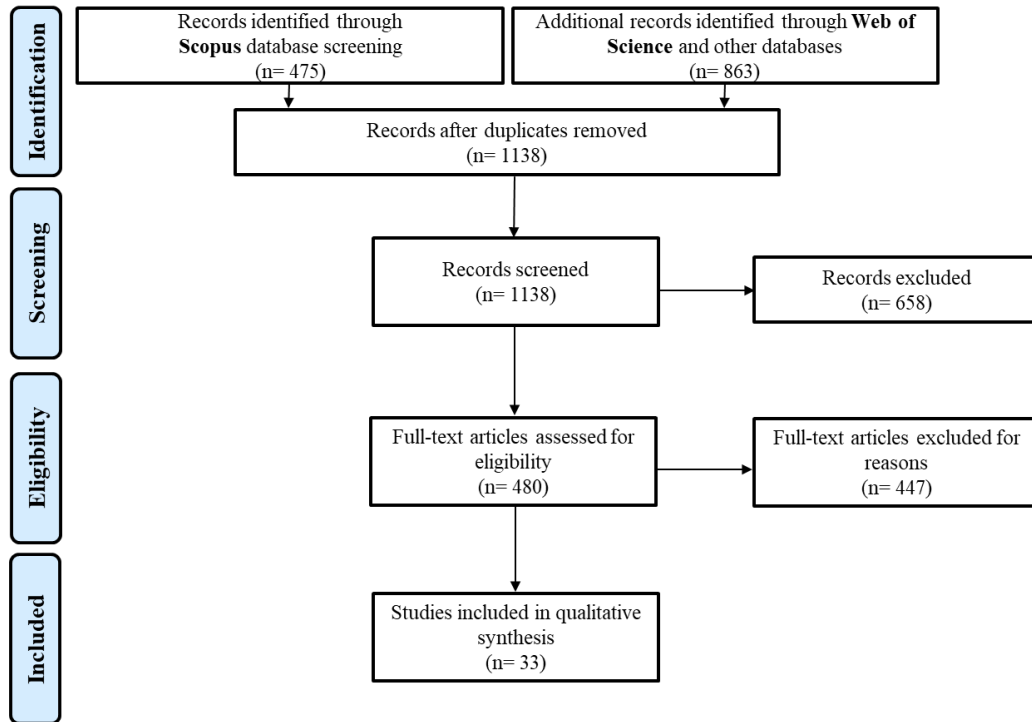


Fig. 1. Paper vetting process based on the PRISMA method

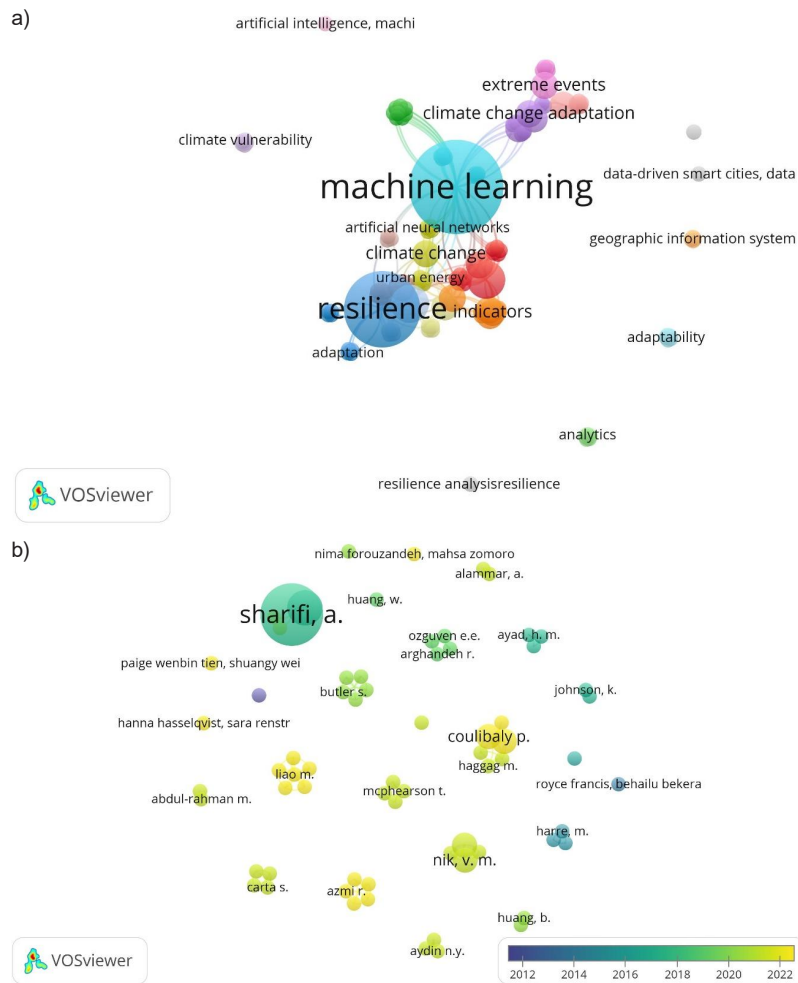


Fig. 2. Bibliometric analysis of: a — co-occurrence and b — authors of related studies

(2020) and O'Dwyer et al. (2020) discussed the impact of AI applications on energy combustion and management, while Perera et al. (2021) researched co-optimization of energy systems in cities. As for building environments, Alammar et al. (2021), Forouzandeh et al. (2022), and Tien et al. (2022) outlined AI applications' contribution to energy efficiency.

Some limited related research also focused on the integration of AI applications and energy systems for the benefit of UER. Thus, this study bridges this gap by creating an integrative framework that can improve UER with ML methods in an acceptable and affordable manner.

Climate Change, SDGs, and Dimensions of Urban Resilience

The resilience and stability of ecological systems is a concept proposed by Holling (1973), who described it as the "ability of a system to absorb changes

of state variables, driving variables, and parameters" (Saikia et al., 2022; Satterthwaite et al., 2020; Woolf et al., 2016). Since sustainability addresses the requirement for a long-term equilibrium among all systems, Ragheb et al. (2017) clarified that resilience as a concept is essential for comprehending the notion of sustainability. Resilience can also be considered a new way of thinking that can help people adjust to vulnerabilities, unprecedented changes, and unforeseen circumstances. Additionally, this concept is closely related to sustainability, an overarching idea that aims to preserve desirable human-environment interactions across time on a social, economic, and environmental level. In this context, resilience has become a central target of the UN's SDGs. For example, a resolution by the UN General Assembly described resilience as "the ability of a system, community or society exposed to hazards to resist, absorb, accommodate, adapt to,

Table 1. Related studies on UER and ML methods

Cluster	Concept	Aims	Main insights	Ref.
Resilience	Resilience and infrastructure systems	To provide a framework for resilience analysis and a metric for measuring resilience.	Proposal for an analysis framework, including: system identification, resilience objective setting, vulnerability analysis, and stakeholder engagement.	(Francis and Bekera, 2014)
	Climate resilience	To identify the research objectives and gaps that must be filled when planning support systems and addressing climate resilience.	A research agenda that integrates the full range of variables and supports choosing appropriate planning responses across multiple infrastructure systems.	(Krishnan et al., 2021)
	Social resilience	To identify, categorize, and evaluate key social resilience indicators, according to the stages of the disaster cycle.	A novel general framework for studying social resilience within communities in different disaster phases.	(Khalili et al., 2015)
	Community resilience	To analyze the similarities and differences between the various assessment tools.	A six-criteria analytical framework for measuring the effectiveness of resilience assessments.	(Sharifi, 2016)
		To analyze and improve resilient communities by optimizing sustainable design principles and using quantitative methods.	Proximity pattern observations in urban typologies, along with density and preliminary correlations.	(Carta et al., 2021)
	Resilience in slums	To examine the need for applying a universal technique to evaluate resilience-related programs in slums.	A framework tool, which was tested in a pilot project for the Kenya Slum Upgrading Program in Kibera, Nairobi.	(Woolf et al., 2016)
	Urban resilience	To carry out a comprehensive analysis of urban resilience studies.	A case study-backed conclusion that urban resilience is a multidisciplinary framework for examining the transformative capabilities of urban systems.	(Olazabal et al., 2012)
		To present a set of standards for creating an index that measures urban resilience.	A list of several major resilience principles, providing decision-makers with resilience-related information.	(Sharifi and Yamagata, 2014a)
		To present a theoretical framework for evaluating and studying the resilience of the urban form.	A framework proposal with emphasis on urban dynamics over time and space.	(Sharifi and Yamagata, 2018)
		To analyze and synthesize theoretical and empirical data on how a city's physical layout affects its resilience.	A conclusion that the urban form has significant impact on cities' resilience and sustainability, as well as on their social, ecological, and economic functions.	(Sharifi, 2019)

Table 1 (continued)

Cluster	Concept	Aims	Main insights	Ref.
Resilience	UER	To review the literature related to energy resilience to develop a conceptual framework for assessing UER.	An integrated framework that provides urban energy systems with the capacity for planning and preparing for, absorbing, recovering from, and adapting to adverse events.	(Sharifi and Yamagata, 2016a)
		To analyze how urban energy systems can remain energy-efficient, low-carbon, and resilient in a changing climate. To consider how climate change impacts both energy supply and energy demand in cities.	An analysis that identifies some common beneficial strategies for urban energy systems: Distributed energy resources Passive and efficient energy systems in buildings Partnerships across governments, businesses, and communities	(Ohshita and Johnson, 2017)
		To bridge the gap in UER by reviewing the concept of urban resilience and related principles.	An UER matrix that addresses energy shortages in cities.	(Ragheb et al., 2017)
		To review the steps taken to adapt urban energy systems to climate change, with a focus on climate resilience.	A methodology for evaluating the effects of climate change, particularly extreme conditions, on the operation of energy systems.	(Nik et al., 2021)
	Energy resilience	To offer a comprehensive outlook on resilience, taking households as a research starting point.	A definition of household energy resilience based on the availability of electricity. A framework for exploring household energy resilience.	(Hasselqvist et al., 2022)
AI applications and ML methods	ML and urban lifeline system resilience	To present a methodology for measuring system resilience.	A methodology capable of categorizing system resilience and offering guidelines for allocating resources and preventing economic loss.	(Huang and Ling, 2019)
	ML and infrastructure co-resilience	To present an advanced causal inference approach with ML integration to describe the multi-domain vulnerability of urban infrastructure systems.	A multi-network technique proposal for vulnerability assessments that can better predict disaster consequences and evaluate overall system resilience.	(Konila Sriram et al., 2019)
	Big spatial data and urban sustainability	To analyze four case studies using deep learning (DL) to identify and assess urban quality of life, as well as classify urban land use.	A set of integrated methods that combine advantages of both traditional data and big spatial data.	(Huang and Wang, 2020)
	ML, urban form, and energy consumption in cities	To discuss the multidimensional effects of urban form on the amount of energy consumed while operating community buildings.	The study found that adding the spatial dimension can improve the energy performance of community microgrids.	(Rahimian et al., 2020)
AI applications and ML methods	Digital twins and energy management tools	To present an energy management solution that can control, schedule, and make forecasts under user-defined objectives.	A single adaptable tool for integrating and improving energy systems, which includes a combination of predictive, modeling, and control features.	(O'Dwyer et al., 2020)
	Big data and community resilience	To review a selection of 12 global community resilience assessment tools.	The researchers found that none of the assessment tools selected use big data.	(Abdul-Rahman et al., 2021)
	ML and the impact of incident solar radiation on a building's envelope	To outline two ML models that can be used to estimate the impact of solar radiation intensity.	Input data with a substantial impact on model selection and prediction accuracy.	(Alammar et al., 2021)
	DL and climate-induced disasters	To develop a DL model for making spatial-temporal disaster predictions.	A food disaster prediction model with a 96% accuracy rate.	(Haggag et al., 2021)

Table 1 (end)

Cluster	Concept	Aims	Main insights	Ref.
AI applications and ML methods	ML applications in urban planning	To present a comprehensive review of ML applications that can be used for mitigating urban planning challenges.	A list of urban form modeling challenges posed by ML methods, as well as future research directions.	(Tekouabou et al., 2021)
	Data-based scenarios and vulnerability in cities	To examine the climate risks of local land use through numerical models.	Co-produced scenarios that can improve the ecosystem services offered to residents.	(Ortiz et al., 2021)
	Climate resilience and co-optimization of energy systems	To present a novel methodology that will optimize urban energy systems as interconnected infrastructures affected by urban morphology.	The study found that an optimized urban morphology can reduce the cost of energy infrastructure by up to 30%.	(Perera et al., 2021)
	Data-based smart eco-cities	To develop an integrated, case study-based model of strategic sustainable urban development.	A model that incorporates the top worldwide paradigms of urbanism, eco-cities, and data-based smart cities.	(Bibri, 2021b)
	Data-based methods of increasing energy efficiency	To examine the feasibility of seven ML algorithms for forecasting annual energy usage and thermal comfort.	A framework for predicting thermal comfort and energy demand compliance at the initial design stage.	(Forouzandeh et al., 2022)
	ML and DL methods in climate change mitigation and adaptation	To examine the most widely used ML and DL techniques in climate change adaptation and mitigation.	The study found that artificial neural networks (ANN) are the most widely used ML technology when it comes to both mitigating and adapting to climate change.	(Ladi et al., 2022)
	ML and DL methods of improving energy efficiency	To review the existing literature on the ML and DL methods used in construction environments over the last 10 years.	The study found that ML and DL have been successfully applied in assessing the energy efficiency of buildings.	(Tien et al., 2022)
	ML and structural resilience	To propose ML methods for evaluating the resilience of buildings in a mountainous area.	Optimization models with random forest generation and support vector features, and a 97.4% accuracy level.	(Zhang et al., 2022)

transform and recover from the effects of a hazard in a timely and efficient manner, including through the preservation and restoration of its essential basic structures and functions through risk management” (Attia et al., 2022; Satterthwaite, 2013).

In light of global trends, such as climate change, urbanization, and globalization, energy demand is increasing, which, in turn, drives the continued use of fossil fuels, with their destructive environmental effects (Forootan et al., 2022). Additionally, the reliability and resilience of energy systems, along with different aspects of the energy flow, from generation to demand, are influenced by the climate. Urban resilience is associated with these three global mega-trends, given that an ability to quickly recover from extreme and unexpected disruptions is what helps cities survive (Holling, 1973; Sharifi and Yamagata, 2014b; Zekry et al., 2020). Hence, urban resilience is one of the most essential topics within SDG discourse, because it addresses such issues as risk reduction and disaster prevention (Huang and

Ling, 2019). For instance, SDG 3 focuses on health and well-being; SDG 9, on industry, innovation, and infrastructure; SDG 11, on sustainable cities and communities; and SDG 13, on climate action. In this context, a resilient system is defined as one capable of retaining its usual functions, structure, identity, and feedback after undergoing change, absorbing disturbance, and reorganizing behavior (Li, 2020; Sharifi and Yamagata, 2018).

Resilience has also been described as a “multidimensional” phenomenon (Erker et al., 2017), which needs to be clarified in order to provide decision-makers with a comprehensive framework for understanding this concept better. To facilitate this, the London School of Economics and Political Science listed four key factors that measure urban resilience: physical, environmental, social, and economic. Moreover, UN-Habitat presented a framework for evaluating urban resilience across five dimensions: spatial, organizational, physical, functional, and temporal (Zekry et al., 2020). Sharifi

(2016, 2019) and Sharifi and Yamagata (2014a) also proposed five criteria that can be used to develop an urban resilience assessment index, including materials and environmental resources, society and well-being, economy, the built environment and infrastructure, and governance and institutions. In this context, the present study starts by defining urban resilience across multiple dimensions: the environmental dimension, the social and well-being dimension, the economic dimension, the organizational dimension, the physical dimension, and the functional dimension (see Fig. 3). We then show ties between these dimensions and specific SDGs that relate to such features of urban resilience as robustness, stability, and creativity (Bibri et al., 2020; Gharai et al., 2018; Satterthwaite and Dodman, 2013; Sharifi, 2016, 2019; Sharifi and Yamagata, 2014a, 2015).

Urban Energy System Resilience

Urban energy systems are responsible for meeting the energy demand in cities and urban areas by employing promising energy strategies.

The Fifth Assessment Report (AR5) of the UN Intergovernmental Panel on Climate Change has defined an energy system as “all components related to the production, conversion, delivery, and use of energy” (Tien et al., 2022), while the International Energy Agency has defined energy system resilience as “the capacity of the energy system and its components to cope with a hazardous event or trend, to respond in ways that maintain its essential functions, identity and structure as well as its capacity for adaptation, learning, and transformation” (Jasiūnas et al., 2021; Molyneaux et al., 2016; To et al., 2021). Additionally, a resilient energy system can rapidly recover from vulnerabilities or disruptions, while continuing to provide affordable energy services (Erker et al., 2017; Jasiūnas et al., 2021; Sharifi, 2016). The aforementioned disruptions include: weather-related incidents, technical failures, and cyberattacks (Farhoumandi et al., 2021; Jasiūnas et al., 2021; Ohshita and Johnson, 2017).

In this context, Tien et al. (2022) indicated that energy systems are becoming the backbone of



Fig. 3. Multiple dimensions of urban resilience and their ties to the UN's SDGs. Source: The authors' insights, based on reviewing (Bibri et al., 2020; Gharai et al., 2018; Ragheb et al., 2017; Satterthwaite and Dodman, 2013; Sharifi, 2016, 2019; Sharifi and Yamagata, 2014a, 2015, 2016b, 2018)

urban infrastructures (despite the many challenges) and their resilience includes four dimensions that address vulnerabilities: climate, resources, infrastructure, and community. Regarding the climate dimension, climate change brings about various physical phenomena. Meanwhile, energy, food, and water are the main resources of cities, and the urban populations are highly vulnerable when they lack such resources. Moreover, infrastructure is a vital need for cities to meet in order to function as centers of habitation, production, and consumption.

Ohshita and Johnson (2017) discussed three initiatives for improving UER. The first initiative includes energy efficiency and renewable energy, while the second initiative focuses on reducing greenhouse gas (GHG) emissions (e.g., low-carbon development and climate change mitigation). The third initiative includes climate resilience or adaptation plans. In other words, the first initiative can directly promote the second and third initiatives. Consequently, this initiative can impact the acceptability, affordability, availability, and accessibility of sustainability-related dimensions via various pathways and subpathways (see Fig. 4). In addition, it mainly covers energy security, including the energy demand, supply, storage, monitoring, and management system subpathways (see Table 2).

AI Technology and Applications

The Third Industrial Revolution significantly impacted the digital age, as production was mechanized, and information, and subsequently technology, became more widely used. Subsequently, 21st-century advancements brought along the Fourth Industrial Revolution, and the focus has shifted to big data and AI applications (Abo El-Einen et al., 2015; Arfanuzzaman, 2021; Megahed, 2017; Megahed et al., 2022). As a multidisciplinary phenomenon,

AI can be used for forecasting power demand and generation, optimizing the maintenance and use of energy assets, gaining a better understanding of energy usage patterns, and making systems more stable and efficient (Elzeni et al., 2021; Hassan et al., 2022; Williams, 1983). AI can also lighten the load on humans by partially automating decision-making, scheduling, and controlling multiple devices (Ahmad et al., 2022; Antonopoulos et al., 2020; Chan et al., 2020; Chan and Zhang, 2019; Megahed, 2015).

Overall, AI applications facilitate real-time monitoring and control, peer-to-peer energy transmission, smart contracts, and cyber protection of energy assets. These aspects can result in expedient supply, better demand management, and energy storage services that are reliable, resilient, flexible, and sustainable. AI applications can also perform highly complex tasks using knowledge- and data-based models (see Fig. 5). Knowledge-based methods include causal models (fault trees) that use human knowledge to support decision-making and pattern classification. This requires predictive modeling of production, consumption, and demand (Dey et al., 2020; Mosavi et al., 2019). Data-based methods, in turn, include principal component analysis of related data and general knowledge of certain systems (Alzghoul et al., 2014; Dey et al., 2020; Mosavi et al., 2019). Data-based methods can be expanded further in several ways, e.g., to ML and deep learning (DL), which offer practical modeling algorithms and techniques (Forootan et al., 2022).

Machine Learning (ML)

ML is based on three technology trends: the rapid advancement of sensors and IoT, which provide a large amount of data (Cantelmi et al., 2022; Huang et al., 2022); ML-oriented chips, such as graphic processing units and tensor processing

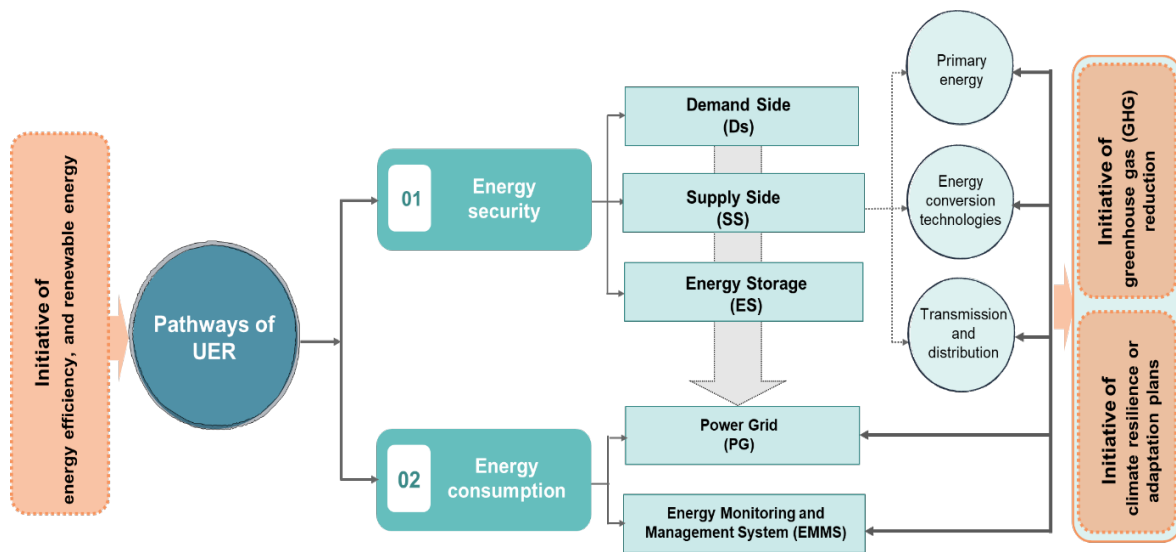


Fig. 4. Urban energy system initiatives and their ties to UER pathways and subpathways. Source: The authors' insights, based on reviewing (Hasselqvist et al., 2022; Sharifi, 2016, 2019; Sharifi and Yamagata, 2014a, 2016b, 2018)

Table 2. UER pathways, subpathways, and descriptions. Source: The authors’ insights, based on reviewing (Allegrini et al., 2015; Badawy et al., 2022; Bibri and Krogstie, 2020b; Chelleri and Olazabal, 2012; Cai et al., 2021; Elgheznavy et al., 2022; Elmokadem et al., 2016a; Hassan et al., 2022; Ismail et al., 2022a; Jasiūnas et al., 2021; Liu et al., 2021; Megahed and Ghoneim, 2021; Noaman et al., 2022; Paraschos et al., 2022; Sugahara and Belmont, 2016)

UER Pathways	UER Subpathways	Description	
Energy security	Demand side	Includes the aspects of efficiency, flexibility, and resilience at a relatively low cost for the overall energy system, which requires dealing with increased complexity and less well-established structures.	
	Supply side	Primary energy	Fossil fuels and renewable energy sources face the issues of security and import dependency.
		Energy conversion technologies	Secure against extreme weather and technical failures.
		Transmission and distribution	Renewable sources have been powering other energy sectors, especially in recent years.
Energy storage	Inherent balance versus supply and demand disruptions. Energy resilience is ensured by inbuilt storage capacity at various points.		
Energy consumption	Power grid	Requires smart meters and communication technologies within electricity networks, supported by hardware, software, and network tools that allow generators to route power to consumers more efficiently.	
	Energy monitoring and management systems	Such systems let the owners use smart technology for remotely regulating, controlling, and monitoring a building’s mechanical and electrical subsystems, such as heating, ventilation, air conditioning, lighting, power, and security.	

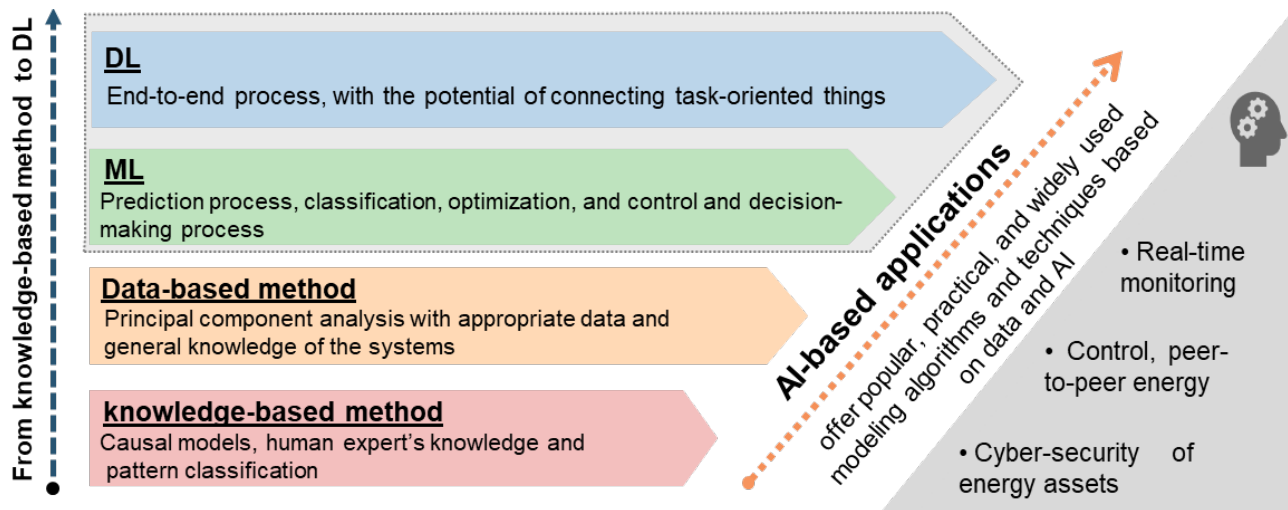


Fig. 5. Evolution of AI and energy system models. Source: The authors’ insights, based on reviewing (Alzghoul et al., 2014; Bibri, 2021a; Bibri and Krogstie, 2019; Dey et al., 2020; Forootan et al., 2022; Mosavi et al., 2019; Seneviratne et al., 2022; Thomas et al., 2021; Wang et al., 2022)

units, which offer better access to powerful and affordable computational resources; and advanced ML algorithms (S. Bibri, 2021b; O’Dwyer et al., 2020; Nashaat, Elmokadem and Waseef, 2022). ML also allows for image-data-based (RGB) numeric labeling, collecting and clustering useful information, and semantic segmentation from large, complex datasets (Alammar et al., 2021). Additionally, accumulating large volumes of data can support comparisons via data deductions and distance calculations (Bibri, 2019; Seneviratne et al., 2022).

Typical ML and UER Workflow

The typical ML workflow includes a process that starts by generating data and then trains and deploys the model (El-Mowafy et al., 2022). Specifically, the first phase includes acquiring input data with parameters that impact or correlate with the output data. ML models can be classified into three main types: supervised, unsupervised, and reinforcement learning. In the context of energy systems, ML can help identify nonlinear correlations within energy systems, such as the relationship

between cooling demand and related variables (e.g., outdoor temperature and occupancy activities), by using mapping functions from a dataset (Tien et al., 2022).

The first learning type, supervised learning, allows for developing algorithms that use fully labeled datasets to classify and regress problems. Regression algorithms can be deployed for determining continuous values or quantities. Classification algorithms, in turn, help predict discrete or distinct values, e.g., when the result needs to be a category. Regression models can also be used in energy demand forecasting to comprehend the variables that influence energy usage, such as building morphology, material, and orientation (Liang, 2020).

In unsupervised learning, the algorithm, once developed, interprets unlabeled data by independently extracting patterns and characteristics, without specific guidance on what to do with its findings. Unsupervised learning techniques are frequently used for various tasks, including dimensionality reduction, association, and clustering. The most common task carried out with unsupervised learning techniques is clustering, which can reveal the structure in an unlabeled dataset (Gull et al., 2021; Wang and Biljecki, 2022).

Finally, reinforcement learning allows algorithms to react to an environment independently. Such methods, via their agents, can maximize the numerical reward signal through trial and error, which makes it possible to learn how to map situations to actions. As the last phase of deploying the model, reinforcement learning methods can also provide optimal strategies for decreasing building energy demand based on real-time data (Tien et al., 2022).

In the context of ML and UER, existing historical input data (collected via energy meters, wireless networks, and sensors, as well as by using the Internet of Things-based techniques that allow energy monitoring solutions to generate vast amounts of data) are highly accurate and relatively easy to deploy. The output parameters, in turn, predict energy demand, energy planning, management, and conservation. They can be used in strategies for reducing energy consumption and CO₂ emissions.

Based on the above, this study uses the Sankey diagram to visualize the relationship flows between pathways that represent UER and their associated ML categories, including: regression, classification, clustering, and models with examples of proposed processes (see Fig. 6). The regression process is based on evaluating the relationship between a dependent variable and independent variables. Regression analysis is one of the most fundamental methods for prediction in the field of ML. In our case, regression includes hourly global solar radiation, system power output, irradiance levels (based on

photovoltaic electrical characteristics), reduction in wind power, photovoltaic power generation, and reduction in wind power. The classification process can categorize a given set of data, either structured or unstructured. The process starts with predicting and labeling the classes of the given data points. Classification can include building energy consumption, renewable energy loads in microgrids, and electricity loads (Alammar et al., 2021; Hosseini and Parvania, 2021). Clustering refers to an algorithm's capacity to generate probable values for each unknown variable in each new data record, allowing the model builder to identify the probable value. For instance, in one case study, a geothermal pump helped provide a district with heat, while simultaneously improving fuel economy and optimizing a railway electric power system (Chan and Zhang, 2019; Wu et al., 2022). Such ML models include multilayer perception (MLP), extreme learning machines, advanced artificial neural networks (ANNs), support vector machines (SVMs), decision trees, and hybrid models such as wavelet neural networks (WNNs) and adaptive neuro-fuzzy inference systems.

ML-Based Integrative Framework for UER

Certain factors, for instance, weather conditions and power generation that uses solar photovoltaic energy or wind turbines, make achieving UER more challenging. Since peak energy demand does not coincide with peak energy production, compensating for this mismatch necessitates the use of auxiliary technologies, such as energy storage. In order to bridge the gap between the different aspects of the UER concept, it is important to create an integrative framework based on UER's four capabilities: preparation, observation, adaptation, and recovery (Francis and Bekera, 2014; Sharifi and Yamagata, 2016a).

This process starts with measuring resilience before, during, and after a disruption, which is associated with UER capabilities and objectives, as well as ML. The framework proposed in this study consists of the following three phases (see Fig. 7):

1. Addressing resilience capabilities: This phase deals with the main components of UER before, during, and after a disruption. This entails predicting and preparing for a disruption by adopting a wide range of design and planning strategies to minimize the potential adverse impacts on energy acceptability, affordability, accessibility, and availability. Here, resilience refers to a system's ability to absorb the impact of a disruption in advance and afterwards. In turn, adaptation is the ability to flexibly adjust during and after a disruption. Finally, recovery refers to processes that occur during and after a disruption and help restore the energy system's capacity and reliability to a normal operational level.

2. Identifying UER priorities: At this phase, UER priorities are identified during and after a disruption.

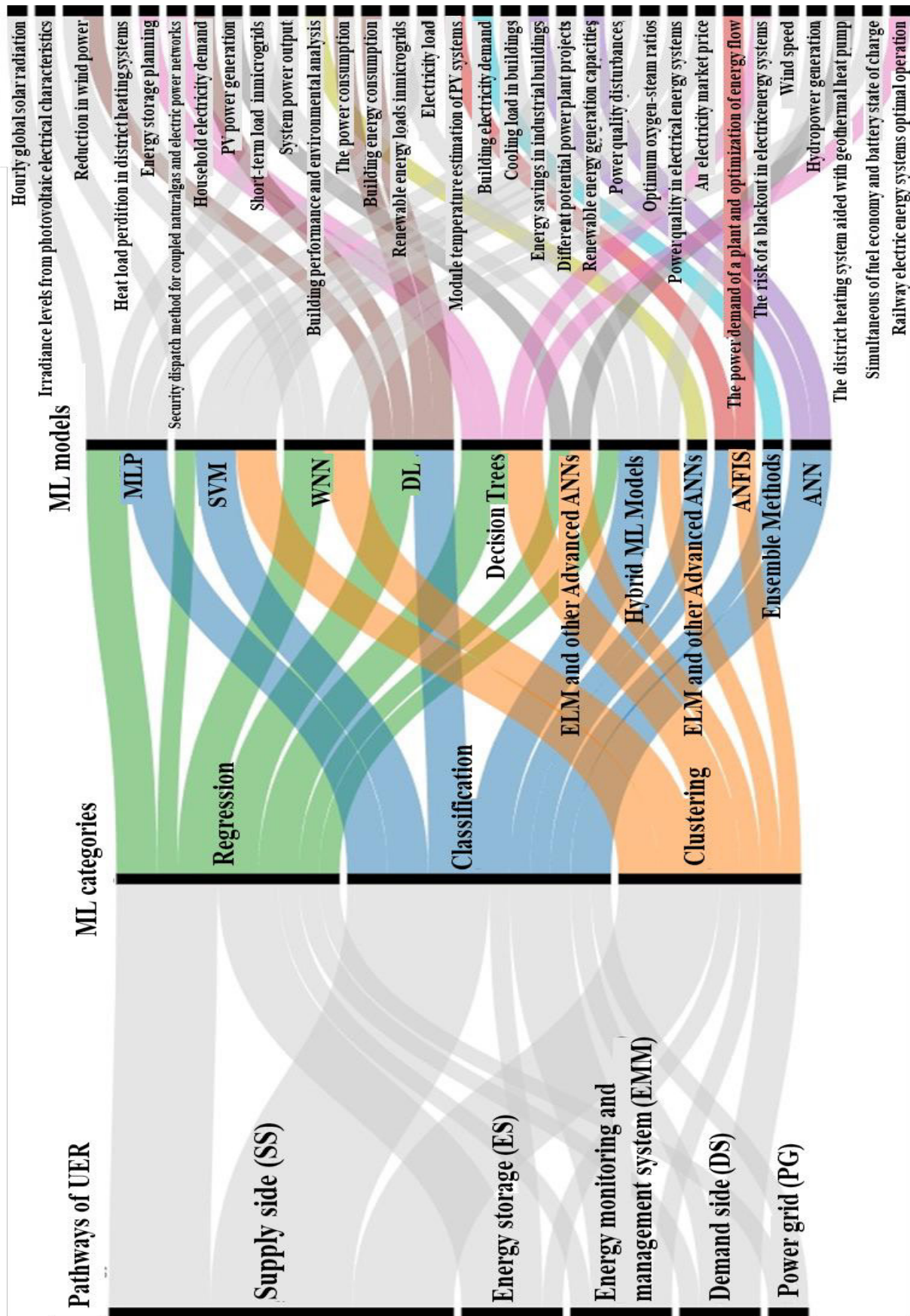


Fig. 6. A Sankey diagram of pathways, representing UER, their associated ML categories, and models with examples. Source: The authors' insights, based on reviewing (Alammar et al., 2021; Bibri and Krogstie, 2020a; Chan and Zhang, 2019; Guvenir et al., 1997; Hasselqvist et al., 2022; Setiadi et al., 2022; Wu et al., 2022)

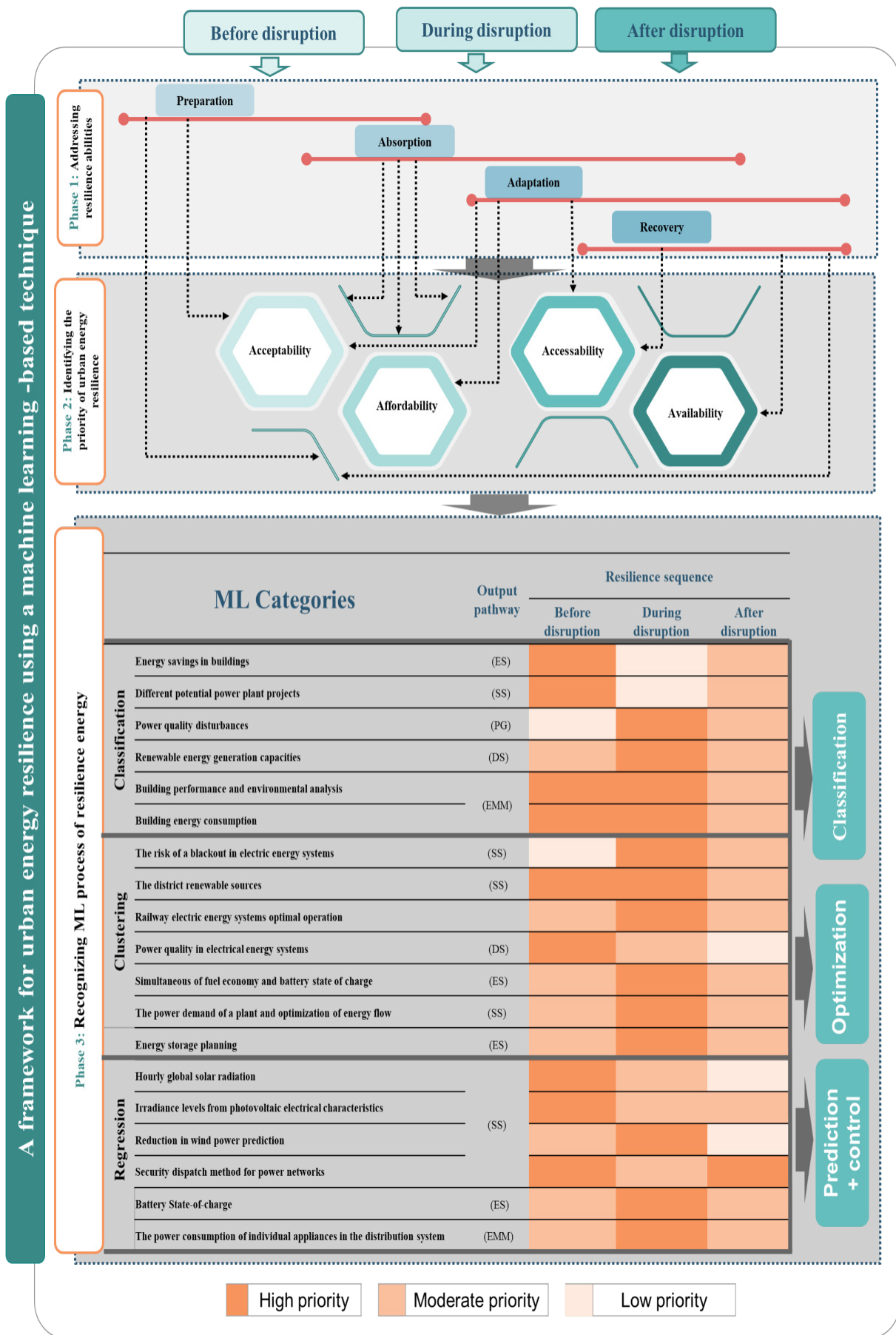


Fig. 7. The ML-based integrative framework for UER

The key capabilities here are preparation, or the process of achieving energy accessibility and affordability, and absorption, which is associated with acceptability, in addition to both accessibility and affordability.

3. Recognizing the ML aspect of energy resilience: At this phase, one identifies how ML can improve UER through three key categories, i.e., regression, classification, and clustering. This involves four main processes: classification, prediction, control, and optimization. This phase is also when one constructs a relationship matrix of the ML categories, the resilience sequences, and their relationships to energy security, including supply- and demand-side management, energy storage, and energy consumption. For instance, ML algorithms, such as SVMs, ANNs, and MLP, can classify potential power plant projects or power quality disturbances that improve energy storage, supply-side management, and power grids, using sensors in a wireless network. These networks first collect data from various sources within a system and then analyze their findings to facilitate real-time preparation, absorption, recovery decision-making, and information transmission, which are high priorities before and during a disruption, and moderate priorities after a disruption. In addition, optimization processes that use ML algorithms, such as MLP, ANNs, and WNNs, predict hourly global solar radiation and irradiance levels based on photovoltaic electrical characteristics, forecast reduction in wind power, assess the risk of blackouts in electric power systems via regression, and operate in clustering categories.

Therefore, the framework proposed in this study can serve as a reference for integrating ML and AI applications in order to improve UER in the three aforementioned phases. Both UER pathways and subpathways can also assist with supply- and demand-side management, power grids, energy storage, and energy monitoring. This framework can ensure that climate risks are considered as part of utility rate cases for investments in new/upgraded infrastructure. It can also provide backup power during emergencies at all critical facilities identified. Moreover, through UER, it is possible to overcome the challenges of global climate change by reducing the demand for fossil fuels, while responding to the increasing need for an expanded sustainable energy supply. Since all of the above aligns with several of the UN's SDGs, future researchers can build on the framework proposed in this study and expand AI and ML applications to optimize UER in general and further support the UN's objectives in particular.

Conclusion

In this study, we created an integrative framework to bridge the gap in previous research on the

potential use of AI and ML applications for sustaining UER systems, even during service disruptions. For this purpose, we carried out a bibliometric analysis and a systematic UER overview in accordance with AI concepts, models, and applications. Since the UER concept has been highlighted among the approaches to addressing the impact of climate change, we examined its significance in this field, as well as its alignment with the UN's SDGs.

In this context, our framework proposal included three phases. The first phase addresses key elements of UER through a series of actions before, during, and after a disruption. The second phase determines the varying importance of UER in achieving accessibility and affordability. The third phase explores how ML can improve UER through three key categories, regression, classification, and clustering, in order to support four main processes: classification, prediction, control, and optimization. This step further includes a relationship matrix between the ML processes, the resilience sequences, and their connections to energy, which are identified via priority variations.

The results of our study show that this integrative framework effectively addresses UER's main capabilities, identifies its priorities, and recognizes how ML can benefit UER as a whole. The framework developed in this study also offers insights in integrating ML methods into UER as strategically as possible, especially in the context of climate change and urban energy systems. Moreover, we found that UER efforts follow the pathways of energy management, encompassing energy security and consumption. Such pathways can ensure an energy system's preparation, absorption, adaptation, and recovery under disruption conditions.

Finally, we hope that the proposed framework can serve as an initial step for researchers and decision-makers focusing on UER in the context of climate change. However, more research is necessary to verify the effectiveness of this framework when aiming to expand AI and ML applications in order to optimize UER.

Data and Material Availability

The data that support the findings of this study can be provided by the corresponding author upon request.

Funding

This study did not receive any specific grant from funding agencies in the public, commercial, or non-profit sectors.

Acknowledgments

The authors intend to thank the editors and reviewers for their efforts at a later point.

Conflict of Interest

The authors declare that there is no conflict of interest.

References

- Abdul-Rahman, M., Chan, E. H. W., Wong, M. S., and Xu, P. (2021). Big Data for community resilience assessment: A critical review of selected global tools. In: Ye, G., Yuan, H., and Zuo, J. (eds.). *Proceedings of the 24th International Symposium on Advancement of Construction Management and Real Estate. CRIOCM 2019*. Singapore: Springer, pp. 1345–1361. DOI: 10.1007/978-981-15-8892-1_94.
- Abo El-Einen, O. M., Ahmed, M. M., Megahed, N. A., and Hassan, A. M. (2015). Interactive-based approach for designing facades in digital era. *Port-Said Engineering Research Journal*, Vol. 19, Issue 1, pp. 72–81.
- Ahmad, T., Madonski, R., Zhang, D., Huang, C., and Mujeeb, A. (2022). Data-driven probabilistic machine learning in sustainable smart energy/smart energy systems: Key developments, challenges, and future research opportunities in the context of smart grid paradigm. *Renewable and Sustainable Energy Reviews*, Vol. 160, 112128. DOI: 10.1016/j.rser.2022.112128.
- Alammar, A., Jabi, W., and Lannon, S. (2021). Predicting Incident solar radiation on building's envelope using machine learning. In: *SimAUD 2021*, April 15–17, 2021, virtually hosted.
- Allegrini, J., Orehounig, K., Mavromatidis, G., Ruesch, F., Dorer, V., and Evins, R. (2015). A review of modelling approaches and tools for the simulation of district-scale energy systems. *Renewable and Sustainable Energy Reviews*, Vol. 52, pp. 1391–1404. DOI: 10.1016/j.rser.2015.07.123.
- Alzghoul, A., Backe, B., Löfstrand, M., Byström, A., and Liljedahl, B. (2014). Comparing a knowledge-based and a data-driven method in querying data streams for system fault detection: A hydraulic drive system application. *Computers in Industry*, Vol. 65, Issue 8, pp. 1126–1135. DOI: 10.1016/j.compind.2014.06.003.
- Antonopoulos, I., Robu, V., Couraud, B., Kirli, D., Norbu, S., Kiprakis, A., Flynn, D., Elizondo-Gonzalez, S., and Wattam, S. (2020). Artificial intelligence and machine learning approaches to energy demand-side response: A systematic review. *Renewable and Sustainable Energy Reviews*, Vol. 130, 109899. DOI: 10.1016/j.rser.2020.109899.
- Arfanuzzaman, M. (2021). Harnessing artificial intelligence and big data for SDGs and prosperous urban future in South Asia. *Environmental and Sustainability Indicators*, Vol. 11, 100127. DOI: 10.1016/j.indic.2021.100127.
- Attia, S., Holzer, P., Homaei, S., Kazanci, O. B., Zhang, C., and Heiselberg, P. (2022). Resilient cooling in buildings – A review of definitions and evaluation methodologies. In: *CLIMA 2022 Conference*, May 22–25, Rotterdam, the Netherlands. DOI: 10.34641/clima.2022.195.
- Badawy, N. M., El Samaty, H. S., and Waseef, A. A. E. (2022). Relevance of monocrystalline and thin-film technologies in implementing efficient grid-connected photovoltaic systems in historic buildings in Port Fouad city, Egypt. *Alexandria Engineering Journal*, Vol. 61, Issue 12, pp. 12229–12246. DOI: 10.1016/j.aej.2022.06.007.
- Bibri, S. (2019) 'Generating a Vision for Smart Sustainable City of the Future: A Scholarly Backcasting Approach', *European Journal of Futures Research*. doi: 10.1186/s40309-019-0157-0.
- Bibri, S. E. (2021a). A novel model for data-driven smart sustainable cities of the future: the institutional transformations required for balancing and advancing the three goals of sustainability. *Energy Informatics*, Vol. 4, No. 1, pp. 1–37. DOI: 10.1186/s42162-021-00138-8.
- Bibri, S. E. (2021b). Data-driven smart eco-cities of the future: an empirically informed integrated model for strategic sustainable urban development. *World Futures*, pp. 1–44. DOI: 10.1080/02604027.2021.1969877.
- Bibri, S. E. and Krogstie, J. (2019). Generating a vision for smart sustainable city of the future: a scholarly backcasting approach. *European Journal of Futures Research*, Vol. 7, Issue 1, pp. 1–20. DOI: 10.1186/s40309-019-0157-0.
- Bibri, S. E. and Krogstie, J. (2020a). Smart eco-city strategies and solutions for sustainability: the cases of Royal Seaport, Stockholm, and Western Harbor, Malmö, Sweden. *Urban Science*, Vol. 4, Issue 1, 11. DOI: 10.3390/urbansci4010011.
- Bibri, S. E. and Krogstie, J. (2020b). The emerging data-driven Smart City and its innovative applied solutions for sustainability: the cases of London and Barcelona. *Energy Informatics*, Vol. 3, 5. doi: 10.1186/s42162-020-00108-6.
- Bibri, S. E., Krogstie, J., and Kärrholm, M. (2020). Compact city planning and development: Emerging practices and strategies for achieving the goals of sustainability. *Developments in the Built Environment*, Vol. 4, 100021. DOI: 10.1016/j.dibe.2020.100021.
- Bosisio, A., Moncecchi, M., Morotti, A., and Merlo, M. (2021). Machine learning and GIS approach for electrical load assessment to increase distribution networks resilience. *Energies*, Vol. 14, Issue 14, 4133. DOI: 10.3390/en14144133.
- Cai, C., Guo, Z., Zhang, B., Wang, X., Li, B., and Tang, P. (2021). Urban morphological feature extraction and multi-dimensional similarity analysis based on deep learning approaches. *Sustainability*, Vol. 13, Issue 12, 6859. DOI: 10.3390/su13126859.
- Cantelmi, R., Steen, R., Di Gravio, G., and Patriarca, R. (2022). Resilience in emergency management: Learning from COVID-19 in oil and gas platforms. *International Journal of Disaster Risk Reduction*, Vol. 76, 103026. DOI: 10.1016/j.ijdrr.2022.103026.

- Carta, S., Pintacuda, L., Owen, I. W., and Turchi, T. (2021). Resilient communities: a novel workflow. *Frontiers in Built Environment*, Vol. 7, 767779. DOI: 10.3389/fbuil.2021.767779.
- Chan, M. F., Witztum, A., and Valdes, G. (2020). Integration of AI and machine learning in radiotherapy QA. *Frontiers in Artificial Intelligence*, Vol. 3, 577620. DOI: 10.3389/frai.2020.577620.
- Chan, J. and Zhang, Y. (2019) *Urban resilience in the smart city*. In: *The 12th Conference of the International Forum on Urbanism: Beyond Resilience*, June 24–26, 2019, Jakarta, Indonesia.
- Chelleri, L. and Olazabal, M. (eds.) (2012). *Multidisciplinary perspectives on urban resilience*. Bilbao: Basque Centre for Climate Change, 78 p.
- Dey, M., Rana, S.P., and Dudley, S. (2020). A case study based approach for remote fault detection using multi-level machine learning in a smart building. *Smart Cities*, Vol. 3, Issue 2, pp. 401–419. DOI: 10.3390/smartcities3020021.
- Du, Z., Palem, K., Lingamneni, A., Temam, O., Chen, Y., and Wu, C. (2014). Leveraging the error resilience of machine-learning applications for designing highly energy efficient accelerators. In: *2014 19th Asia and South Pacific Design Automation Conference (ASP-DAC)*, January 20–23, 2014, Singapore. DOI: 10.1109/ASPAC.2014.6742890.
- Elgheznavy, D., El Enein, O. A., Shalaby, G., Seif, A. (2022). An experimental study of indoor air quality enhancement using breathing walls. *Civil Engineering and Architecture*, Vol. 10, No. 1, pp. 194–209. DOI: 10.13189/cea.2022.100117.
- Elmokadem, A. A., Megahed, N. A., and Noaman, D. S. (2016a). Systematic framework for the efficient integration of wind technologies into buildings. *Frontiers of Architectural Research*, Vol. 5, Issue 1, pp. 1–14. DOI: 10.1016/j.foar.2015.12.004.
- EL-Mokadem, A. A., Megahed, N. A., and Noaman, D. S. (2016b). Towards a Computer Program for building-integrated wind technologies. *Energy and Buildings*, Vol. 117, pp. 230–244. DOI: 10.1016/j.enbuild.2016.02.022.
- El-Mowafy, B. N., Elmokadem, A. A., and Waseef, A. A. (2022). Evaluating adaptive facade performance in early building design stage: an integrated daylighting simulation and machine learning. In: Hassanien, A. E., Rizk, R. Y., Snášel, V., and Abdel-Kader, R. F. (eds.). *The 8th International Conference on Advanced Machine Learning and Technologies and Applications (AMLTA2022)*. AMLTA 2022. *Lecture Notes on Data Engineering and Communications Technologies*, Vol. 113. Cham: Springer, pp. 211–223. DOI: 10.1007/978-3-031-03918-8_20.
- Elzeni, M. M., Elmokadem, A. A., and Badawy, N. M. (2021). Genetic algorithms application in urban morphology generation. *Port-Said Engineering Research Journal*, Vol. 26, No. 1, pp. 21–34. DOI: 10.21608/pserj.2021.87367.1129.
- Elzeni, M. M., Elmokadem, A. A., and Badawy, N. M. (2022). Impact of urban morphology on pedestrians: A review of urban approaches. *Cities*, Vol. 129, 103840. DOI: 10.1016/j.cities.2022.103840.
- Erker, S., Stangl, R., and Stoeglehner, G. (2017). Resilience in the light of energy crises – Part I: A framework to conceptualise regional energy resilience. *Journal of Cleaner Production*, Vol. 164, pp. 420–433. DOI: 10.1016/j.jclepro.2017.06.163.
- Eslamlou, M. S., Tabibian, M., and Mirmoghtadaee, M. (2022). Developing a conceptual framework of urban resilience for its application in urban literature, through thematic analysis of texts. *Quarterly Journal of Iranian Islamic City Studies*, Vol. 12, Issue 45, pp. 71–84.
- Farhoumandi, M., Zhou, Q., and Shahidehpour, M. (2021). A review of machine learning applications in IoT-integrated modern power systems. *The Electricity Journal*, Vol. 34, Issue 1, 106879. DOI: 10.1016/j.tej.2020.106879.
- Forootan, M. M., Larki, I., Zahedi, R., and Ahmadi, A. (2022). Machine learning and deep learning in energy systems: a review. *Sustainability*, Vol. 14, Issue 8, 4832. DOI: 10.3390/su14084832.
- Forouzandeh, N., Zomorodian, Z. S., Shaghaghian, Z., and Tahsildoost, M. (2022). Room energy demand and thermal comfort predictions in early stages of design based on the Machine Learning methods. *Intelligent Buildings International*. DOI: 10.1080/17508975.2022.2049190.
- Francis, R. and Bekera, B. (2014). A metric and frameworks for resilience analysis of engineered and infrastructure systems. *Reliability Engineering & System Safety*, Vol. 121, pp. 90–103. DOI: 10.1016/j.ress.2013.07.004.
- Gharai, F., Masnavi, M., and Hajibandeh, M. (2018). Urban local-spatial resilience: developing the key indicators and measures, a brief review of literature. *The Monthly Scientific Journal of Bagh-e Nazar*, Vol. 14, Issue 57, pp. 19–32.
- Gull, C. Q., Aguilar, J., and R-Moreno, M. D. (2021). A semi-supervised learning approach to study the energy consumption in smart buildings. In: *2021 IEEE Symposium Series on Computational Intelligence (SSCI)*, December 5–7, 2021, Orlando, FL, USA. DOI: 10.1109/SSCI50451.2021.9659911.
- Gültekin, Y. (2021). Strategies to improve urban energy efficiency for urban resilience. *IOP Conference Series: Materials Science and Engineering*, Vol. 1203, 022020. DOI: 10.1088/1757-899X/1203/2/022020.
- Güvenir, H. A., Acar, B., Demiroz, G., and Cekin, A. (1997). A supervised machine learning algorithm for arrhythmia analysis. In: *Computers in Cardiology 1997*. Lund: IEEE, pp. 433–436. DOI: 10.1109/CIC.1997.647926.

- Haggag, M., Siam, A. S., El-Dakhakhni, W., Coulibaly, P., and Hassini, E. (2021). A deep learning model for predicting climate-induced disasters. *Natural Hazards*, Vol. 107, Issue 1, pp. 1009–1034. DOI: 10.1007/s11069-021-04620-0.
- Hassan, A. M., El Mokadem, A. A. F., Megahed, N. A., and Abo Eleinen, O. M. (2020a). Improving outdoor air quality based on building morphology: Numerical investigation. *Frontiers of Architectural Research*, Vol. 9, Issue 2, pp. 319–334. DOI: 10.1016/j.foar.2020.01.001.
- Hassan, A. M., ElMokadem, A. A., Megahed, N. A., and Abo Eleinen, O. M. (2020b). Urban morphology as a passive strategy in promoting outdoor air quality. *Journal of Building Engineering*, Vol. 29, 101204. DOI: 10.1016/j.job.2020.101204.
- Hassan, S. R., Megahed, N. A., Abo Eleinen, O. M., and Hassan, A. M. (2022). Toward a national life cycle assessment tool: Generative design for early decision support. *Energy and Buildings*, Vol. 267, 112144. DOI: 10.1016/j.enbuild.2022.112144.
- Hasselqvist, H., Renström, S., Strömberg, H., and Håkansson, M. (2022). Household energy resilience: Shifting perspectives to reveal opportunities for renewable energy futures in affluent contexts. *Energy Research & Social Science*, Vol. 88, 102498. DOI: 10.1016/j.erss.2022.102498.
- Holling, C. S. (1973). Resilience and stability of ecological systems. *Annual Review of Ecology and Systematics*, Vol. 4, pp. 1–23. DOI: 10.1146/annurev.es.04.110173.000245.
- Hosseini, M. M. and Parvania, M. (2021). Artificial intelligence for resilience enhancement of power distribution systems. *The Electricity Journal*, Vol. 34, Issue 1, 106880. DOI: 10.1016/j.tej.2020.106880.
- Huang, Y., Huang, L., and Zhu, Q. (2022). Reinforcement Learning for feedback-enabled cyber resilience. *Annual Reviews in Control*, Vol. 53, pp. 273–295. DOI: 10.1016/j.arcontrol.2022.01.001.
- Huang, W. and Ling, M. (2019). Machine learning-based method for urban lifeline system resilience assessment in GIS*. In: Rocha, J. and Abrantes, P. (eds.). *Geographic Information Systems and Science. Chapter 3*. London: IntechOpen. DOI: 10.5772/intechopen.82748.
- Huang, B. and Wang, J. (2020). Big spatial data for urban and environmental sustainability. *Geo-spatial Information Science*, Vol. 23, Issue 2, pp. 125–140. DOI: 10.1080/10095020.2020.1754138.
- Hunter, M. (2021). Resilience, fragility, and robustness: cities and COVID-19. *Urban Governance*, Vol. 1, Issue 2, pp. 115–125. DOI: 10.1016/j.ugj.2021.11.004.
- Ismail, R. M., Megahed, N. A., and Eltarabily, S. (2022a). Numerical investigation of the indoor thermal behaviour based on PCMs in a hot climate. *Architectural Science Review*, Vol. 65, Issue 3, pp. 196–216. DOI: 10.1080/00038628.2022.2058459.
- Ismail, R. M., Megahed, N. A., and Eltarabily, S. (2022b). The strategy of using PCMs in building sector applications. *Port-Said Engineering Research Journal*, Vol. 26, No. 3, pp. 1–12. DOI: 10.21608/pserj.2022.135558.1185.
- Jasiūnas, J., Lund, P. D., and Mikkola, J. (2021). Energy system resilience – a review. *Renewable and Sustainable Energy Reviews*, Vol. 150, 111476. DOI: 10.1016/j.rser.2021.111476.
- Kapucu, N., Ge, Y., Martín, Y., and Williamson, Z. (2021). Urban resilience for building a sustainable and safe environment. *Urban Governance*, Vol. 1, Issue 1, pp. 10–16. DOI: 10.1016/j.ugj.2021.09.001.
- Khalili, S., Harre, M., and Morley, P. (2015). A temporal framework of social resilience indicators of communities to flood, case studies: Wagga wagga and Kempsey, NSW, Australia. *International Journal of Disaster Risk Reduction*, Vol. 13, pp. 248–254. DOI: 10.1016/j.ijdr.2015.06.009.
- Konila Sriram, L. M., Ulak, M. B., Ozguven, E. E., and Arghandeh, R. (2019). Multi-network vulnerability causal model for infrastructure co-resilience. *IEEE Access*, Vol. 7, pp. 35344–35358. DOI: 10.1109/ACCESS.2019.2904457.
- Krishnan, S., Aydin, N. Y., and Comes, T. (2021). Planning support systems for long-term climate resilience: a critical review. In: Geertman, S. C. M., Pettit, C., Goodspeed, R., and Staffans, A. (eds.). *Urban Informatics and Future Cities. The Urban Book Series*. Cham: Springer, pp. 465–498. DOI: 10.1007/978-3-030-76059-5_24.
- Kumar, K. and Saini, R. P. (2021). Application of artificial intelligence for the optimization of hydropower energy generation. *EAI Endorsed Transactions on Industrial Networks and Intelligent Systems*, Vol. 8, Issue 28, e1. doi: 10.4108/eai.6-8-2021.170560.
- Ladi, T., Jabalameli, S., and Sharifi, A. (2022). Applications of machine learning and deep learning methods for climate change mitigation and adaptation. *Environment and Planning B: Urban Analytics and City Science*, Vol. 49, Issue 4, pp. 1314–1330. DOI: 10.1177/23998083221085281.
- Li, Q. (2020). Resilience thinking as a system approach to promote China's sustainability transitions. *Sustainability*, Vol. 12, Issue 12, 5008. DOI: 10.3390/su12125008.
- Liang, X. (2020). Supervised and unsupervised learning models. In: Liang, X. (ed.). *Social Computing with Artificial*

Intelligence. Singapore: Springer, pp. 27–82. DOI: 10.1007/978-981-15-7760-4_4.

Liu, J., Jian, L., Wang, W., Qiu, Z., Zhang, J., and Dastbaz, P. (2021). The role of energy storage systems in resilience enhancement of health care centers with critical loads. *Journal of Energy Storage*, Vol. 33, 102086. DOI: 10.1016/j.est.2020.102086.

Masnavi, M. R., Gharai, F., and Hajibandeh, M. (2018). Exploring urban resilience thinking for its application in urban planning: a review of literature. *International Journal of Environmental Science and Technology*, Vol. 16, Issue 1, pp. 567–582. DOI: 10.1007/s13762-018-1860-2.

Megahed, N. A. (2015). Towards a theoretical framework for HBIM approach in historic preservation and management. *Archnet-IJAR: International Journal of Architectural Research*, Vol. 9, Issue 3, pp. 130–147. DOI: 10.26687/archnet-ijar.v9i3.737.

Megahed, N. A. (2017). An exploration of the control strategies for responsive umbrella-like structures. *Indoor and Built Environment*, Vol. 27, Issue 1, pp. 7–18. DOI: 10.1177/1420326X16669750.

Megahed, N. A., Abdel-Kader, R. F., and Soliman, H. Y. (2022). Post-pandemic education strategy: framework for artificial intelligence-empowered education in engineering (AIEd-Eng) for lifelong learning. In: Hassaniien, A. E., Rizk, R. Y., Snášel, V., and Abdel-Kader, R. F. (eds.). *The 8th International Conference on Advanced Machine Learning and Technologies and Applications (AMLT2022)*. AMLTA 2022. *Lecture Notes on Data Engineering and Communications Technologies*, Vol. 113. Cham: Springer, pp. 544–556. DOI: 10.1007/978-3-031-03918-8_45.

Megahed, N. A. and Ghoneim, E. M. (2021). Indoor air quality: rethinking rules of building design strategies in post-pandemic architecture. *Environmental Research*, Vol. 193, 110471. DOI: 10.1016/j.envres.2020.110471.

Molyneaux, L., Brown, C., Wagner, L., and Foster, J. (2016). Measuring resilience in energy systems: Insights from a range of disciplines. *Renewable and Sustainable Energy Reviews*, Vol. 59, pp. 1068–1079. DOI: 10.1016/j.rser.2016.01.063.

Mosavi, A., Salimi, M., Faizollahzadeh Ardabili, S., Rabczuk, T., Shamshirband, S., and Varkonyi-Koczy, A. R. (2019). State of the art of machine learning models in energy systems, a systematic review. *Energies*, Vol. 12, Issue 7, 1301. DOI: 10.3390/en12071301.

Nashaat, B., Elmokadem, A. and Waseef, A. (2022) 'Evaluating Adaptive Facade Performance in Early Building Design Stage: An Integrated Daylighting Simulation and Machine Learning', in, pp. 211–223. doi: 10.1007/978-3-031-03918-8_20.

Nik, V. M., Perera, A. T. D. and Chen, D. (2021). Towards climate resilient urban energy systems: A review. *National Science Review*, Vol. 8, Issue 3, nwaa134. DOI: 10.1093/nsr/nwaa134.

Noaman, D. S., Moneer, S. A., Megahed, N. A., and El-Ghafour, S. A. (2022). Integration of active solar cooling technology into passively designed facade in hot climates. *Journal of Building Engineering*, Vol. 56, 104658. DOI: 10.1016/j.jobe.2022.104658.

O'Dwyer, E., Pan, I., Charlesworth, C., Butler, S., and Shah, N. (2020). Integration of an energy management tool and digital twin for coordination and control of multi-vector smart energy systems. *Sustainable Cities and Society*, Vol. 62, 102412. DOI: 10.1016/j.scs.2020.102412.

Ohshita, S. and Johnson, K. (2017). Resilient urban energy: making city systems energy efficient, low carbon, and resilient in a changing climate. *ECEEE Summer Study Proceedings*, pp. 719–728. [online] Available at: https://www.eceee.org/library/conference_proceedings/eceee_Summer_Studies/2017/3-local-action/resilient-urban-energy-making-city-systems-energy-efficient-low-carbon-and-resilient-in-a-changing-climate.

Olazabal, M., Chelleri, L., Waters, J. J., and Kunath, A. (2012). Urban resilience: towards an integrated approach. In: *1st International Conference on Urban Sustainability & Resilience*, November 5–6, 2012, London, UK.

Ortiz, L., Mustafa, A., Rosenzweig, B., Carrero, R., and McPhearson, T. (2021). Correction to: Modeling urban futures: Data-driven scenarios of climate change and vulnerability in cities. In: Hamstead, Z. A., Iwaniec, D. M., McPhearson, T., Berbés-Blázquez, M., Cook, E. M., and Muñoz-Erickson, T. A. (eds.). *Resilient Urban Futures. The Urban Book Series*. Cham: Springer, p. C1. DOI: 10.1007/978-3-030-63131-4_13.

Paraschos, P. D., Xanthopoulos, A. S., Koulinas, G. K., and Koulouriotis, D. E. (2022). Machine learning integrated design and operation management for resilient circular manufacturing systems. *Computers & Industrial Engineering*, Vol. 167, 107971. DOI: 10.1016/j.cie.2022.107971.

Perera, A. T. D., Javanroodi, K., and Nik, V. M. (2021). Climate resilient interconnected infrastructure: Co-optimization of energy systems and urban morphology. *Applied Energy*, Vol. 285, 116430. DOI: 10.1016/j.apenergy.2020.116430.

Ragheb, S. A., Ayad, H. M., and Galil, R. A. (2017). An energy-resilient city, an appraisal matrix for the built environment. *WIT Transactions on Ecology and the Environment*, Vol. 226, pp. 667–678. DOI: 10.2495/SDP170581.

Rahimian, M., Cervone, G., Duarte, J. P., and lulo, L. D. (2020). A machine learning approach for mining the

- multidimensional impact of urban form on community scale energy consumption in cities. In: Gero, J. S. (eds.). *Design Computing and Cognition'20*. Cham: Springer, pp. 607–624. DOI: 10.1007/978-3-030-90625-2_36.
- Saikia, P., Beane, G., Garriga, R. G., Avello, P., Ellis, L., Fisher, S., Leten, J., Ruiz-Apilánez, I., Shouler, M., Ward, M., and Jiménez, A. (2022). City Water Resilience Framework: A governance based planning tool to enhance urban water resilience. *Sustainable Cities and Society*, Vol. 77, 103497. DOI: 10.1016/j.scs.2021.103497.
- Satterthwaite, D. (2013). The political underpinnings of cities' accumulated resilience to climate change. *Environment and Urbanization*, Vol. 25, Issue 2, pp. 381–391. DOI: 10.1177/0956247813500902.
- Satterthwaite, D., Archer, D., Colenbrander, S., Dodman, D., Hardoy, J., Mitlin, D., and Patel, S. (2020). Building resilience to climate change in informal settlements. *One Earth*, Vol. 2, Issue 2, pp. 143–156. DOI: 10.1016/j.oneear.2020.02.002.
- Satterthwaite, D. and Dodman, D. (2013). Towards resilience and transformation for cities within a finite planet. *Environment and Urbanization*, Vol. 25, Issue 2, pp. 291–298. DOI: 10.1177/0956247813501421.
- Seneviratne, S., Nice, K. A., Wijnands, J. S., Stevenson, M., and Thompson, J. (2022). *Self-supervision, remote sensing and abstraction: representation learning across 3 million locations*. [online] Available at: <https://arxiv.org/pdf/2203.04445v1.pdf>. DOI: 10.48550/arXiv.2203.04445.
- Setiadi, H., Mithulanathan, N., Shah, R., Md. Islam, R., Fekih, A., Krismanto, A. U., and Abdillah, M. (2022). Multi-mode damping control approach for the optimal resilience of renewable-rich power systems. *Energies*, Vol. 15, Issue 9, 2972. DOI: 10.3390/en15092972.
- Sharifi, A. (2016). A critical review of selected tools for assessing community resilience. *Ecological Indicators*, Vol. 69, pp. 629–647. DOI: 10.1016/j.ecolind.2016.05.023.
- Sharifi, A. (2019). Resilient urban forms: A macro-scale analysis. *Cities*, Vol. 85, pp. 1–14. DOI: 10.1016/j.cities.2018.11.023.
- Sharifi, A. and Yamagata, Y. (2014a). Major principles and criteria for development of an urban resilience assessment index. In: *2014 International Conference and Utility Exhibition on Green Energy for Sustainable Development (ICUE)*, March 19–21, 2014, Pattaya, Thailand.
- Sharifi, A. and Yamagata, Y. (2014b). Resilient urban planning: major principles and criteria. *Energy Procedia*, Vol. 61, pp. 1491–1495. DOI: 10.1016/j.egypro.2014.12.154.
- Sharifi, A. and Yamagata, Y. (2015). A conceptual framework for assessment of urban energy resilience. *Energy Procedia*. Vol. 75, pp. 2904–2909. DOI: 10.1016/j.egypro.2015.07.586.
- Sharifi, A. and Yamagata, Y. (2016a). Principles and criteria for assessing urban energy resilience: A literature review. *Renewable and Sustainable Energy Reviews*, Vol. 60, pp. 1654–1677. DOI: 10.1016/j.rser.2016.03.028.
- Sharifi, A. and Yamagata, Y. (2016b). Urban resilience assessment: multiple dimensions, criteria, and indicators. In: Yamagata, Y. and Maruyama, H. (eds). *Urban Resilience. Advanced Sciences and Technologies for Security Applications*. Cham: Springer, pp. 259–276. DOI: 10.1007/978-3-319-39812-9_13.
- Sharifi, A. and Yamagata, Y. (2018). Resilient urban form: a conceptual framework. In: Yamagata, Y. and Sharifi, A. (eds.). *Resilience-Oriented Urban Planning. Lecture Notes in Energy*, Vol. 65. Cham: Springer, pp. 167–179. DOI: 10.1007/978-3-319-75798-8_9.
- Sugahara, M. and Bermont, L. (2016) *Energy and resilient cities. OECD Regional Development Working Papers 2016/5*. Paris: OECD Publishing, 94 p. DOI: 10.1787/5jlwj0rl3745-en.
- Tekouabou, S. C. K., Diop, E. B., Azmi, R., Jalignot, R., and Chenal, J. (2021). Reviewing the application of machine learning methods to model urban form indicators in planning decision support systems: Potential, issues and challenges. *Journal of King Saud University - Computer and Information Sciences*, Vol. 34, Issue 8, Part B, pp. 5943–5967. DOI: 10.1016/j.jksuci.2021.08.007.
- Thomas, E., Wilson, D., Kathuni, S., Libey, A., Chintalapati, A., and Coyle, J. (2021). A contribution to drought resilience in East Africa through groundwater pump monitoring informed by in-situ instrumentation, remote sensing and ensemble machine learning. *Science of The Total Environment*, Vol. 780, 146486. DOI: 10.1016/j.scitotenv.2021.146486.
- Tien, P. W., Wei, S., Darkwa, J., Wood, C., and Calautit, J. K. (2022). Machine learning and deep learning methods for enhancing building energy efficiency and indoor environmental quality – a review. *Energy and AI*, Vol. 10, 100198. DOI: 10.1016/j.egyai.2022.100198.
- To, L. S., Bruce, A., Munro, P., Santagata, E., MacGill, I., Rawali, M., and Raturi, A. (2021). A research and innovation agenda for energy resilience in Pacific Island Countries and Territories. *Nature Energy*, Vol. 6, pp. 1098–1103. DOI: 10.1038/s41560-021-00935-1.
- Tumini, I., Arriagada Sickinger, C., and Baeriswyl Rada, S. (2017). Model to integrate resilience and sustainability into urban planning. In: Mercader-Moyano, P. (ed.). *Sustainable Development and Renovation in Architecture, Urbanism*

and Engineering. Cham: Springer, pp. 39–49. DOI: 10.1007/978-3-319-51442-0_4.

Wang, J. and Biljecki, F. (2022). Unsupervised machine learning in urban studies: A systematic review of applications. *Cities*, Vol. 129, 103925. DOI: 10.1016/j.cities.2022.103925.

Wang, Y., Qiu, D., and Strbac, G. (2022). Multi-agent deep reinforcement learning for resilience-driven routing and scheduling of mobile energy storage systems. *Applied Energy*, Vol. 310, 118575. DOI: 10.1016/j.apenergy.2022.118575.

Williams, C. (1983). A brief introduction to artificial intelligence. In: *Proceedings OCEANS '83*, August 29, 1983 – September 1, 1983, San Francisco, CA, USA. DOI: 10.1109/OCEANS.1983.1152096.

Wolf, S., Twigg, J., Parikh, P., Karaoglou, A., and Cheaib, T. (2016). Towards measurable resilience: A novel framework tool for the assessment of resilience levels in slums. *International Journal of Disaster Risk Reduction*, Vol. 19, pp. 280–302. DOI: 10.1016/j.ijdrr.2016.08.003.

Wu, J., Lu, Y., Gao, H., and Wang, M. (2022). Cultivating historical heritage area vitality using urban morphology approach based on big data and machine learning. *Computers, Environment and Urban Systems*, Vol. 91, 101716. DOI: 10.1016/j.compenvurbsys.2021.101716.

Xie, J., Alvarez-Fernandez, I., and Sun, W. (2020). A review of machine learning applications in power system resilience. In: *2020 IEEE Power & Energy Society General Meeting (PESGM)*, August 2–6, 2020, Montreal, QC, Canada. DOI: 10.1109/PESGM41954.2020.9282137.

Zekry, M., Al-Hagla, K., and Saadallah, D. (2020) Urban governance as a tool for enhancing resilient urban form: case study Alexandria, Egypt. In: Schrenk, M., Popovich, V. V., Zeile, P., Elisei, P., Beyer, C., Ryser, J., Reicher, C., and Çelik, C. (eds.). *REAL CORP 2020. Shaping Urban Change – Livable City Regions for the 21st Century*, September 15–18, 2020, Aachen, Germany, pp. 939–948.

Zhang, C., Wei, H., Liao, M., Lin, Y., Wu, Y., and Zhang, H. (2022). Study on machine learning models for building resilience evaluation in mountainous area: a case study of Banan District, Chongqing, China. *Sensors*, Vol. 22, Issue 3, 1163. DOI: 10.3390/s22031163.

SMART MULTI-FUNCTIONAL MICRO-HUB FOR NEIGHBORHOODS: SUSTAINABLE MOBILITY AND ENVIRONMENTAL RESTORATION IN HIGH-DENSITY SOCIAL NEIGHBORHOODS

Carlos Rosa-Jiménez*, Carlos Prados-Gomez

Institute for Habitat, Territory and Digitalization. University of Malaga
Avda. Cervantes, 2, 29016, Málaga, Andalucía, Spain

*Corresponding author: cjrosa@uma.es

Abstract

Introduction: Outdoor parking lots have been a common and cost-effective solution for private mobility in European social housing districts built between the 1960s and 1980s, but this solution has significant, particularly environmental and spatial, impacts. The future of urban mobility requires changes to an electrified community model, based on shared vehicle fleets. **Purpose of the study:** We aimed to analyze the transport, social, and environmental improvements of a smart multi-functional micro-hub for neighborhoods — a theoretical proposal designed to facilitate the transition toward a decarbonized city. **Methods:** The literature is therefore reviewed and a case study of the city of Malaga is provided. **Results:** On the one hand, the findings show the environmental, economic, and spatial advantages of this model compared to traditional underground parking lots. On the other hand, the paper proposes the design characteristics that could be adopted by a particular type of buildings and their urban space. Finally, the paper discusses the implications of setting up a citywide network of micro-hubs and the ensuing benefits.

Keywords

automatic parking system, green parking, car sharing, public transport, active facades.

Introduction

Transport accounts for 50% of liquid fossil fuel consumption and for 25% of carbon dioxide (CO₂) emissions (International Energy Agency, 2017). The use of private cars as the main means of mobility in the urban environment causes serious economic (consumption of fuel and time spent looking for where to park in saturated spaces), environmental (noise and gas emissions), and spatial (related to undermining the public space and social relations) problems. The spatial impact of the extensive use of the private vehicle has led to the large surface area needed for parking, compared to low passenger occupancy rates. The ratio between the surface and the number of people transported is 6.7 m²/person, which is very high as vehicles are parked for an average of 20 to 22 hours a day and between 82–95% of their useful life (Barter, 2013). Outdoor parking lots have been a common and cost-effective solution for private mobility in many European social housing neighborhoods built between the 1960s and 1980s and consisting of high-rise residential blocks without garages. Replacing those outdoor parking lots with underground ones in large tree-less areas partially solved the issue with the lack

of parking. However, their building often required expensive construction work and only partially solved the spatial problem.

Research into sustainable and alternative urban transport plans is a priority in urban planning. However, public transport still cannot compete with private transport for many journeys (Graham-Rowe et al., 2011). According to Kane and Whitehead (2017), the future mobility disruption framework is based on a community mobility model using electrified, self-driving, shared vehicle fleets. Therefore, the incorporation of private-public interim systems based on the sharing economy driven by information and communication technologies (ICTs) is needed, particularly by means of developing car-sharing (Carlorosi et al., 2015; Kane and Whitehead, 2017; Shaheen and Cohen, 2013) and bike-sharing (Shaheen et al., 2010a) platforms. Furthermore, electrified vehicles can be charged while they are parked, unlike combustion vehicles that need to be taken to gas stations. This revolution in mobility offers new strategies to peripheral social neighborhoods with high population density and few parking lots, based on setting up a community car-sharing service for the local residents to

supplement the available public transport. Thus, a resident does not need to own a vehicle but can rather choose from a diversity of different means of transport and thus can avoid having to invest in purchasing a vehicle, its maintenance and parking.

The Smart Multi-functional Micro-hub for Neighborhoods (SMMN) is a theoretical proposal designed to facilitate the transition towards a decarbonized city. This model combines both public transport and sharing system. The literature has focused on the intermodality of large urban or regional public transport systems, but there is little research at neighborhood scale. There are also few contributions that analyze public design, environmental and spatial improvements. In this vein, authors such as Maienschein-Cline (2014) highlight the crisis in the design and concept of garages and seek to turn parking into a catalyst for innovative suburban development. New parking systems based on automatic parking lots, which also include community amenities and facilities and are able to generate energy and important environmental benefits in the neighborhoods, are therefore needed. The first section reviews the scientific literature in relation to the main characteristics of this model at the neighborhood level. In the second section the methodology and case study are presented. The third section proposes its theoretical implementation in a high-density social housing neighborhood in the city of Malaga (Spain). Finally, in the discussion, the architectural and urban results can therefore be assessed and the impact of this model can be analyzed, along with its social and environmental improvements.

Background

The SMMN is designed to replace the model of privately owned vehicles parked in outdoor parking lots by an as-a-service mobility model. Furthermore, it is specifically designed to increase resources, green areas, and neighborhood spaces. The public space will thus be recovered for social and environmental uses thanks to a significant drop in the number of vehicles and space required for their storage. There are precedents in the literature that address multi-functional hubs — architectural-engineering elements that combine multimodal mobility, public services, and parking zones in areas saturated by private transport (Carlorosi et al., 2015). Obsolete or underused major public transport infrastructures, such as train stations, are thus recovered. The Social Condenser concept of Soviet Constructivism, ecological theories, and the pedestrian Metropolis are incorporated, along with highly technological elements. However, this model is focused on large territorial and urban mobility infrastructures. There is a gap in the application of those concepts at the urban microscale

of neighborhoods and spatial results of their implementation. Similarly to multi-functional hubs (Carlorosi et al., 2015), the main characteristics of the SMMN are as follows:

- (a) multimodal mobility hub that leads to a reduction in private traffic,
- (b) environmental improvements with an increase in green areas,
- (c) recovery of the public space,
- (d) social hub and sustainable architectural design.

Multimodal mobility hub and reduction in private traffic

Multimodal hubs offer a minimum of two different means of transport. Their impact on reducing the use of cars depends on the size of the city area and the density of the existing public transport (Verbavatz and Barthelemy, 2019). According to Shaheen and Cohen (2020), the multimodal integration occurs at the meeting points of the mobility on demand (MOD) — consisting of sharing mobility services and public transport — with mobility as a service (MaaS). Alarcos and Ginés (2017) defined mobility stations as physical hubs of integrated multimodal mobility services managed using ICTs. Efthymiou et al. (2019) differentiated between seven categories of shared mobility, of which we focus on three: car sharing, bike sharing, and scooter sharing. The latter two are also known as shared micromobility. The use of shared mobility means an average vehicle reduction of around 50% (Martin et al., 2010), which leads to a drop in urban travel costs (Belk, 2014) and in private and public parking spaces (Shaheen et al., 2010b).

Car-sharing companies offer the residents of neighborhoods mobility without the need to own a vehicle. Car sharing — the model of hiring cars for short time periods and distances — stands out among the emerging transport systems driven by the development of ICTs (Tyrinopoulos and Antoniou, 2020). One-way car sharing or station-based car sharing is the most appropriate model for the residents of a neighborhood for their daily journeys, as the user will tend to use the vehicles for those trips and return to the same SMMN. Shared micromobility uses the same bicycle, scooter and other low-speed transport model (Shaheen and Chan, 2015), even though the use of shared electric scooters (e-scooters) is more desirable, as many of the journeys undertaken by the residents in a neighborhood are in the immediate vicinity (Bachand-Marleau et al., 2012; Fishman et al., 2015).

In the literature, we can find two types of neighborhood mobility hubs: those that come from an evolution of public garages and those organized by the residents themselves. In the first case, special mention should be made of *Mobiway* as a new concept of parking lot building that provides

advanced services and the user with a multimodal selection system. It was developed in 2009 by Vinci Park in the business district of La Défense in Paris and had three characteristics (Bates and Leibling, 2012): (a) access to the greatest possible offer of transport in the district: private cars, public transport, car-pooling, taxis, motorbike taxis, bicycles, and hire vehicles; (b) a centralized system with specific information on all the mobility solutions available in the neighborhood; and (c) carefully designed parking waiting areas, integration with public spaces, and providing amenities such as news kiosks, car washes, baggage lockers, toilets, drinks dispensers, and umbrella hire. The model was implemented in one of the main financial districts and a wealthy residential area in Paris. There are no examples of its replicability in other types of middle-class neighborhoods.

In the second case, organized by the residents themselves, the Domagkpark residential complex with 1600 dwellings in Munich stands out. This is a sustainable mobility pilot project that is part of a residential complex. It has managed to reduce the vehicles/dwelling ratio to a rate of under 0.5 by means of shared electric vehicles with the possibility of their use being managed online (Alarcos and Ginés, 2017). However, the development of these multimodal platforms requires external factors (Efthymiou et al., 2019) offered by the neighborhoods for car sharing to be a success (see Fig. 1). Furthermore, the status of place has to be taken into account in the urban and architectural design of transport interchanges.

Hernandez and Monzón (2016) made a distinction between at least three areas: commercial and amenities area, transport and transfer area — where the users deliver and receive the means of transport — and access area. The latter, with a greater urban ramification, must take into account the signage for the users (pedestrians, cyclists, and vehicles) and establish four access routes: vehicles, motorbikes, bicycles, scooters; the safe pedestrian area route; and the SMMN connection with public transport.

Environmental improvements of the Automatic Parking System (APS)

Incorporating APSs in SMMNs provides important environmental advantages. APSs are an alternative to conventional garages and traditional multi-level ramp parking, which occupy large spaces (Idris et al., 2009). APSs have a diversity of definitions and options (Wu et al., 2019), including automatic/robotic parking systems on several stories, which are an ideal solution for commercial and residential settings due to their four advantages — space efficiency, design flexibility, security, and sustainability — compared to traditional parking (Batra, 2014). APSs are high-density parking solutions that allow secondary vehicle access spaces, such as car ramps and lanes, to be eliminated; along with user access, such as space between cars, stairs, walkways, elevators for users, in addition to reducing the clear height. It is estimated that the building volume can be reduced by up to 50% compared to the same number of cars being parked in a multi-story conventional

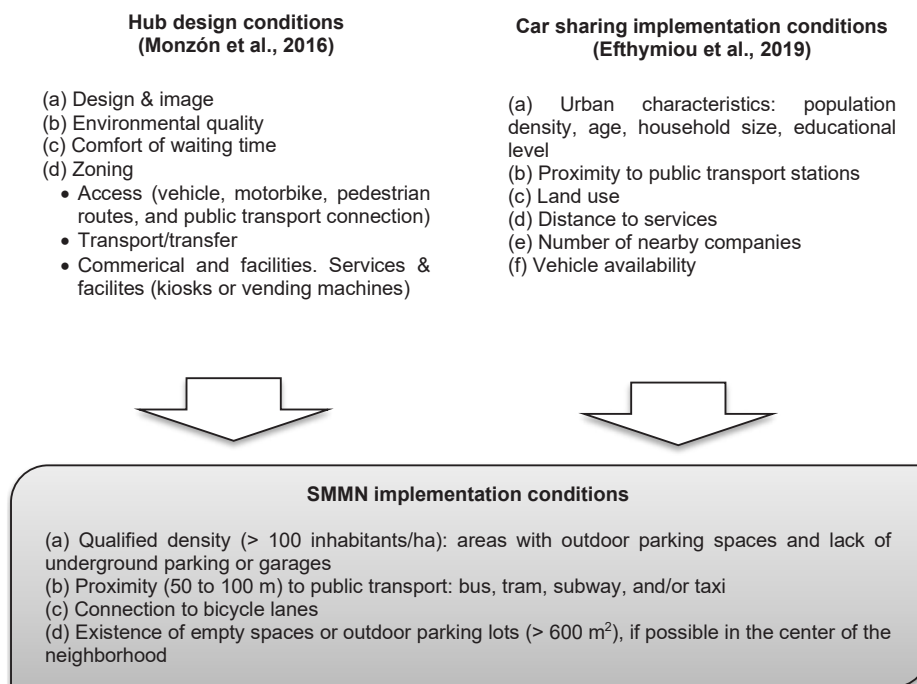


Fig. 1. SMMN implementation characteristics based on the design conditions of transport hubs and car sharing location. Source: authors

garage (Batra, 2014; Frankel, 1998; Robotic Parking System, 2020b). The design flexibility is achieved thanks to its modularity, and a 20-story-structure with an incorporated computerized system can be obtained. The greater safety and security is due to no access for users, and injuries, theft, or car damage can be avoided (Frankel, 1998).

Finally, in terms of an environmental approach, the green parking concept has been developed thanks to the smaller area occupied by the APS, which leads to a progressive gain in green areas due to the smaller need for parking space (Robotic Parking System, 2020b). This encourages the greening of compact areas of the city (Robotic Parking System, 2020a). CO₂ emissions can be reduced by over 80% due to the shorter time spent on construction and search for parking spaces (Batra, 2014). All these improvements are added to the reduction in traffic congestion and environmental pollution offered by an integrated transport system (Dacko and Spalteholz, 2014). There are also economic advantages due to the lower construction and maintenance costs (Robotic Parking System, 2020b). The construction cost is estimated to be 30% lower than that of a conventional underground parking lot (Frankel, 1998), or 55% if we take into account the maintenance and staff costs, particularly in large parking lots (900 spots) (Robotic Parking System, 2020b).

Recovery of the public space

The important space recovery by APSs increases opportunities for better urban design and increased walkability (Kane and Whitehead, 2017). The SMMN fosters the transit-oriented development (TOD) model (Loo and du Verle, 2017), as it reduces the neighborhood carbon footprint as well as improves quality and pedestrian/public transport. Neighborhood pedestrianization is a process that began with the traffic calming techniques developed in Dutch residential districts in the 1970s (Gehl, 1987) and which currently converge in the slow metropolis concept where the public space design is prioritized to encourage pedestrian mobility (Mezoued et al., 2021). As regards the size of the pedestrian residential areas, authors such as Rueda (2011, 2012, 2016) proposed the superblock as the optimum size for pedestrianization. It is roughly 400 x 400 metres in size and involves traffic calming measures to encourage walking and cycling, while the motorized transport is on the perimeter roads. Based on these dimensions, the location of the SMMN in a central position allows for 200–250 m ranges of journey, which would make equipping it with social amenities feasible, in a similar way to Clarence Perry's neighborhood unit (Perry, 1929), where its size is likewise restricted by pedestrian accessibility to local stores and amenities such as a school (Barcellos de Souza, 2006).

Social hubs and architectural renewal

In the literature, some authors advocate a necessary overhaul of the design and programming of uses of transport hubs and garages. The latter are traditionally side-lined in architectural culture (Kay, 2001), even with important values as elements of contemporary architecture (Henley, 2007). In this vein, APSs allow for a renewal of the design by adopting iconic photos of towers (Batra, 2014), either large ones such as the Car Towers (Wolfsburg, Germany, 20 stories and 400 vehicles), and the Emirates Financial Towers (Dubai, 9 stories and 1191 vehicles); or small ones of the Smart Car Towers project (Europe), transparent towers with a surface area of 100 m² (7 to 11 stories and a total of up to 43 vehicles). Furthermore, ARUP (2019) advocates for a new station concept adapted to the needs of the users and neighborhoods, with coworking facilities and even recreational activities. One such example is a mixed-used garage at Cincinnati University. In addition to parking spaces, it provides storage and meeting facilities for university departments (Seeley, 2008).

Methodology and case study

The methodology is structured into two phases. The first reviewed the literature on mobility hubs, green parking lots, APSs and shared mobility systems, with special emphasis on the neighborhood scale. We complemented the published literature with an online-based review. That allowed us to define a theoretical SMMN model. The second phase proposed the city of Malaga as a case study. According to Johansson (2003), the case study is fundamental in research fields with a practical component, such as architecture and urban planning.

Malaga is a coastal city in southern Spain with a population of around 569,000 inhabitants. Its metropolitan area includes 13 municipalities and a population of nearly 1 million inhabitants. The city is administratively organized into 11 districts and 297 neighborhoods. Its Sustainable Urban Mobility Plan (Ayuntamiento de Málaga, 2011) structures the city into large reduced mobility sectors demarcated by primary routes. Primary routes are the main arterial roads, which connect the main sectors. The study area is in the west of the city, within No. 27 reduced mobility sector (Fig. 2). It has an area of 19.3 hectares (193,280 m²) and is demarcated by the Avenida de Andalucía (north) and Avenida de las Américas (east) primary routes and the Calle Conde de Guadalhore (east) and Calle Gerona (south) secondary routes. An area that is approximately the side of a 400 x 400 m superblock (Rueda, 2011, 2012, 2016) would facilitate its pedestrianization potential.

As of 2021, the sector had a population of 6094 inhabitants (IECA, 2022), which makes it an urban



Fig. 2. Study area chosen from the sector structure established by the Malaga Mobility Plan. Source: Ayuntamiento de Málaga (2011)

area with a high average population density of 315.29 inhabitants/ha. The main age bracket in its age structure is between 16–64 years old (59.94%), followed by the over 65 (28.8%) and then the under 16 (11.26%). Fig. 3 shows the land use structure. The sector has two types of building: high-rise blocks (7–15 stories) with the plinth made up of offices on the first, second, and third floors, located in the north sector and built between 1975 and 1982; and 6-story residential blocks, with mainly neighborhood retail activity on the first floor, located in the east sector and built around 1967. It also has a district of single-family dwellings in the south sector. The amenities

are limited to a school and a social services centre, with a rather low occupancy rate (2114 m², 1.1%). Green areas make up a very small surface area, with only 4832 m² (2.50%). Meanwhile, the surface area used for roadways is 33,700 m² (17.44%) and has a total of 1001 private surface parking spaces in outdoor parking lots and spaces alongside the road. That number is approximately the same as the number of dwellings without private garages (1096 dwellings).

The central outdoor parking lot is large and easily reached, as it is off Avenida de la Aurora and has good connections with public transport (buses), a



Fig. 3. Land use structure of the study sector with parking areas highlighted. Source: authors

bike lane, and pedestrian ways (Fig. 4). An SMMN located in this central area would mean that the outdoor parking lots could be eliminated and the central hub of the proposed superblock could be fitted out with amenities for its pedestrianization. Subsequently, the other outdoor car parking lots would be replaced by new SMMNs or by enlarging the existing one.

SMMN proposal

The creation of an SMMN environmentally restores an urban space that has been highly degraded by vehicle occupancy (Fig. 5) and provides a sustainable mobility solution for the neighboring housing. The three outdoor car parking lots provide a total of 236 public parking spaces, while the adjoining buildings have 919 private parking spaces in underground garages, which means a real current allocation of 1155 spaces. The parking needs according to the regulations are 1486 private spaces. The removal of the 236 spaces would mean that 567 parking spaces would be required. Those spaces could be provided by building a public parking lot or by opting for constructing an SMMN.

The three outdoor parking lots have a total of 4795 m² of tarmac and impermeable ground surface. The traditional option of building an underground parking lot with 567 spaces would require a three-story building with 190 parking spaces per level. For a ratio of 25 m²/parking space, it is estimated that the building could have a built surface of 14,250 m² and a ground occupancy of 4750 m², i.e., the whole of the ground occupied by the outdoor parking lots. The SMMN option allows for a large area to be released by converting the outdoor parking lots into three green areas (Fig. 6) with a total of 3660 m² (2100 m² + 840 m² + 720 m²), which accounts for 76.33%, in addition to the building roof with a surface area of 915 m², which would be used for allotments and relaxation areas.

The SMMN incorporates three distinct parts (Fig. 7): (a) the shared mobility module with a ground occupancy of 915 m², where the electric car-sharing storage is on the four upper levels and the first floor is used for the shared micromobility; (b) the facilities and amenities module of the neighborhood consisting of an 8-story tower with a ground occupancy of 220 m² metres; and (c) the first floor, which is a specially-

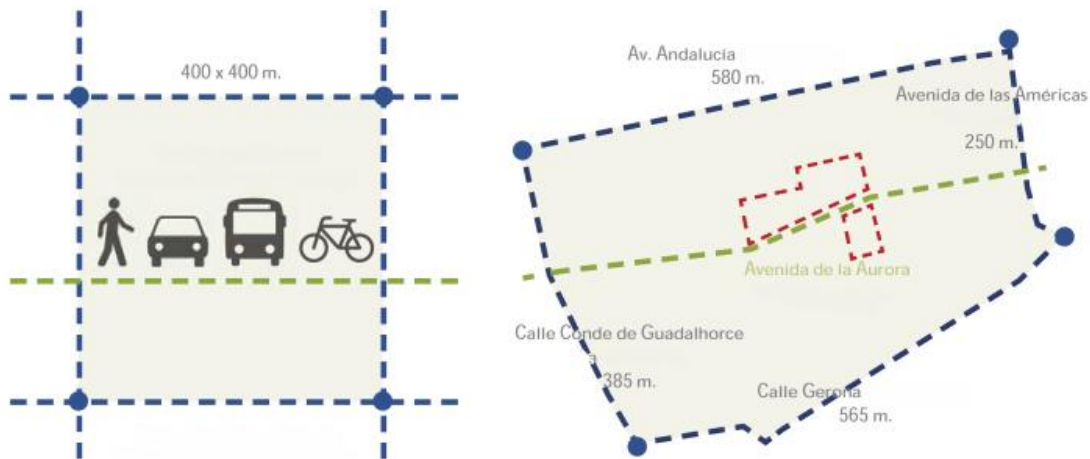


Fig. 4. Adaptation of the theoretical superblock model to the case study, showing the surface area renovated by the SMMN. Source: authors



Fig. 5. Photo of the outdoor parking lot being studied. Source: authors



Fig. 6. Environmental recovery of 3660 m² as a result of eliminating the outdoor parking lots (left) after setting up the SMMN (right). Cycle lane (red line) and concentration of public transport: buses (red dot) and taxis (blue dot). Source: authors

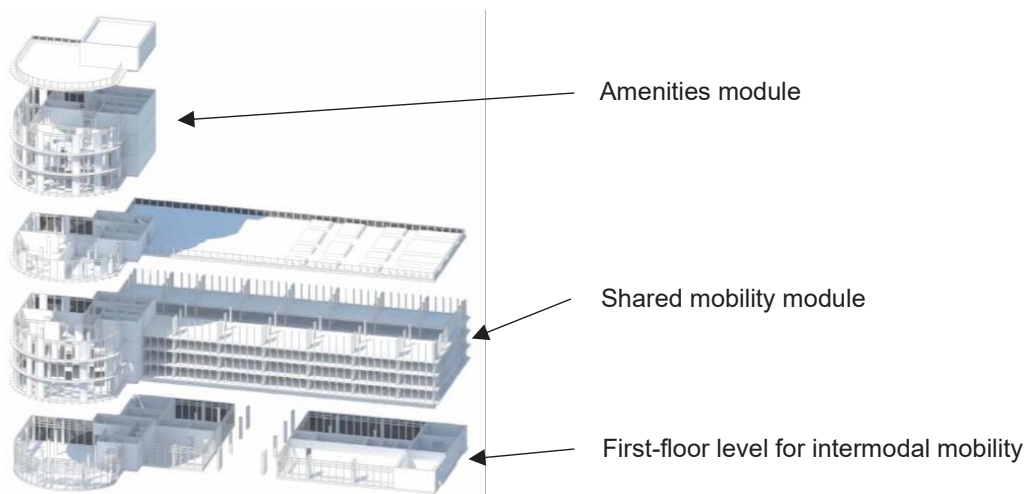


Fig. 7. SMMN modules and functional parts. Source: authors

designed area, as it is the contact area of the building with the SMMN and the connection point between the different means of transport. The car-sharing and bike-sharing office (85 m²), the e-bike and bicycle storage, vehicle maintenance and cleaning are located there, along with shops and coffee bars. Furthermore, special importance is given to keeping pedestrian, bicycle, and vehicle access totally separate for greater security.

Given that the car-sharing module allows the vehicle fleet to be reduced by 50%, the size of the SMMN is designed for just 284 vehicles. The module to be used for car parking has a surface area of 915 m², with 5 levels and a built surface area of 3660 m². The low private vehicle occupancy rate, which ranges between 1 and 1.5 people per vehicle, allows a more diversified offer to be adjusted to the standardized size of family utility vehicles, which are usually 4–5 seaters. It is therefore possible to differentiate between three types of storage place

size (Fig. 8): A1 for a maximum length of 3 m, single-seater (e.g., Renault Twizy e-tech electric) or two-seater (e.g., Smart EQ Fortwo); A2 for a maximum length of 4 m (e.g., Citroën C-Zero); and A3 for a maximum length of 5 m. Applying this differentiation can reduce the width of the building, compared to a traditional parking lot where all the spaces are sized for a private owner, who tends to purchase a vehicle with the greatest number of features (the same vehicle is used to travel alone to work and to travel with the family of 3 or 4 people). The SMMN would thus require 71 modules per story (23 A1, 24 A2 and 23 A3), with a total of 284 vehicles on the four levels.

Building a parking lot at the surface level means that its roof and façades can be used, unlike in traditional parking lots, where they play a minor role. The façades in SMMNs are active skins that play an important function in the environmental recovery of the urban space. There is a system

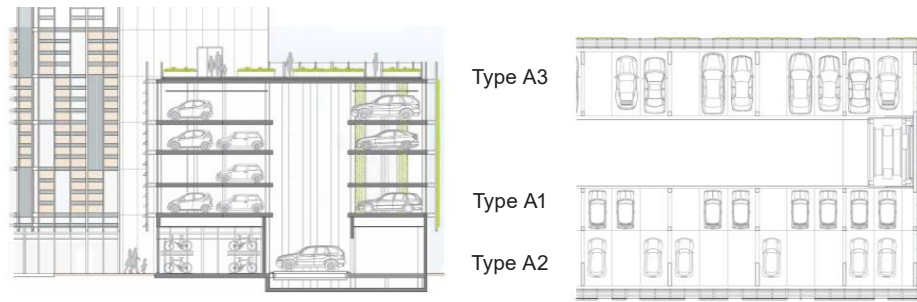


Fig. 8. On the left: mobility module section; on the right: different platform sizes for a diversified vehicle offer. Source: authors

to collect and reuse rainwater on the roof (Fig. 9). Demartini et al. (2019) showed the beneficial effects of water accumulation systems to avoid overloading the sewage network in climates with torrential rain such as the Mediterranean. Savings of 87% were reported in office buildings in the United Kingdom (Ward et al., 2012). Rain water can satisfy over 60% of the garden irrigation demands both in single- and multi-family buildings (Domènech and Saurí, 2011). In the case study and according to Malaga rainfall data, the average water catchment is 485 mm/year/m², which, for a roof surface of 900 m², means that a total of 436,500 l/year can be obtained. Its storage in tanks under the first-floor joists means the filtered water can be piped to irrigate the roof allotments, the hydroponic panels and used to clean vehicles.

Tulpule et al. (2013) showed the feasibility of the charging points for plug-in electric hybrid vehicles and electric vehicles located in workplace parking lots. Part of this energy can be supplied by

photovoltaic panels in the façades, an emerging and necessary system to harness solar energy in the built environment (Xiang et al., 2021) either as full panels or slats. Tablada et al. (2020) defined productive façades as systems integrating photovoltaic systems and vertical farming, which could contribute to transforming buildings and communities from consumers to producers. The incorporation of environmentally-friendly panels would add the possibility of capturing CO₂ (Yoshioka et al., 2013).

Thus, the north-facing façades in the proposed model would have passive systems to improve the air quality and create favorable urban microclimates by incorporating green concrete and plant panels, while the solar panels and photovoltaic slats to generate electricity for the building's self-consumption and the electric vehicle fleet would be located on the other façades (south-, east- and west-facing) (Fig. 10).

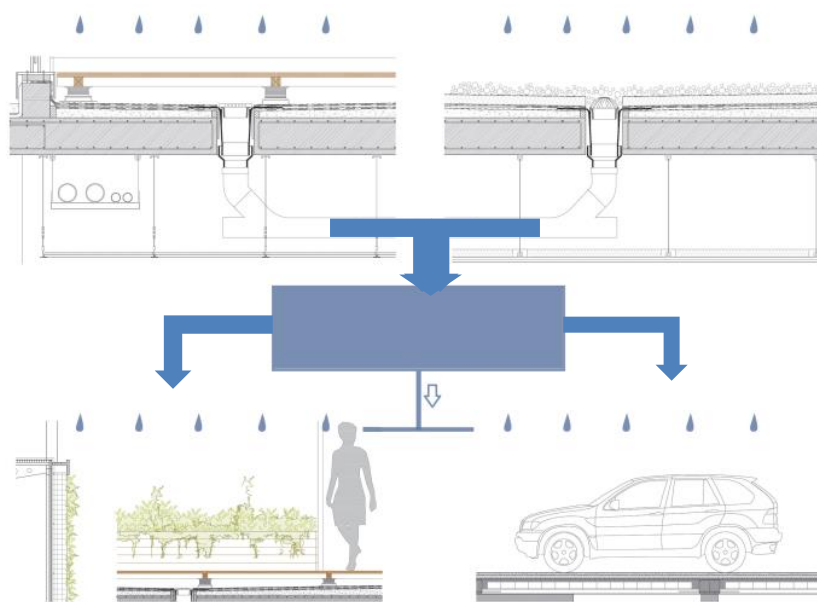


Fig. 9. SMMN active roof collecting rain water to irrigate allotments and clean vehicles. Source: authors

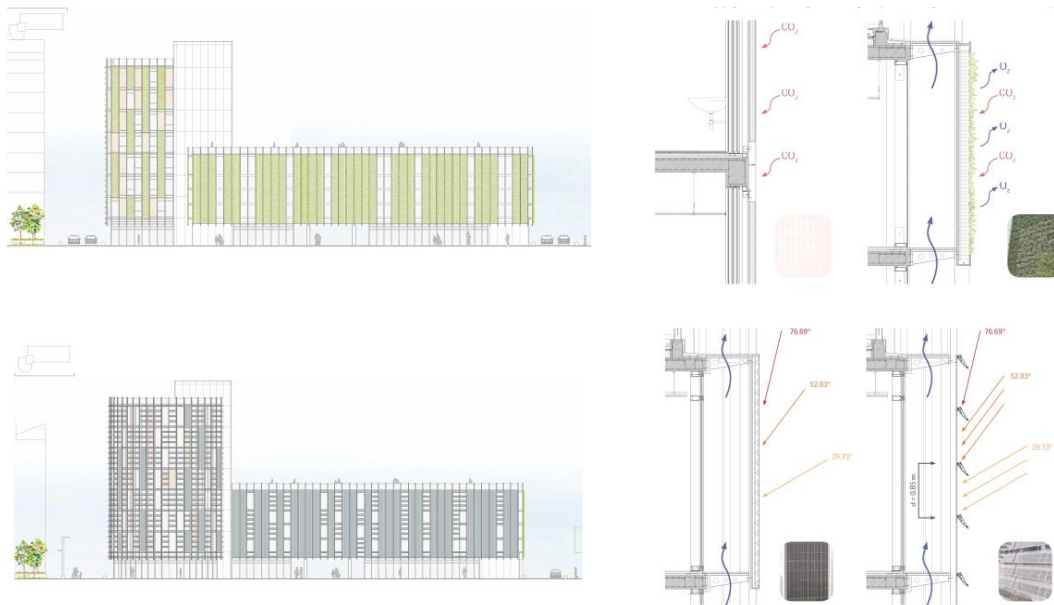


Fig. 10. Above: north-facing active skins comprising plant panels and green concrete; below: east, south- and west-facing active skins comprising photovoltaic panels and slats. Source: authors

Discussion

The SMMNs involve adapting the multi-dimensional hubs of large transport infrastructures (Carlorosi et al., 2015) to the intermediate or neighborhood scale. Therefore, environmental improvement — with the recovery of green space — and improving amenities are closely related to the residents’ community benefitting from the mobility service. In this regard, the SMMN is at the intersection between the Mobiway model (Moran, 2009) and the model proposed in Domagkpark (Alarcos and Ginés, 2017). The first contributes to the concentration of mobility services and the second — to the relationship with the residents’ community. In this vein, research should continue into the possibility of creating social-based cooperatives as the business model to manage this infrastructure. The SMMN is designed for residential neighborhoods and middle-/

low-income population sectors. Thus, personalized mobility without having to purchase a vehicle can be an incentive, particularly as the change to electric technology requires a charging infrastructure and users do not have parking spaces.

On the other hand, its implementation throughout the city would generate a second level of interchanges. Thus, in the Malaga case study, whose intermodal system is currently made up of the metropolitan interurban and urban transport stations associated with large transport and/or social amenities (Fig. 11, on the left), the SMMNs would generate a secondary network associated with the residential blocks. For each of the Sustainable Urban Mobility Sectors (Ayuntamiento de Málaga, 2011), an area of opportunity can be pinpointed, which will also be a social and environmental regeneration space (Fig. 11, on the right). Thus,



Fig. 11. On the left: primary system of large transport interchanges in Malaga; on the right: overlapping of the secondary system consisting of the SMMN network in different superblocks. Source: authors

each resident would be able to travel using different SMMNs, which would generate a large network of interchanges and facilitate more sustainable mobility for the whole city.

The integration of the SMMN of the public transport system would foster transit-oriented development (TOD), help reduce the carbon footprint, reduce the number of private vehicles, and increase the public space. The latter offers important environmental improvements compared to the underground parking lots, as SMMNs release land that allows evapotranspiration, and, therefore, the environmental advantages are much greater as it helps to recharge the aquifers. It should be stressed that the case study allows the existing green area surface of 4382 m² to be duplicated to a ratio of 1.2 m²/inhabitant. This results in the creation of a neighborhood network of green areas that would approve its accessibility and also foster, in tandem, the development of a network of urban allotments.

As regards the facelifts of the garages, SMMNs are not focused on iconic and aesthetic design but rather on being core elements in the environmental improvement of the existing neighborhoods and facilitate the transition to electricity mobility in urban sectors, with difficulties for vehicle charging due to the lack of space. In the new mobility revolution, parking lots can no longer be mere spaces containing vehicles, but rather they have to be active hotspots of mobility, accessibility, urban amenities, and obtaining energy.

Another advantage of SMMNs over traditional underground parking lots is that the ground

occupancy is minimum, as what is occupied by the building itself is recovered on the roof. It also allows for the development of a large surface of active skins with environmental improvement functions (increasing solar and water capturing, and green façades). The development of façades to capture photovoltaic energy helps to produce electricity to charge electric cars and thus reduce electricity demand. Similarly, collecting rainwater allows water consumption for cleaning the vehicles to be reduced; and developing green façades turns the infrastructures into vertical allotments that foster food production at the neighborhood scale (Tablada et al., 2020).

Therefore, given the need to renew the architectural design (Kay, 2001), the SMMN shows that this renewal must not be exclusively aimed at a facelift inspired, e.g., by the Car Towers (Wolfsburg, Germany), but rather it must be focused on increasing the environmental improvement that this type of facilities may produce, particularly in the existing city. In this vein, it should be noted that the case study in question tallies with open block and high-density neighborhoods. This research should continue by analyzing the feasibility of the model in other urban areas such as low-density zones and in historical centers where free spaces are rare and where the introduction of this type of environmental improvement infrastructure seems not to be very viable.

Funding

This research was funded by the 1st Smart-Campus Plan of University of Malaga [project Microsol].

References

- Alarcos A. and Ginés, Á. (2017). *Evaluation of the mobility station in Domagkpark, Munich - Development and test of a methodology for the impact and process evaluation of sustainable mobility measures in the framework of the ECCENTRIC project*. [online] Available at: <https://mediatum.ub.tum.de/doc/1446939/1446939.pdf> [Date accessed November 1, 2022].
- ARUP (2019). *Tomorrow's living station*. [online] Available at: <https://www.arup.com/perspectives/publications/promotional-materials/section/tomorrows-living-station> [Date accessed November 1, 2022].
- Ayuntamiento de Málaga (2011). *Plan de Movilidad Urbana Sostenible*. [online] Available at: <https://movilidad.malaga.eu/opencms/export/sites/movilidad/.content/galerias/Documentos-del-site/PMUS.pdf> [Date accessed November 1, 2022].
- Bachand-Marleau, J., Lee, B. H. Y., and El-Geneidy, A. M. (2012). Better understanding of factors influencing likelihood of using shared bicycle systems and frequency of use. *Transportation Research Record*, Vol 2314, Issue 1, pp. 66–71. DOI: 10.3141/2314-09.
- Barter, P. (2013). "Cars are parked 95% of the time". *Let's check!* [online] Available at: <https://www.reinventingparking.org/2013/02/cars-are-parked-95-of-time-lets-check.html> [Date accessed November 1, 2022].
- Barcellos de Souza, G. (2006). About the deployments of the Neighborhood Unit. The communitarian space in Leon Krier's Polycentric City. *Bitácora*, 10(1), 7–26.
- Bates, J. and Leibling, D. (2012). Spaced out. Perspectives on parking policy. [online] Available at: http://www.racfoundation.org/assets/rac_foundation/content/downloadables/spaced_out-bates_leibling-jul12.pdf [Date accessed November 1, 2022].
- Batra, A. (2014). Optimum car parking solutions. *Institute of Town Planners, India Journal*, Vol. 11, No. 3, pp. 39–46.
- Belk, R. (2014). You are what you can access: Sharing and collaborative consumption online. *Journal of Business Research*, Vol. 67, Issue 8, pp. 1595–1600. DOI: 10.1016/j.jbusres.2013.10.001.
- Carlorosi, C., Pugnali, F., and Filippini, G. (2015). Eco-infrastructure labs for urban utopias Moscow as slow metropolis. *GSTF Journal of Engineering Technology (JET)*, Vol. 3, Issue 3, 25. DOI: 10.7603/s40707-014-0025-z.
- Dacko, S. G. and Spalteholz, C. (2014). Upgrading the city: Enabling intermodal travel behaviour. *Technological Forecasting and Social Change*, Vol. 89, pp. 222–235. DOI: 10.1016/j.techfore.2013.08.039.
- Demartini, J. I., Bertoni, G. A., and Piga, L. (2019). Recolección y reutilización de las aguas de lluvia en edificios como beneficio para las ciudades. *Arquitecto*, No. 13, pp. 35–46. DOI: 10.30972/arq.0134160.
- Domènech, L. and Sauri, D. (2011). A comparative appraisal of the use of rainwater harvesting in single and multi-family buildings of the Metropolitan Area of Barcelona (Spain): social experience, drinking water savings and economic costs. *Journal of Cleaner Production*, Vol. 19, Issues 6–7, pp. 598–608. DOI: 10.1016/j.jclepro.2010.11.010.
- Efthymiou, D., Chaniotakis, E., & Antoniou, C. (2019). Factors affecting the adoption of vehicle sharing systems. In: Antoniou, C., Efthymiou, D., and Chaniotakis, E. (eds.). *Demand for Emerging Transportation Systems: Modeling Adoption, Satisfaction, and Mobility Patterns*. Amsterdam: Elsevier, pp. 189–209. DOI: 10.1016/B978-0-12-815018-4.00010-3.
- Fishman, E., Washington, S., Haworth, N., and Watson, A. (2015). Factors influencing bike share membership: an analysis of Melbourne and Brisbane. *Transportation Research Part A: Policy and Practice*, Vol. 71, pp. 17–30. DOI: 10.1016/j.tra.2014.10.021.
- Frankel, E. H. (1998). The future robotic parking and the ever-changing dynamics of land use. *Architectural Record*, Vol. 186, Issue 6, 232.
- Gehl, J. (1987). *Life Between Buildings. Using Public Space*. Van Nostrand Reinhold.
- Graham-Rowe, E., Skippon, S., Gardner, B., and Abraham, C. (2011). Can we reduce car use and, if so, how? A review of available evidence. *Transportation Research Part A: Policy and Practice*, Vol. 45, Issue 5, pp. 401–418. DOI: 10.1016/j.tra.2011.02.001.
- Henley, S. (2007). *The Architecture of Parking*. Thames & Hudson. <https://doi.org/10.1111/j.1531-314x.2010.01118.x>
- Hernandez, S. and Monzon, A. (2016). Key factors for defining an efficient urban transport interchange: Users' perceptions. *Cities*, Vol. 50, pp. 158–167. DOI: 10.1016/j.cities.2015.09.009.
- Idris, M. Y. I., Leng, Y. Y., Tamil, E. M., Noor, N. M., and Razak, Z. (2009). Car park system: A review of smart parking system and its technology. *Information Technology Journal*, Vol. 8, Issue 2, pp. 101–113. DOI: 10.3923/itj.2009.101.113.
- IECA (2022). *Distribución espacial de la población en Andalucía*. [online] Available at: <http://www.juntadeandalucia.es/institutodeestadisticaycartografia/distribucionpob/index.htm> [Date accessed November 1, 2022].

- International Energy Agency (2017). *CO₂ Emissions from Fuel Combustion Highlights 2017*. [online] Available at: www.iea.org/publications/freepublications/publication/CO2-emissions-from-fuel-combustion-highlights-2017.html [Date accessed January 12, 2018].
- Johansson, R. (2003). *Case study methodology*. [online] Available at: http://www.psyking.net/htmlobj-3839/case_study_methodology-_rolf_johansson_ver_2.pdf [Date accessed November 1, 2022].
- Kane, M. and Whitehead, J. (2017). How to ride transport disruption—a sustainable framework for future urban mobility*. *Australian Planner*, Vol. 54, Issue 3, pp. 177–185. DOI: 10.1080/07293682.2018.1424002.
- Kay, J. H. (2001). A brief history of parking: the life and after-life of paving the planet. *Architecture*, Vol. 90, No. 2, 78.
- Loo, B. P. Y., & du Verle, F. (2017). Transit-oriented development in future cities: towards a two-level sustainable mobility strategy. *International Journal of Urban Sciences*, 21, 54–67. <https://doi.org/10.1080/12265934.2016.1235488>
- Maienschein-Cline, L. M. (2014). *Catalytic parking: creating new possibilities in an integrated suburban parking garage*. Seattle: University of Washington, 73 p.
- Martin, E., Shaheen, S. A., and Lidicker, J. (2010). Impact of carsharing on household vehicle holdings: results from North American shared-use vehicle survey. *Transportation Research Record*, Vol. 2143, Issue 1, pp. 150–158. DOI: 10.3141/2143-19.
- Mezoued, A. M., Letesson, Q., & Kaufmann, V. (2021). Making the slow metropolis by designing walkability: a methodology for the evaluation of public space design and prioritizing pedestrian mobility. *Urban Research & Practice*, 1–20. <https://doi.org/10.1080/17535069.2021.1875038>
- Monzón, A., Hernández, S., and Di Ciommo, F. (2016). Efficient urban interchanges: the City-HUB model. *Transportation Research Procedia*, Vol. 14, pp. 1124–1133. DOI: 10.1016/j.trpro.2016.05.183.
- Perry, C. A. (1929). City Planning for Neighborhood Life. *Social Forces*, 8(1), 98–100. <https://doi.org/10.2307/2570059>
- Robotic Parking Systems (2020a). *Changing the dynamics of land use*. [online] Available at: <https://www.roboticparking.com/do-more-with-less/changing-the-dynamics-of-land-use/> [Date accessed November 1, 2022].
- Robotic Parking Systems (2020b). *Green Parking*. [online] Available at: <https://www.roboticparking.com/green-parking/> [Date accessed November 1, 2022].
- Rueda, S. (2011). Las supermanzanas: reinventando el espacio público, reinventando la ciudad. In: Armand, L. (ed.). *Ciudades (im) propias: la tensión entre lo global y lo local*. Valencia: Centro de Investigación Arte y Entorno, pp. 123–132.
- Rueda, S. (2012). *El urbanismo ecológico: su aplicación en el diseño de un ecobarrio en Figueres*. Barcelona: Agencia de Ecología Urbana, 304 p.
- Rueda, S. (2016). *La supermanzana, nueva célula urbana para la construcción de un nuevo modelo funcional y urbanístico de Barcelona*. [online] Available at: http://bcnecologia.net/sites/default/files/proyectos/la_supermanzana_nueva_celula_poblenou_salvador_rueda.pdf [Date accessed November 1, 2022].
- Seeley, M. (2008). How a hillside impacts parking garage design: the Calhoun Street parking garage. *Parking*, Vol. 47, Issue 7, pp. 38–41.
- Shaheen, S. and Chan, N. (2015). *Mobility and the sharing economy: impacts synopsis*. [online] Available at: http://innovativemobility.org/wp-content/uploads/Innovative-Mobility-Industry-Outlook_SM-Spring-2015.pdf [Date accessed November 1, 2022].
- Shaheen, S. A. and Cohen, A. P. (2013). Carsharing and personal vehicle services: worldwide market developments and emerging trends. *International Journal of Sustainable Transportation*, Vol. 7, Issue 1, pp. 5–34. DOI: 10.1080/15568318.2012.660103.
- Shaheen, S. and Cohen, A. (2020). Mobility on demand (MOD) and mobility as a service (MaaS): Early understanding of shared mobility impacts and public transit partnerships. In: Antoniou, C., Efthymiou, D., and Chaniotakis, E. (eds.). *Demand for Emerging Transportation Systems: Modeling Adoption, Satisfaction, and Mobility Patterns*. Amsterdam: Elsevier, pp. 37–59. DOI: 10.1016/B978-0-12-815018-4.00003-6.
- Shaheen, S. A., Guzman, S., and Zhang, H. (2010a). Bikesharing in Europe, the Americas, and Asia: past, present, and future. *Transportation Research Record*, Vol. 2143, Issue 1, pp. 159–167. DOI: 10.3141/2143-2.
- Shaheen, S. A., Rodier, C., Murray, G., Cohen, A., and Martin, E. (2010b). *Carsharing and public parking policies: assessing benefits, costs, and best practices in North America. MTI Report 09-09*. San José, CA: Mineta Transportation Institute, 76 p.
- Tablada, A., Kosorić, V., Huang, H., Lau, S. S. Y., and Shabunko, V. (2020). Architectural quality of the productive façades integrating photovoltaic and vertical farming systems: Survey among experts in Singapore. *Frontiers of Architectural Research*, Vol. 9, Issue 2, pp. 301–318. DOI: 10.1016/j.foar.2019.12.005.

Tulpule, P. J., Marano, V., Yurkovich, S., and Rizzoni, G. (2013). Economic and environmental impacts of a PV powered workplace parking garage charging station. *Applied Energy*, Vol. 108, pp. 323–332. DOI: 10.1016/j.apenergy.2013.02.068.

Tyrinopoulos, Y. and Antoniou, C. (2020). Review of factors affecting transportation systems adoption and satisfaction. In: Antoniou, C., Efthymiou, D., and Chaniotakis, E. (eds.). *Demand for Emerging Transportation Systems: Modeling Adoption, Satisfaction, and Mobility Patterns*. Amsterdam: Elsevier, pp. 11–36. DOI: 10.1016/B978-0-12-815018-4.00002-4.

Verbavatz, V. and Barthelemy, M. (2019). Critical factors for mitigating car traffic in cities. *PloS One*, Vol. 14, Issue 7, e0219559. DOI: 10.1371/journal.pone.0219559.

Ward, S., Memon, F. A., and Butler, D. (2012). Performance of a large building rainwater harvesting system. *Water Research*, Vol. 46, Issue 16, pp. 5127–5134. DOI: 10.1016/j.watres.2012.06.043.

Wu, G., Xu, X., Dong, Y., De Koster, R., and Zou, B. (2019). Optimal design and planning for compact automated parking systems. *European Journal of Operational Research*, Vol. 273, Issue 3, pp. 948–967. DOI: 10.1016/j.ejor.2018.09.014.

Xiang, C., Matusiak, B. S., Røyset, A., and Kolås, T. (2021). Pixelization approach for façade integrated coloured photovoltaics-with architectural proposals in city context of Trondheim, Norway. *Solar Energy*, Vol. 224, pp. 1222–1246. DOI: 10.1016/j.solener.2021.06.079.

Yoshioka, K., Obata, D., Nanjo, H., Yokozeki, K., Torichigai, T., Morioka, M., and Higuchi, T. (2013). New ecological concrete that reduces CO₂ emissions below zero level ~ new method for CO₂ capture and storage ~. *Energy Procedia*, Vol. 37, pp. 6018–6025. DOI: 10.1016/j.egypro.2013.06.530.

ANALYSIS OF COOLING SYSTEM EFFICIENCY

Yuri Dmitriev

Saint Petersburg State University of Architecture and Civil Engineering
Vtoraja Krasnoarmeyskaya st., 4, 190005, Saint Petersburg, Russia

E-mail: 6377227@mail.ru

Abstract

Introduction: The main task of cooling systems in the machine room of a data center is to maintain optimal air parameters at the inlet to IT equipment in accordance with the applicable regulatory documents. If the value of air temperature at the inlet to IT equipment exceeds the optimal value, then so-called hot spots occur — the operation of IT equipment in such places can lead to its overheating and failure. The main reason for the occurrence of hot spots is the violation of air circulation between the hot and cold aisles. **Purpose of the study:** We aimed to analyze the influence of different methods of hot aisle isolation on the efficiency of IT equipment cooling. **Methods:** We performed modeling of different methods of hot aisle isolation at different capacity values of IT equipment in the STAR-CCM+ program. **Result:** As a result of studying temperature and air conditions in a data center, we found the most rational way of isolating the hot aisle — top horizontal containments with vertical blind panels in the free rack space.

Keywords

data center, ambient temperature, cold aisle, hot aisle, computational fluid dynamics (CFD).

Introduction

In recent decades, row arrangement of equipment racks in data centers have been widely used. In such an arrangement, rows of racks are divided into so-called hot and cold aisles. IT equipment is installed in racks in such a way that heat is removed to the hot aisle, and cooled air is supplied from the cold aisle.

IT equipment in a data center is cooled using the following systems:

- 1) surface air coolers and cooling units as well as monoblock air conditioners with a remote condenser;
- 2) evaporative cooling;
- 3) with ventilation air.

Cooling with ambient ventilation air makes it possible to significantly save on power consumption of the data center cooling system. However, this system can be used at outdoor temperature $t_{out} \leq 27^\circ\text{C}$. In cases when outdoor temperature is higher than this limit value ($t_{out} \geq 27^\circ\text{C}$) set by the effective standard (ASHRAE, 2016), additional air cooling is required.

The efficiency of cooling with ventilation air can be improved by using evaporative cooling. This method is based on adiabatic cooling of ambient air due to mist spraying or the use of wetted pads made of various materials. It should be noted that in winter an evaporative cooling system can serve as a humidifier to increase relative humidity to the optimal values (ASHRAE, 2016) without the need to use steam humidifiers characterized by high power consumption.

Air cooling in surface air coolers is carried out with the use of freon coolant or cooling media such as water or non-freezing liquid. When cooling

media are used, chilled water or non-freezing liquid from a steam compression (chiller) or absorption refrigerating machines is fed to an air cooler. Air cooling with freon coolant takes place in an air cooler located in a monoblock air conditioner.

Depending on arrangement in a data center, cooling system equipment can be classified into central and local. The first group includes central air conditioners using ambient air and evaporative cooling (Figs. 1 and 2). The second group includes surface air coolers that can be installed:

- 1) in monoblock air conditioners located either around the perimeter of a machine room (Fig. 3) or in rows of racks (Fig. 4);
- 2) in the machine room space (Fig. 5);
- 3) in each rack (Fig. 6).

The choice of a particular data center cooling solution depends on the feasibility study. During that study, the following should be taken into account: the climatic conditions of the region where the data center is constructed, the cost of available energy resources, the impact on the environment, and the capacity of IT equipment placed in racks. Today, racks with a capacity from 5 to 15 kW are widespread (Timonin, 2018). Systems using surface air coolers installed in monoblock air conditioners have become very popular in cooling IT equipment in such racks.

Many researchers performed comparative analysis of monoblock air conditioners located around the perimeter of the machine room and monoblock air conditioners located in rows of racks in a data center. As a result of comparative analysis performed by some researchers (Abbas

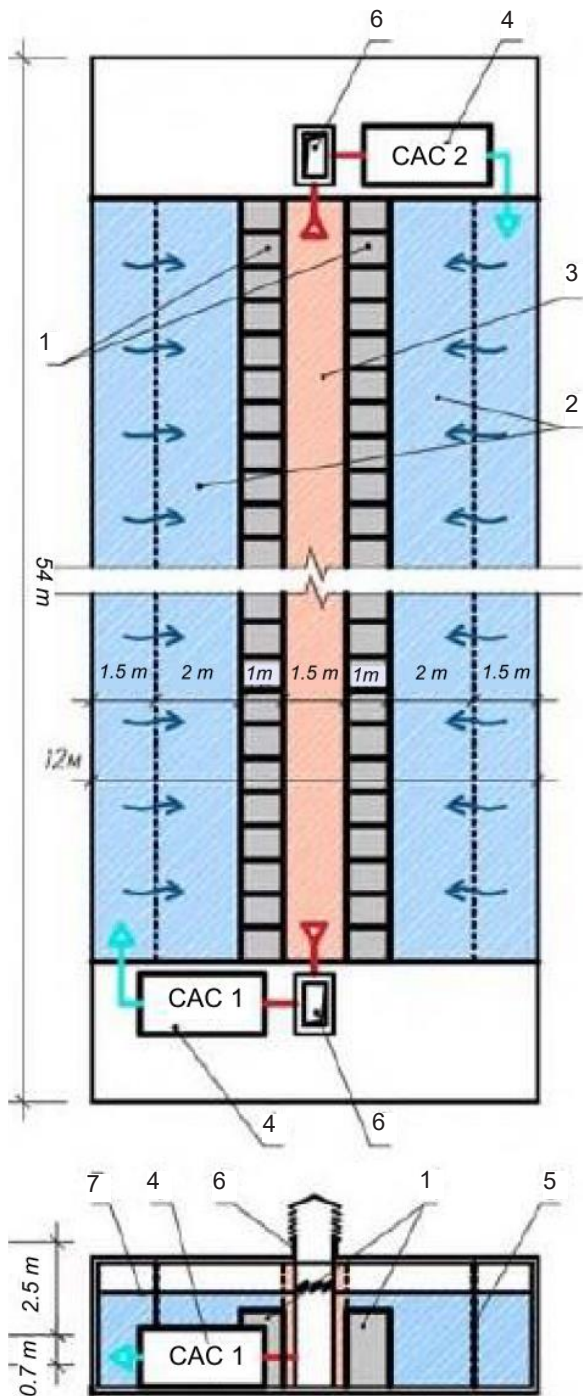


Fig. 1. Diagram of a data center air cooling system using central air conditioners: 1 — racks with IT equipment; 2 — cold aisle; 3 — hot aisle; 4 — central air conditioner; 5 — drop separator; 6 — air inlet duct; 7 — suspended ceiling; CAC 1, CAC 2 — central air conditioner

et al., 2021; Priyadumkol and Kittichaikarn, 2014), it was revealed that when air conditioners are located around the perimeter of the machine room, an uneven distribution of air throughout the height of the racks is observed. But when air conditioners are located in rows of racks, air is distributed evenly. As a result of another comparative analysis (Cho and Woo, 2020), it was revealed that the intensity

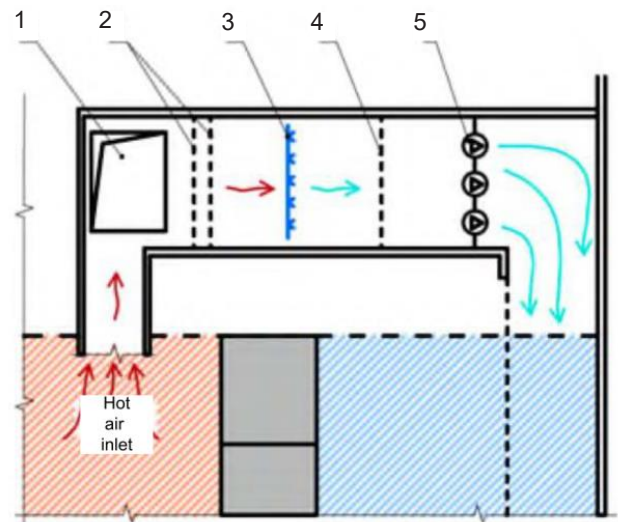


Fig. 2. Diagram of a data center air cooling system using a central air conditioner: 1 — air inlet duct; 2 — coarse and fine filters; 3 — evaporative cooling system; 4 — drop separator; 5 — fans (axial or radial)

of air circulation between the aisles is higher when air conditioners are located around the perimeter of the machine room. It was also revealed that as a result of air circulation between the aisles, the heating of supply air in the cold aisle is $\Delta T = 4.6^{\circ}\text{C}$ when air conditioners are located in rows of racks and $\Delta T = 8.3^{\circ}\text{C}$ when air conditioners are located around the perimeter of the machine room. Thus, the arrangement of air conditioners in rows of racks is at least 50% more efficient than the arrangement around the perimeter of the machine room.

To increase the efficiency of cooling systems in a data center, hot and cold aisles are isolated using containment (Fig. 7) and blind panels in the rack space free from IT equipment (Fig. 8). Such researchers as Nada et al. (2016) and Zhang et al. (2017) addressed the issue of aisle isolation with the use of containments. They established that the use of containments to isolate the cold aisle reduces air circulation between the aisles and decreases the temperature of air supplied to the racks by 5°C compared to the option without containments. Cho et al. (2021) as well as Niemann et al. (2008) found out that hot aisle isolation allows for 24.9% improvement in the temperature conditions in the machine room and 43% reduction in the annual power consumption of the data center compared to cold aisle isolation. Other researchers studied isolation with blind panels in the rack space free of IT equipment (Rasmussen, 2012; Tatchell-Evans et al., 2017). They established that the use of blind panels for isolation reduces air circulation in the rack and decreases the temperature of air supplied to cool IT equipment by 12°C .

In continuation of the above studies, we performed comparative analysis for the efficiency of a cooling

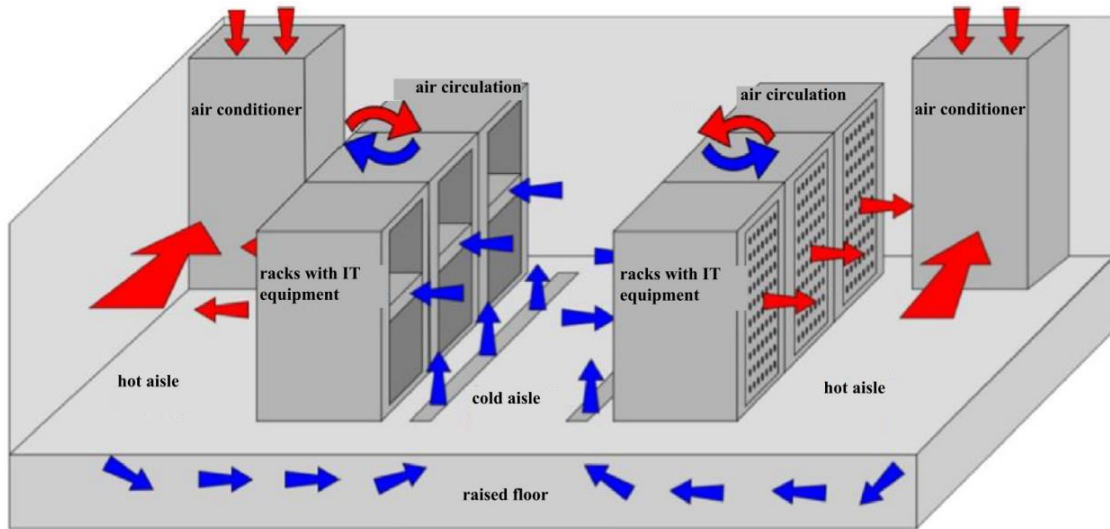


Fig. 3. Diagram of an air cooling system using air conditioners located around the perimeter of the data center machine room. The blue arrows indicate the air flow entering the rack, the red arrows indicate the air flow leaving the rack with IT equipment

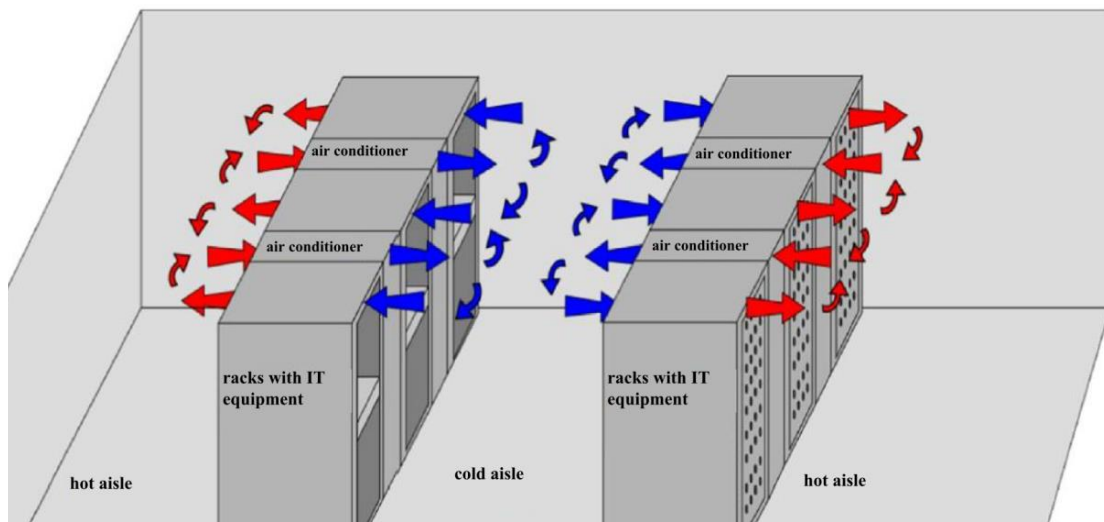


Fig. 4. Diagram of a data center air cooling system using air conditioners located in rows of racks with IT equipment. The blue arrows indicate the air flow entering the rack, the red arrows indicate the air flow leaving the rack with IT equipment

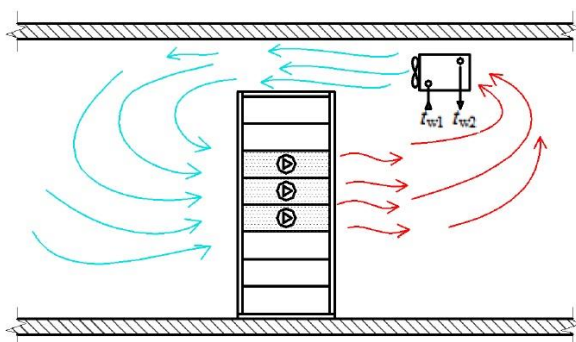


Fig. 5. Diagram of a data center air cooling system using a surface air cooler located in the machine room space. The blue arrows indicate the air flow entering the rack, the red arrows indicate the air flow leaving the rack with IT equipment

system in a data center with different options of hot aisle isolation (using containments and blind panels in the free rack space) at different values of IT equipment capacity. Air conditioners located inside the rows of racks were used as cooling system equipment. To perform analysis, we conducted numerical studies of cooling with regard to IT equipment with a capacity of 4.7 and 9.5 kW in each rack for the following methods of hot aisle isolation:

- A) without top containment (hereinafter — containment) and without blind panels in the free rack space (hereinafter — panels);
- B) without containment but with panels;
- C) with containment but without panels;
- D) with containment and panels.

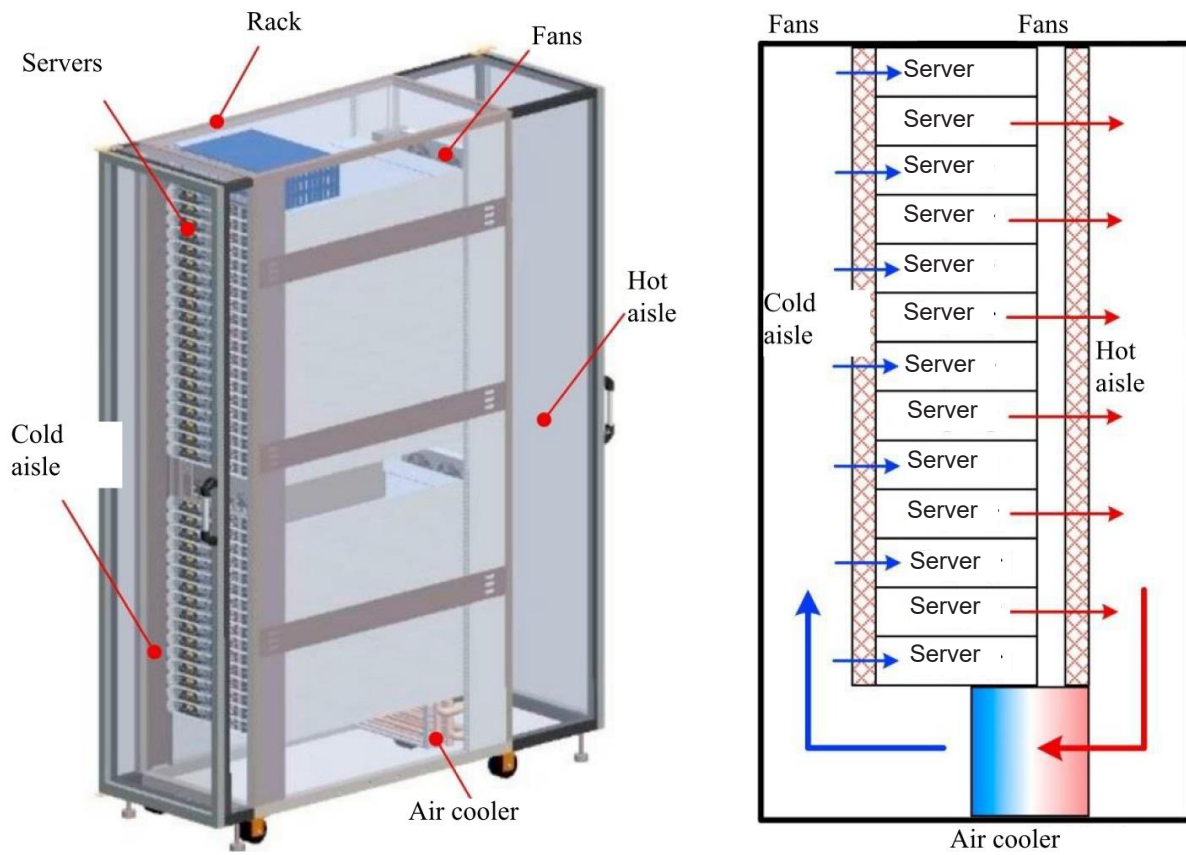


Fig. 6. Diagram of an air cooling system using air coolers located in rows of racks with IT equipment. The blue arrows indicate the air flow entering the rack, the red arrows indicate the air flow leaving the rack with IT equipment

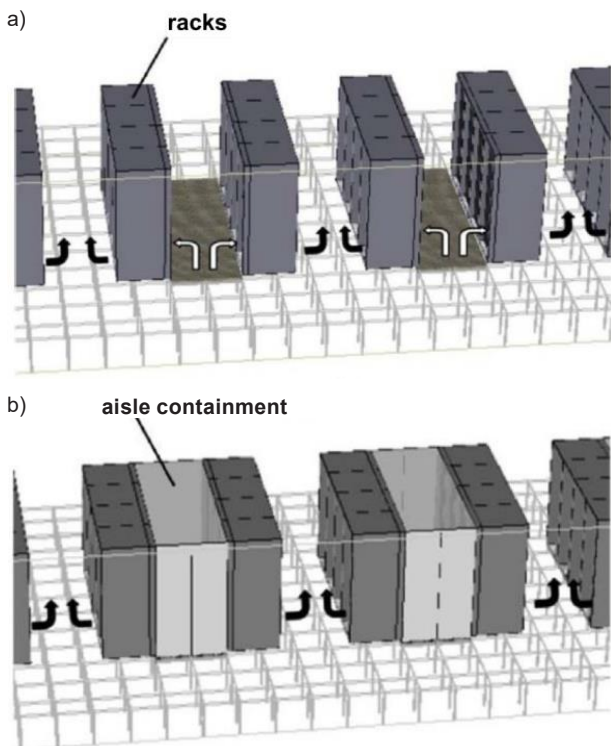


Fig. 7. An example of using containments to isolate the aisles between the racks: a — without containments, b — with containments

Materials and methods

We chose a real data center machine room in St. Petersburg (Fig. 9) using row arrangement or racks as an object for analysis in the STAR-CCM+ program. In each rack of the machine room, one IT equipment is placed (chassis with blade servers) (Almoli, 2013). The air conditioners are located between the rows of racks and are equipped with an

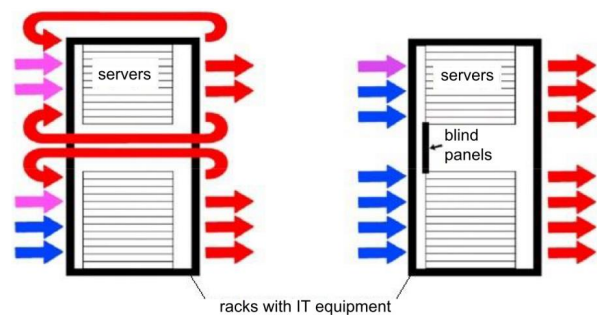


Fig. 8. An example of using blind panels in the racks with IT equipment. The blue arrows indicate the air flow entering the rack, the red arrows indicate the air flow leaving the rack with IT equipment:
 a — without blind panels in the racks
 b — with blind panels in the racks

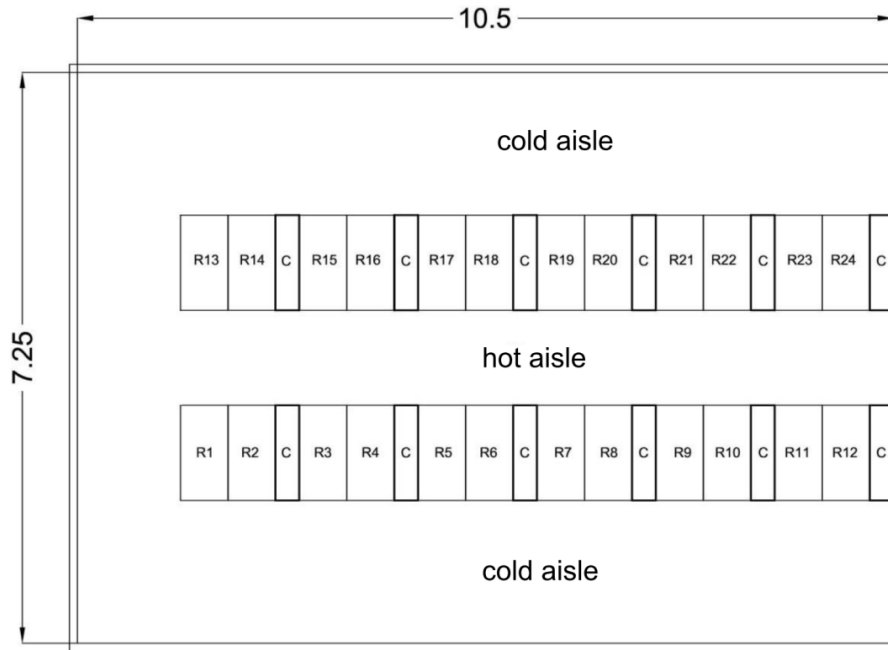


Fig. 9. Layout of the machine room in the data center in St. Petersburg. Designations: R1–R24 — racks with IT equipment; C — air conditioners

inverter compressor and fans with EC motors (Vertiv, 2022).

Tables 1 and 2 present the initial data for model construction and calculation in the STAR-CCM+ program.

The values of IT equipment capacity (4.7 kW) and fan capacity (853 m³/h) in each rack are taken in accordance with experimental data that correspond to 10% of the computational load of this IT equipment in the data center machine room (Ponomarev et al., 2021). The maximum estimated capacity of this IT

equipment in each rack is 9.5 kW (Ponomarev et al., 2021). The capacity of fans of IT equipment in each rack for the capacity of IT equipment = 9.5 kW can be obtained by the following equation:

$$Q = \frac{L \cdot \rho \cdot c \cdot \Delta T}{3.6}, \text{ W}, \quad (1)$$

where L — capacity of fans of IT equipment, m³/h; ρ — air density, kg/m³; c — specific heat capacity of air, kJ/(kg·K); ΔT — maximum temperature difference of incoming and outgoing air in IT equipment, K $\Delta T = 20$ K (Huawei, 2019).

The values of air capacity and cooling capacity of the air conditioners are taken to be equal to the needs of IT equipment in the racks.

To evaluate the modeling results, dimensionless indices RCI_{HIGH} and K_T are used.

The RCI_{HIGH} index was first introduced by Herrlin (2007) and is used to estimate the average air temperature at the inlet to IT equipment in racks, comparing it with the maximum permissible $T_{\text{max-perm}} = 32$ °C and recommended $T_{\text{max-rec}} = 27$ °C temperatures (ASHRAE, 2016). If the values of the average air temperature at the inlet to IT equipment in the racks exceed the maximum recommended value, then so-called hot spots occur —

Table 1. Initial data for model construction in the STAR-CCM+ program

Machine room dimensions (LxWxH), m	10.5 x 7.25 x 3.3
Number of racks with IT equipment, pcs.	24
Brand of IT equipment	Huawei E9000 chassis with Huawei CH242 V3 blade servers
Number of air conditioners, pcs.	12
Brand of air conditioners	Liebert CRV CR021RA
Supply air temperature T_{sup} , °C (ASHRAE, 2016)	20

Table 2. Initial data for model calculation in the STAR-CCM+ program

Capacity of IT equipment in each rack, kW	Capacity of fans of IT equipment in each rack, m ³ /h	Cooling capacity of one air conditioner, kW	Air capacity of one air conditioner, m ³ /h
4.7	853	9.4	1706
9.5	1424	19	2848

the operation of IT equipment in such places can lead to its overheating and failure.

$$RCI_{HIGH} = \left[1 - \frac{\sum_{i=1}^n (T_{inc\ i} - T_{max-rec})_{T_{inc\ i} > T_{max-rec}}}{n \times (T_{max-perm} - T_{max-rec})} \right] \times 100 \%, \quad (2)$$

where:

$T_{inc\ i}$ — average temperature of incoming air entering IT equipment in the rack, °C;

$T_{max-rec}$ — maximum recommended temperature ($T_{max-rec} = 27$ °C) of incoming air entering IT equipment in the racks, °C;

$T_{max-perm}$ — maximum permissible temperature ($T_{max-perm} = 32$ °C) of incoming air entering IT equipment in the racks, °C;

n — the number of racks with IT equipment.

If $RCI_{HIGH} = 100\%$, it means that the average air temperature at the inlet to IT equipment in all the racks of the machine room does not exceed the recommended value $T_{max-rec} = 27$ °C. If $RCI_{HIGH} < 100\%$, that indicates that the recommended value $T_{max-rec} = 27$ °C in one or more IT equipment in the racks is exceeded (the lower the value of $RCI_{HIGH} < 100\%$, the more IT equipment is there in the racks where the average air temperature at the inlet exceeds the recommended value).

Such researchers as Capozzoli et al. (2014) as well as Norouzi-Khangah et al. (2016) studied the efficiency of cooling systems in data centers using this index.

The K_T index (Huang et al., 2017) characterizes the deviation of the average temperature values of air entering IT equipment relative to the temperature $T_{sup} = 20$ °C of air supplied by air conditioners. The K_T index can be calculated by the following equation:

$$K_T = \frac{1}{T_{sup}} \sqrt{\frac{\sum_{i=1}^n (T_{inc\ i} - T_{sup})^2}{n-1}}, \quad (3)$$

T_{sup} — supply air temperature, °C;

$T_{inc\ i}$ — average temperature of incoming air entering IT equipment in the rack, °C;

n — the number of racks with IT equipment.

The lower the K_T index, the more efficient is air distribution in the data center machine room.

Results and discussion

To present the results of the study, we made sections in the x-y and y-z planes in the model (Fig. 10). The results of the study are represented by air temperature fields for different methods of hot aisle isolation (Fig. 11):

- A) without containment and panels;
- B) without containment but with panels;
- C) with containment but without panels;
- D) with containment and panels.

Besides, each method is represented by air temperature fields for the capacity of IT equipment in each rack of 4.7 and 9.5 kW.

To evaluate the modeling results, we constructed graphs of the average values of air temperature at the inlet to IT equipment in the racks $T_{inc\ i}$ (Figs. 12 and 13) and calculated the dimensionless indices RCI_{HIGH} and K_T (Figs. 14 and 15).

Thus, as a result of the analysis of the RCI_{HIGH} index values for different isolation methods and capacity of IT equipment, the following was established:

- 1) The maximum values (100%) of the RCI_{HIGH} index were obtained for methods B) and D), which assume the arrangement of panels in the racks. This means that the average air temperature at the inlet to IT equipment in the racks for these methods does not exceed the maximum recommended value $T_{max-rec} = 27$ °C. Besides, the value of the RCI_{HIGH}

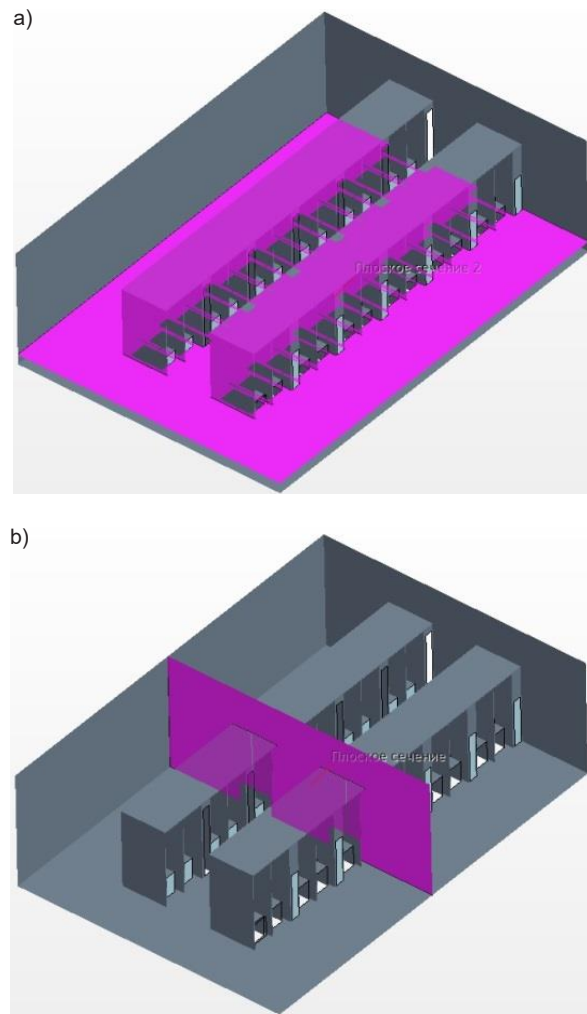


Fig. 10. Location of the sections for the model of the data center machine room in St. Petersburg. a) section of the model in the x-y plane at el. +0.300 m from the floor level (level of IT equipment location in the racks); b) section of the model in the y-z plane perpendicular to the center of the rows of the racks

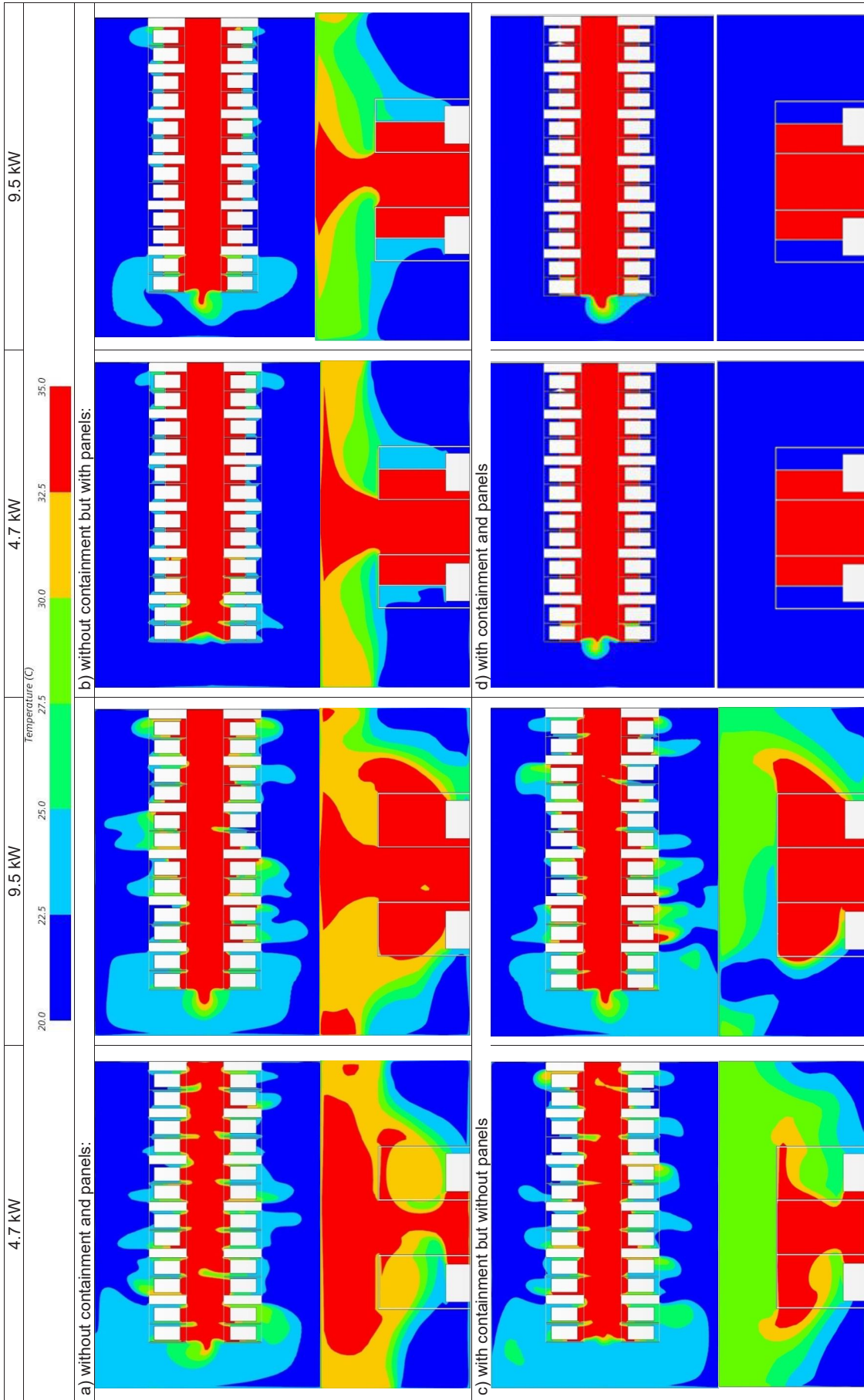


Fig. 11. Air temperature fields (°C) for the machine room for different methods of hot aisle isolation and capacity of IT equipment in each rack in the y-z and x-y section planes

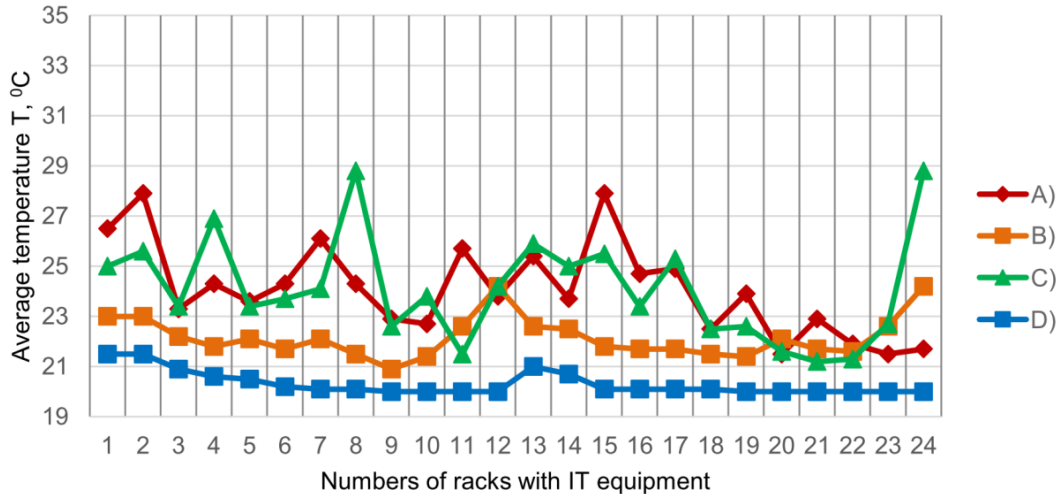


Fig. 12. Average air temperature $T_{inc,i}$ (°C) at the inlet to IT equipment in the racks. Capacity of IT equipment in each rack = 4.7 kW

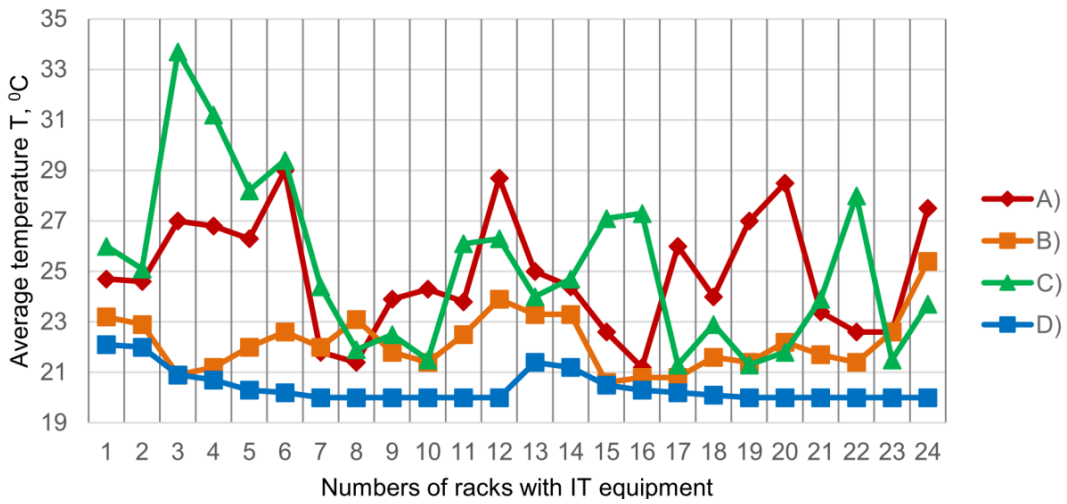


Fig. 13. Average air temperature $T_{inc,i}$ (°C) at the inlet to IT equipment in the racks. Capacity of IT equipment in each rack = 9.5 kW

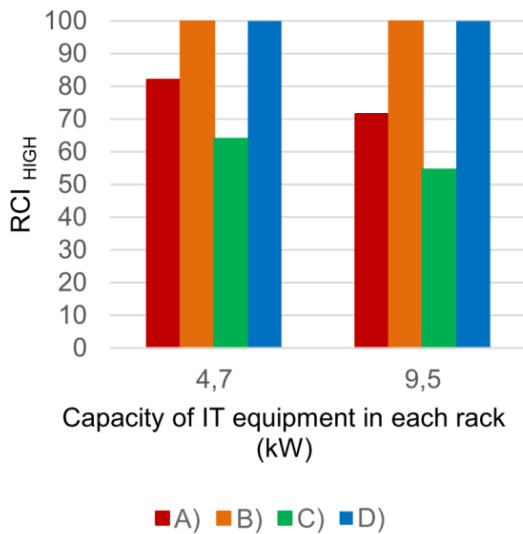


Fig. 14. Values of the dimensionless RCI_{HIGH} index for different methods of hot aisle isolation and capacity of IT equipment in each rack

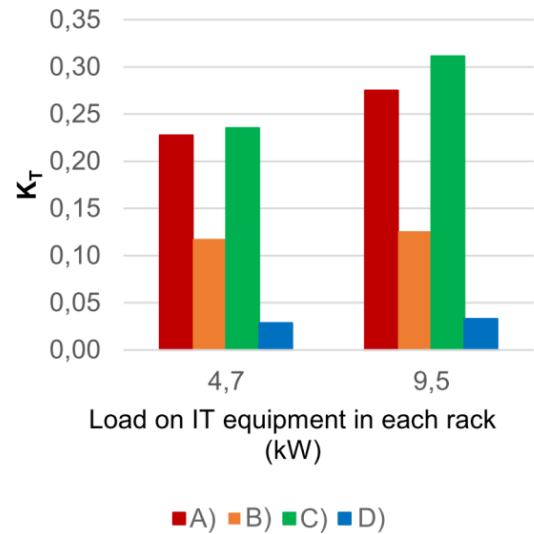


Fig. 15. Values of the dimensionless K_T index for different methods of hot aisle isolation and capacity of IT equipment in each rack

index for these methods does not change with an increase in the capacity of IT equipment in the racks.

2) The minimum values of the RCI_{HIGH} index were obtained for methods A) and C), which do not assume the arrangement of blind panels in the racks. It was also revealed that the value of the RCI_{HIGH} index for isolation method C) (with containment but without panels) is lower than its value for method A) (without containment and panels). This is due to the fact that top containment increases the rate of hot air flow through the racks that are not equipped with panels.

3) With an increase in the capacity of IT equipment in the racks for methods A) and C), the RCI_{HIGH} index becomes lower, i.e., the number of hot spots increases.

As a result of the analysis of the K_r index values for different isolation methods and capacity of IT equipment, the following was established:

1) The isolation method D) is the most effective in terms of air distribution in the data center machine room.

2) The highest value of the K_r index is typical for methods A) and C), which do not assume the arrangement of blind panels in the racks. This means that the efficiency of air distribution for these methods is the lowest among those considered. Besides, the efficiency of air distribution for these methods decreases with an increase in the capacity of IT equipment in the racks.

Conclusions

The comparative analysis of different methods of hot aisle isolation at different capacity values of IT equipment in the data center machine room allows us to draw the following conclusions:

1) The arrangement of top containment for the hot aisle without blind panels in the free rack space as well as the absence of any hot aisle isolation result in the occurrence of hot spots — places where air temperature at the inlet to IT equipment exceeds the maximum recommended value $T_{max-rec} = 27^{\circ}C$. The arrangement of blind panels in the free rack space without top containment for the hot aisle makes it possible to ensure optimal air temperature values at the inlet to IT equipment in the racks. The most effective method to isolate the hot aisle in terms of air distribution in the data center machine room is the one that takes into account the joint arrangement of blind panels in the free rack space and top containment for the hot aisle.

2) For the methods of hot aisle isolation, taking into account the arrangement of blind panels in the free rack space, an increase in the capacity of IT equipment in the racks does not result in the occurrence of hot spots. For the methods of hot aisle isolation without blind panels in the free rack space, an increase in the capacity of IT equipment leads to an increase in the number of hot spots, a deterioration in the circulation of air flows, and a decrease in the efficiency of IT equipment cooling in the data center machine room.

References

- Abbas, A. M., Huzayyin, A. S., Mouneer, T. A., and Nada, S. A. (2021). Effect of data center servers' power density on the decision of using in-row cooling or perimeter cooling. *Alexandria Engineering Journal*, Vol. 60, Issue 4, pp. 3855–3867. DOI: 10.1016/j.aej.2021.02.051.
- Almoli, A. M. (2013). Air flow management inside data centres. PhD Thesis in Mechanical Engineering.
- ASHRAE (2016). ASHRAE TC9.9 Data Center Power Equipment Thermal Guidelines and Best Practices. [online] Available at: https://www.ashrae.org/File%20Library/Technical%20Resources/Bookstore/ASHRAE_TC0909_Power_White_Paper_22_June_2016_REVISED.pdf [Date accessed September 12, 2022].
- Capozzoli, A., Serale, G., Liuzzo, L., and Chinnici, M. (2014). Thermal metrics for data centers: a critical review. *Energy Procedia*, Vol. 62, pp. 391–400. DOI: 10.1016/j.egypro.2014.12.401.
- Cho, J., Park, C., and Choi, W. (2021). Numerical and experimental study of air containment systems in legacy data centers focusing on thermal performance and air leakage. *Case Studies in Thermal Engineering*, Vol. 26, 101084. DOI: 10.1016/j.csite.2021.101084.
- Cho, J. and Woo, J. (2020). Development and experimental study of an independent row-based cooling system for improving thermal performance of a data center. *Applied Thermal Engineering*, Vol. 169, 114857. DOI: 10.1016/j.applthermaleng.2019.114857.
- Herrlin, M. K. (2007). Improved data center energy efficiency and thermal performance by advanced airflow analysis. *Digital Power Forum*, San Francisco, USA, pp. 10–12.
- Huang, Z., Dong, K., Sun, Q., Su, L., and Liu, T. (2017). Numerical simulation and comparative analysis of different airflow distributions in data centers. *Procedia Engineering*, Vol. 205, pp. 2378–2385. DOI: 10.1016/j.proeng.2017.09.854.
- Huawei (2019). E9000 Server V100R001 User Guide. [online] Available at: <https://www.manualslib.com/manual/1668286/Huawei-E9000.html> [Date accessed September 12, 2022].
- Nada, S. A., Said, M. A., and Rady, M. A. (2016). CFD investigations of data centers' thermal performance for different configurations of CRACs units and aisles separation. *Alexandria Engineering Journal*, Vol. 55, Issue 2, pp. 959–971. DOI: 10.1016/j.aej.2016.02.025.
- Niemann, J., Brown, K., and Avelar, V. (2008). Hot-aisle vs. cold-aisle containment for data centers. White Paper 135. [online] Available at: https://www.missioncriticalmagazine.com/ext/resources/MC/Home/Files/PDFs/WP-APC-Hot_vs_Cold_Aisle.pdf [Date accessed September 12, 2022].
- Norouzi-Khangah, B., Mohammadsadeghi-Azad, M. B., Hoseyni, S. M., and Hoseyni, S. M. (2016). Performance assessment of cooling systems in data centers; Methodology and application of a new thermal metric. *Case Studies in Thermal Engineering*, Vol. 8, pp. 152–163. DOI: 10.1016/j.csite.2016.06.004.
- Ponomarev, N. S., Martianova, A. Yu., and Dmitriev, Yu. A. (2021). Assessment of heat gain from server equipment. *Bulletin of Civil Engineers*, Vol. 2 (85), pp. 166–172. DOI: 10.23968/1999-5571-2021-18-2-166-172.
- Priyadumkol, J. and Kittichaikarn, C. (2014). Application of the combined air-conditioning systems for energy conservation in data center. *Energy and Buildings*, Vol. 68, Part A, pp. 580–586. DOI: 10.1016/j.enbuild.2013.07.082.
- Rasmussen, N. (2012). Improving rack cooling performance using airflow management blanking panels. White Paper 44. [online] Available at: https://www.apc.com/us/en/download/document/SPD_SADE-5TPLKQ_EN/ [Date accessed September 12, 2022].
- Tatchell-Evans, M., Kapur, N., Summers, J., Thompson, H., and Oldham, D. (2017). An experimental and theoretical investigation of the extent of bypass air within data centres employing aisle containment, and its impact on power consumption. *Applied Energy*, Vol. 186, Part 3, pp. 457–469. DOI: 10.1016/j.apenergy.2016.03.076.
- Timonin, Yu. (2018). Concepts of data center cooling arrangement: in search of maximum efficiency. *STA*, No. 1, pp. 84–90.
- Vertiv (2022). Liebert CRV, Row-based Cooling Unit. [online] Available at: <https://www.vertiv.com/ru-emea/products-catalog/thermal-management/in-row-cooling/liebert-crv-row-based-cooling-unit/> [Date accessed September 12, 2022].
- Zhang, M., An, Q., Long, Z., Pan, W., Zhang, H., and Cheng, X. (2017). Optimization of airflow organization for a small-scale data center based on the cold aisle closure. *Procedia Engineering*, Vol. 205, pp. 1893–1900. DOI: 10.1016/j.proeng.2017.10.279.

АНАЛИЗ ЭФФЕКТИВНОСТИ СИСТЕМЫ ОХЛАЖДЕНИЯ

Юрий Александрович Дмитриев
Санкт-Петербургский государственный архитектурно-строительный университет
2-я Красноармейская ул., д. 4, 190005, Санкт-Петербург, Россия

E-mail: 6377227@mail.ru

Аннотация

Введение: Основной задачей систем охлаждения в помещении машинного зала центра обработки данных является поддержание оптимальных параметров воздуха на входе в IT-оборудование в соответствии с действующими нормативными документами. Если значение температуры воздуха на входе в IT-оборудование превышает оптимальное значение, то возникают так называемые «горячие точки» – работа IT-оборудования в таких местах может привести к его перегреву и выходу из строя. Основной причиной возникновения «горячих точек» является нарушение циркуляции воздуха между «горячим» и «холодным» коридорами. **Целью данного исследования** является анализ влияния различных способов изоляции «горячего» коридора на эффективность системы охлаждения IT-оборудования. Использован следующий метод: Моделирование в программном комплексе STAR-CCM+ различных способов изоляции «горячего» коридора при различных значениях мощности IT-оборудования. **В результате** исследования теплового и воздушного режимов в ЦОД выявлен наиболее рациональный способ устройства изоляции «горячего» коридора – горизонтальные ограждения над коридором с вертикальными глухими панелями в свободном пространстве стоек.

Ключевые слова: центр обработки данных, температура воздуха, холодный коридор, горячий коридор, вычислительная гидродинамика (CFD).

REPAIR MORTARS OBTAINED BY PLASMA MODIFICATION AND VORTEX ACTIVATION

Valentin Ushkov¹, Ruslan Ibragimov*², Oleg Figovsky³, Svetlana Samchenko¹

¹ National Research University Moscow State University of Civil Engineering
Yaroslavskoye Shosse, 26, 129337, Moscow, Russia

² Kazan State University of Architecture and Engineering
Zelenaya st., 1, 420043, Kazan, Russia

³ Polymate International Nanotechnology Research Center, Israeli Association of Inventors
Shimkin Street, 3a, 34750, Haifa, Israel

*Corresponding author: rusmag007@yandex.ru

Abstract

Introduction: The service life of reinforced-concrete structures can be increased with the use of effective repair compositions obtained by activating the original components. **Purpose of the study:** We aimed to develop effective repair compounds obtained by activating the original components. **Methods:** To process the original components, low-temperature non-equilibrium plasma (LTNP) and electromagnetic activation in a vortex layer device were used. In the course of the study, we used polypropylene, steel, glass, and basalt fiber and fiber made of structured ferromagnetic microwire. Electron microscopy and X-ray diffraction analysis were applied. **Results:** It was established that the combined use of the above methods for the modification of raw components makes it possible to improve the strength of these materials by more than 50%, which is due to the characteristics of structure formation in the developed compositions. For instance, LTNP increases the amount of portlandite and reduces the main phases of cement stone — C_3S and $\beta-C_2S$, and vortex activation contributes to an increase in the total number of crystalline phases. Quartz powder particles processed in an electromagnetic mill are characterized by layered structure, high surface roughness, large developed cracking, as well as inclusions as a result of impact action. All that improves the physical and mechanical properties of the resulting repair compositions by an average of 20%. Repair compositions additionally treated with plasma modification feature new hydrated formations on quartz grains.

Keywords

activation, fiber, plasma, vortex layer.

Introduction

Improving performance of fine-grained cement concretes and repair mortars (hereinafter referred to as repair compositions) is one of the actively developing areas in construction material engineering (Chun et al., 2022; Teixeira et al., 2019). The analysis of scientific and technical literature showed that the handling ability as well as the physical and mechanical properties of building composites based on Portland cement can be improved by the following methods:

- activation of raw components:
 - mechanical, chemical, mechanochemical, and plasma activation of Portland cement (Fediuk, 2016; Ibragimov et al., 2019; Sun et al., 2021);
 - mechanical, magnetochemical, electrochemical, and plasma activation of mixing water (Fedosov et al., 2017);
 - mechanochemical and plasma activation of mineral filler and/or fine aggregate (Abbas et al., 2023; Kalyadin et al., 2019);
- dispersed reinforcement of concretes and repair compositions (metal, natural (glass and

basalt), polymer (polypropylene or glass composite), vegetable (cellulose) fiber or organic (carbon) fiber) (Fediuk et al., 2017; Ruslan et al., 2022);

- the use of nano-additives of various chemical nature (Khuzin and Ibragimov, 2021);
- combination of the methods listed above to improve the performance of building composites (Ma et al., 2017).

Mechanochemical (or mechanical) activation of the binder and fine aggregates is widely used to improve the performance of building composites. Mechanochemical activation of Portland cement not only increases its specific surface area but also changes the structure of the surface layer of Portland cement particles, promotes its amorphization (Chun et al., 2022). To ensure such Portland cement activation, vortex layer devices (Ibragimov and Korolev, 2022) and vibration mills of various designs or high-energy ball milling (Khamatova et al., 2017) are most often used. During activation, the shape of Portland cement particles changes from angular to a more rounded one. At the same time, the milling fineness of Portland cement increases, which leads

to a significant increase in compressive strength (up to 49%) and tensile strength in bending (up to 26%) of sand-cement mortars without increasing their water-cement ratio (in equally easily workable mixes) (Khozin et al., 2021).

Silica-containing components (fillers, fine aggregate) activated in centrifugal planetary mills and vortex layer devices play a significant role in the structure formation of cement composites. Plasma modification of raw components (Portland cement, quartz sand, and mixing water), used to improve the performance of cement composites, in particular, repair compositions, is of particular interest (Kalyadin et al., 2019). The shape of quartz sand particles after processing is quite important since it affects the hydration parameters and the structure formation of cement stone. This issue shall be studied more thoroughly (Li et al., 2022).

To obtain repair compositions with low shrinkage, high physical and mechanical properties and crack resistance, fibers of various chemical nature and size are used: metal (steel), polymer (polypropylene, polyethylene terephthalate, or glass composite), mineral (glass or basalt), and vegetable (cellulose). The effectiveness of the fiber depends on its chemical nature, and, consequently, its adhesion to cement stone, fiber diameter and length, volume content, and its distribution in the mineral matrix (Feng et al., 2020; Yang et al., 2020).

One of the effective methods to obtain repair compositions is a combination of low-temperature non-equilibrium plasma or vortex activation and effective fiber reinforcement. In this regard, the purpose of our study is to obtain highly effective repair compositions with application of low-temperature non-equilibrium plasma or vortex activation and fiber modification.

Subject, tasks, and methods

To prepare the compositions, we used Portland cement CEM I 42.5 N, corresponding to GOST 31108, and fractionated quartz sand of class I, corresponding to GOST 8736 with a content of dust-like and clay particles of less than 3% by weight.

Polypropylene, steel, glass, and basalt fibers as well as fiber made of structured ferromagnetic microwire

were used as the fiber. Its physical and mechanical properties are shown in Table 1. To obtain the fiber, we used alkali-resistant glass fiber manufactured by Owens Corning (Spain), basalt fiber manufactured by Alyans-Strointelnie Tekhnologii LLC, and polypropylene fiber manufactured by Fibra Lyuks LLC.

Portland cement, quartz sand, and water were treated in low-temperature non-equilibrium plasma (LTNP) in a barrier discharge and flow mode, with the use of a laboratory installation and according to the method proposed by Bruyako et al. (2014). Portland cement, gypsum plaster, and limestone were treated in an electromagnetic mill (EM), model 297, manufactured by Regionmettrans LLC. In their paper, Ibragimov et al. (2019) presented a standard design of a vortex layer device.

The samples of repair compositions hardened under normal physical conditions: relative humidity — 100%, temperature — $20 \pm 2^\circ\text{C}$. The strength of the samples in compression, bending and tension was determined according to GOST 5802 in 1, 3, 7, 14, and 28 days of hardening, with the use of an Instron 3382 hydraulic press and a WDW-100E tensile testing machine, and the setting time was determined according to GOST 56587.

The microstructure of cement stone was studied using a Merlin high-resolution field-emission scanning electron microscope by CARL ZEISS. The splits of the cement stone samples were coated with Au/Pd alloy in the ratio 80/20 using a Quorum T150 ES high-vacuum unit.

The X-ray diffraction analysis was carried out using a D2 Phaser diffractometer manufactured by Bruker (Germany) to study raw materials and new formations in the structure of hardened cement stone in the Bragg–Brentano geometry with application of monochromatic CuK α radiation ($\lambda = 1.54178 \text{ \AA}$), in step scanning mode.

To evaluate the effectiveness of the developed repair composition, industrial construction mixes of such brands as Mapegrout Thixotropic, Structurite 100, and CarbonWrap® Repair ST, manufactured by Mapei, Thoro, and NTsK LLC, were used.

The repair compositions were prepared in accordance with GOST 58277. The consistency of

Table 1. Physical and mechanical properties of fiber used in the course of study

Fiber	Dimensions		Density, kg/m ³	Tensile strength, MPa	Relative elongation at break, %	Modulus of elasticity in tension, GPa
	Length, mm	Diameter, μm				
Steel	15	300	7800	1870	3.6	200.6
Glass	6	14	2680	2500	2.5	72.4
Basalt	6	16	2670	2200	2.5	76.9
Polypropylene, grade VSM 6 (0.6)	6	20	910	240	212	3.8
Fiber made of structured ferromagnetic microwire	10	15.2	7300	3500	3.2	154.7

mortar mixes was evaluated in accordance with GOST 5802. The bond strength of the repair compositions with concrete was determined according to GOST 58277, frost resistance — according to GOST 10060, water resistance — according to GOST 12730.5.

Results and discussion

Mechanical and thermal action in an EM destroy the crystalline structure of cement clinker minerals, which is manifested in reduced coherent scattering regions. The most significant changes are observed for C₃S (the average size of crystallites decreases by 21%), C₂S (by 18%), and periclase (by 29%); the average size of C₃A cubic and C₄AF crystallites remains virtually unchanged. Table 2 shows the analysis of the X-ray diffraction patterns of cement stone obtained by treating Portland cement with LTNP.

Under the action of low-temperature plasma, the crystal hydrate layer on the surface of Portland cement particles is destroyed and water evaporates from their surface. This is confirmed by a large difference in the hardening rates of aged and partially hydrated Portland cement and Portland cement treated with LTNP.

The action of LTNP in Portland cement treatment (or vortex activation in the EM) changes the mineralogical composition of cement stone studied after 28 days of hardening. LTNP increases the amount of portlandite and reduces the main phases of cement stone — C₃S and β-C₂S, which indicates a more complete hydration of Portland cement. Vortex activation contributes to an increase in the total number of crystalline phases, portlandite, which naturally causes a decrease in the content of the initial phases of Portland cement, increasing the degree of its hydration.

In the course of the study, we analyzed the microstructure of cement stone obtained as a result of Portland cement treatment with LTNP (Fig. 1). The influence of Portland cement activation on the structure of cement stone is characterized by such a

distinctive feature as new crystalline formations with far less dispersion. The new formations crystallize in a more finely dispersed form, smaller pores and capillaries of cement stone are formed. Together with the higher degree of hydration, this leads to the formation of a dense structure of cement stone, which naturally has a higher strength.

The compressive strength of cement stone during Portland cement treatment with LTNP increases by 16.2–20.4%, and the bending strength of sand-cement mortar increases by 18.1–22.3%. Portland cement activation in the EM makes it possible to increase the compressive strength of cement stone on the first day 2.2 times, on the 28th day — by 35% (Fig. 2).

The treatment of quartz sand grains with LTNP results in a decrease in the total surface area of the grains by 10.6–20.3%. It was established that with an increase in the geometric dimensions of quartz

Table 2. Mineralogical composition of cement stone based on the initial Portland cement and Portland cement treated with LTNP

Phase composition of cement	Phase content in Portland cement, % wt.		
	Initial cement	Cement treated with LTNP	Cement treated in the EM
Ca ₃ SiO ₅ (C ₃ S)	22.7	21.5	19.9
Ca ₂ SiO ₄ (β-C ₂ S)	14.4	14.0	13.8
Amorphous phase	40.0	40.0	38.6
C ₄ AF	8.5	8.3	7.9
Ca(OH) ₂	8.5	11.2	12.8
Ettringite	4.0	3.5	5.4
CaCO ₃	1.9	1.5	1.6

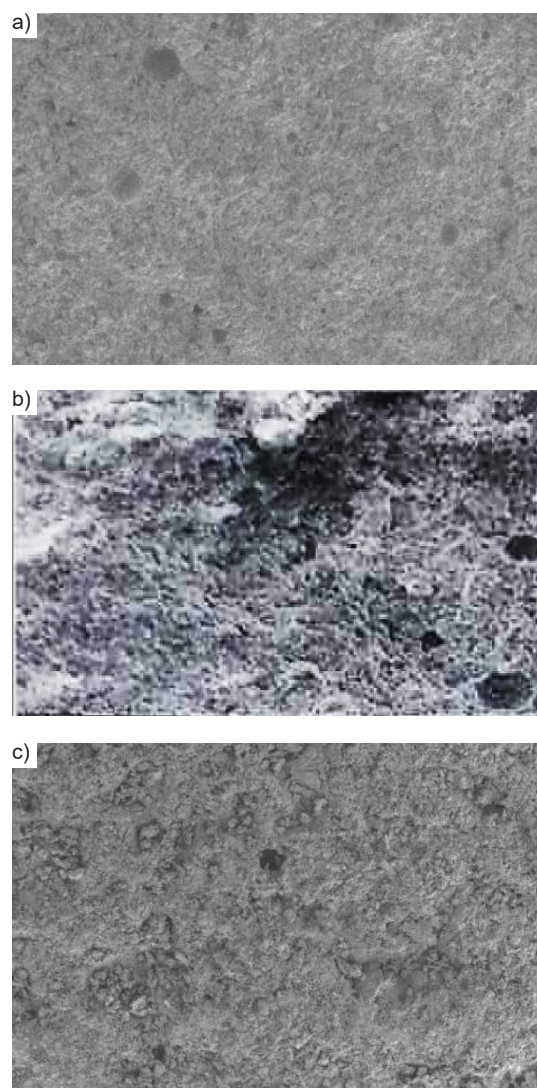


Fig. 1. Microstructure of cement stone (X100 magnification): a — reference composition; b — obtained by Portland cement treatment with LTNP; c — obtained by activation in the EM

sand grains, a more significant decrease in the pore surface area is observed. The latter is associated with sand particle surface melting, which naturally leads to amorphization (Fig. 3b).

Quartz powder particles processed in an electromagnetic mill are characterized by layered structure, high surface roughness, large developed cracking, as well as inclusions as a result of impact action. The treatment in an EM is characterized by the following distinctive feature: when quartz sand particles are milled, the grains are separated along individual conglomerates (Fig. 3c) and not along cleavage planes as with the use of a ball or centrifugal mill, which indicates high EM energy density.

The treatment of mixing water and quartz sand with LTNP, followed by repair composition obtaining, ensures a synergistic effect in strength increasing (Fig. 4).

Fig. 5 shows the microstructure of the obtained repair compositions No. 1 (based on quartz sand two times treated with LTNP and mixing water consisting of a mixture of untreated and plasma-modified water at a ratio of 1:1) and No. 5 (reference composition) with X500 magnification. The data presented in Fig. 5 show that the hydration of the compositions obtained by Portland cement treatment with LTNP differs from that of the reference ones. The compositions additionally treated with plasma

modification feature new hydrated formations on quartz grains.

An important parameter of repair compositions is their crack resistance. Rong et al. (2021) as well as Wang et al. (2021) proposed to indirectly evaluate crack resistance by the following ratio: R_{bt}/R_b (R_{bt} — tensile strength, R_b — compressive strength). Table 3 shows how the type of fiber affects the ratio of the samples of the repair compositions obtained by Portland cement activation in the EM.

The data in Table 3 show that the highest crack resistance (value of the ratio) of the repair compositions is observed with the introduction of metal fiber (the indicator increases by 40%). With the introduction of polypropylene fiber, this indicator increases by 27%.

Shen et al. (2020) indicated that the introduction of fiber makes it possible to increase the impact strength of building materials. Also of interest is the study of the effect of polypropylene and metal fibers on the impact strength of the repair compositions obtained by Portland cement activation in the EM (Fig. 6). The data in Fig. 6 show the obvious result of dispersed reinforcement, which is an increase in impact strength. Of practical interest are the abscissas of functions, at which the impact strength as well as its relative increase have the maximum value. For instance, the introduction of

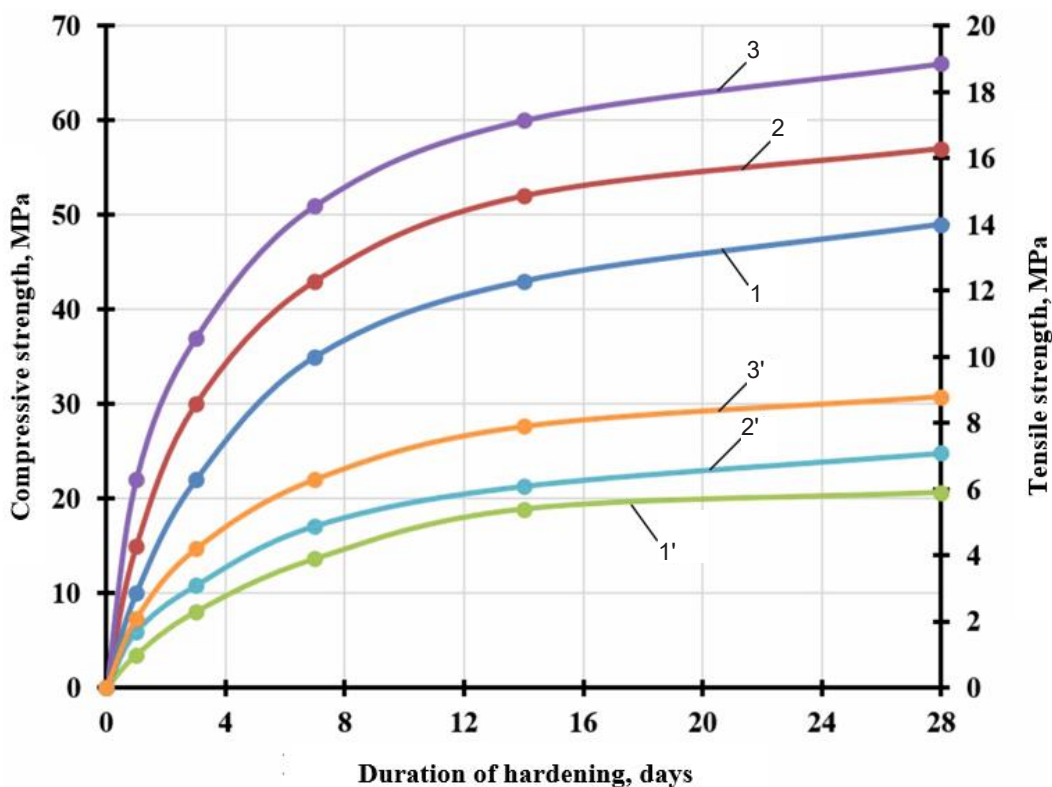


Fig. 2. Compressive strength (1, 2, 3) and bending strength (1', 2', 3') of cement stone vs. duration Portland cement hardening: 1 — reference composition; 2 — treated with LTNP; 3 — obtained by vortex activation

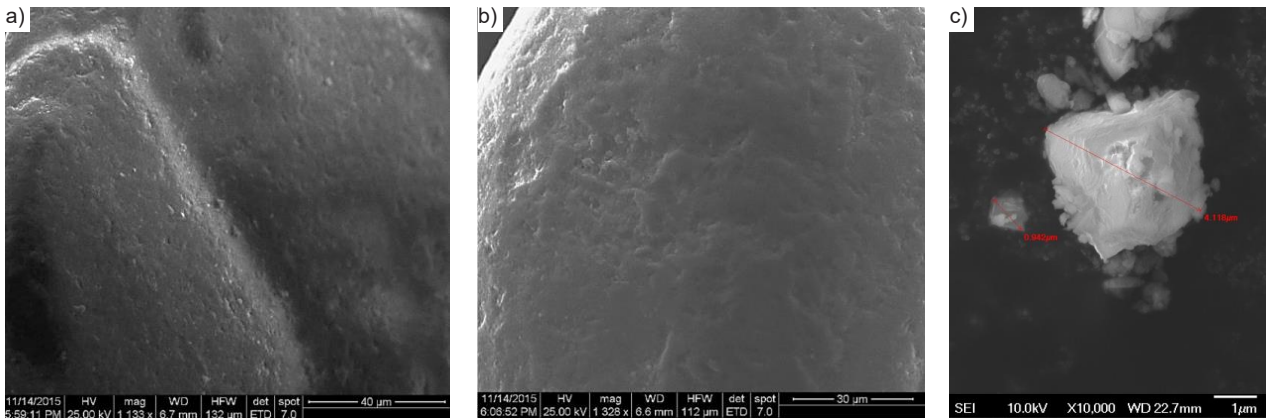


Fig. 3. Photos of quartz sand grains: a — before treatment (X1000) b — after treatment with LTNP (X1300); c — in a vortex mill (X10000)

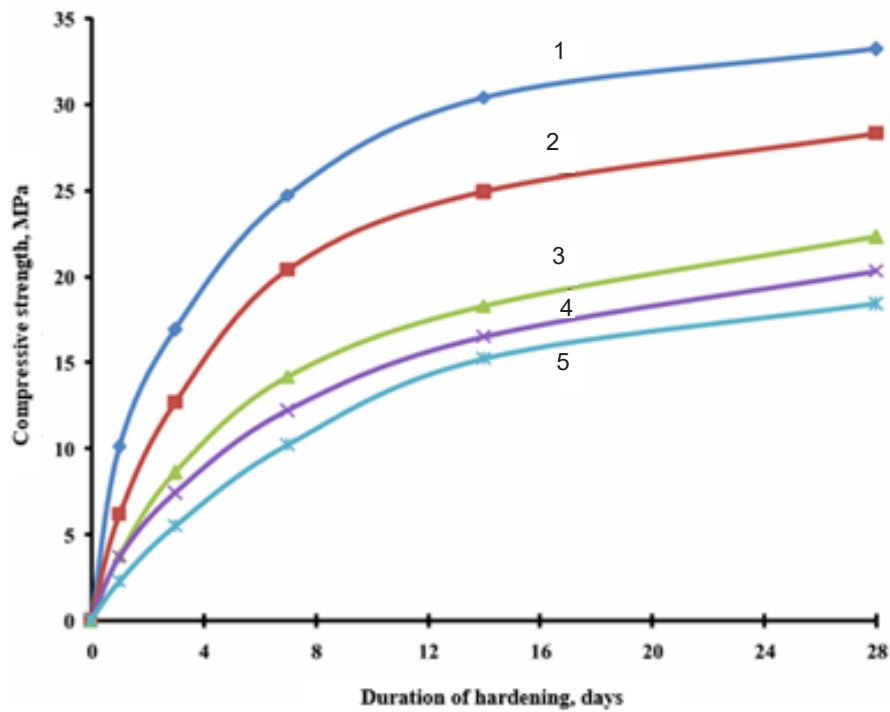


Fig. 4. Dynamics of strength gain in the studied compositions

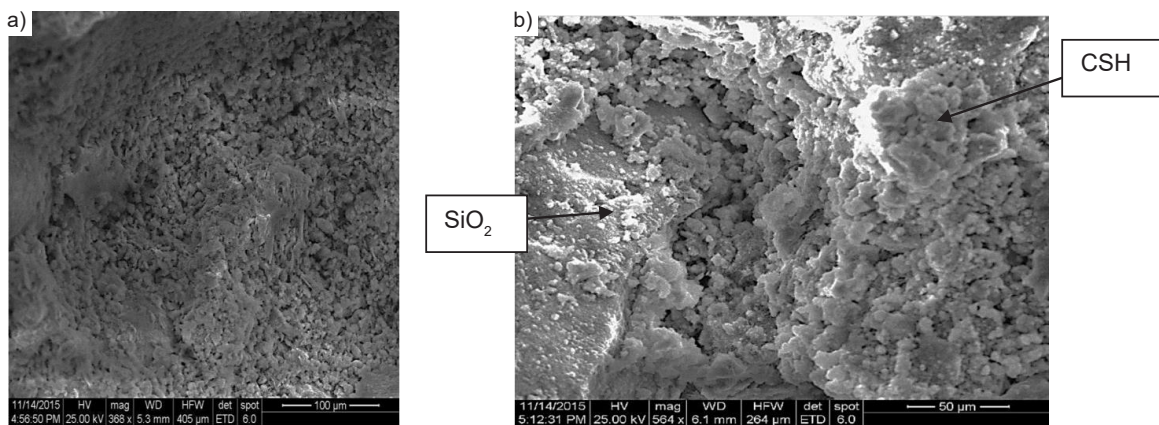


Fig. 5. Microstructure of the repair compositions: a — No. 5; b — No. 1

Table 3. Ratio for the repair compositions under study

Fiber type	Geometric characteristics of the fiber		R_{br}/R_b
	d, mm	L, mm	
Reference composition			0.131
Metal	0.3	15	0.183
Polypropylene	$20 \cdot 10^{-3}$	6	0.167

polypropylene fiber increases the impact strength 1.72 times at its volume content of 1%, and the introduction of metal fiber — 2.6 times at its volume content of 1.5%. It should be noted that the volume content of fiber, at which is more than. Moreover, for polypropylene fiber, more than for metal fiber and equals 2. Although they noted an increase in impact strength with fiber introduction, Shen et al. (2019) did not show how the ratio depends on the type of fiber.

One of the most important structural indicators of repair compositions is durability. In this regard, the influence of aggressive media on the corrosion resistance of cement stone obtained by Portland cement activation in the EM was studied. As aggressive media, 0.1 N nitric, sulfuric and hydrochloric acids were used. The test results show that Portland cement treatment in the EM allows for the formation of cement stone that is more resistant to the effects of the considered aggressive media, which complements the findings of our colleagues (Shen et al., 2019). The resistance of the repair compositions in aggressive media increases by 11–15%, depending on the medium, which increases the durability of such compositions and their service life.

Table 4 shows the handling ability of the developed repair composition as well as its physical and mechanical properties in comparison with the existing repair compositions. The developed repair composition has steel fiber reinforcement in the amount of 0.4% by volume.

The data in Table 4 show that the developed dispersion-reinforced repair composition obtained by Portland cement treatment with LTNP or activation in the EM outmatches the known industrial repair compositions used to eliminate defects and damages in reinforced-concrete structures.

Conclusions

1. LTNP increases the amount of portlandite and reduces the main phases of cement stone — C_3S and $\beta-C_2S$, which indicates a more complete hydration of Portland cement. Vortex activation contributes to an increase in the total number of crystalline phases, portlandite, which naturally causes a decrease in the content of the initial phases of Portland cement, increasing the degree of its hydration. The influence of Portland cement activation on the structure of cement stone is characterized by such a distinctive feature as new crystalline formations with far less dispersion. The new formations crystallize in a more finely dispersed form, smaller pores and capillaries of cement stone are formed.

2. The treatment of quartz sand grains with LTNP results in the amorphization of the surface. Quartz powder particles processed in an electromagnetic mill are characterized by layered structure, high surface roughness, large developed cracking, as well as inclusions as a result of impact action. All that improves the physical and mechanical properties of the resulting repair compositions by an average of 20%. Repair compositions additionally treated with plasma modification feature new hydrated formations on quartz grains.

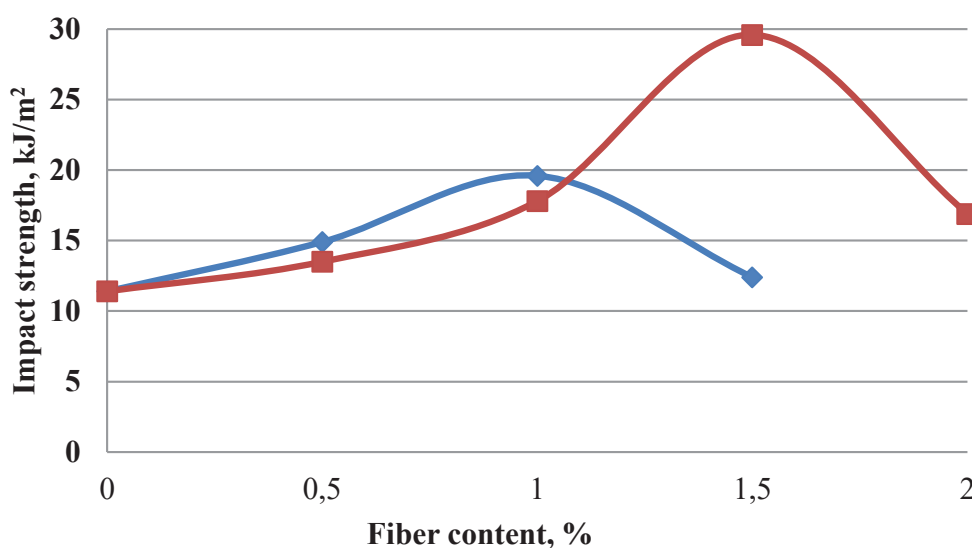


Fig. 6. Impact strength vs. fiber content

Table 4. Handling ability and physical and mechanical properties of the repair compositions

Indicator	Industrial repair compositions			Developed repair composition
	Structurite 100	Mapegrout Thixotropic	CarbonWrap® Repair ST	
Mortar mix consistency	PK 2	PK 2	PK 2	PK 2
Mortar mix properties preservation, min	60	About 60	60	45–50
Maximum filler size, mm	1.5	2.5	2.5	1.5
Mortar mix strength after 28 days of normal hardening, MPa, under: compression bending	65 >7	≥60 ≥8.5	50 ≥8.5	>72 >9.5
Mortar mix adhesion strength after 28 days of hardening, with a concrete base, MPa	>1.5	≥2.0	1.5	>2.8
Frost resistance, number of cycles	200	300	200	300
Watertightness, grade	W10	–	W8	W10

3. Dispersion reinforcement improves the physical and mechanical properties of the developed repair compositions. The value of crack resistance increases with the introduction of metal fiber 40%. With the introduction of polypropylene fiber, this indicator increases by 27%.

4. It was established that the developed dispersion-reinforced repair composition obtained by Portland cement treatment with LTNP or activation

in the EM outmatches the known industrial repair compositions used to eliminate defects and damages in reinforced-concrete structures.

Acknowledgments

The authors express their gratitude to the manufacturers of the repair compositions for the samples provided.

Funding

The study has not received any funding.

References

- Abbas, I. S., Abed, M. H., and Canakci, H. (2023). Development and characterization of eco- and user-friendly grout production via mechanochemical activation of slag/rice husk ash geopolymer. *Journal of Building Engineering*, Vol. 63, Part A, 105336. DOI: 10.1016/j.jobe.2022.105336.
- Bruyako, M. G., Kravtsova, D. V. Yurchenko, V. V., Solov'ev, V. G., and Ushkov, V. A. (2014). Effect of raw materials processing with low temperature non-equilibrium plasma on properties of building mortars. *Stroitel'nye Materialy (Construction Materials)*, No. 12, pp. 68–71.
- Chun, B., Oh, T., Jang, Y. S., Lee, S. K., Lee, J.-H., and Yoo, D.-Y. (2022). Strengthening effect of concrete beams using ultra-rapid-hardening fiber-reinforced mortar under flexure. *Construction and Building Materials*, Vol. 352, 129064. DOI: 10.1016/j.conbuildmat.2022.129064.
- Fediuk, R. (2016). High-strength fibrous concrete of Russian Far East natural materials. *IOP Conference Series: Materials Science and Engineering*, Vol. 116, 012020. DOI: 10.1088/1757-899X/116/1/012020.
- Fediuk, R., Pak, A., and Kuzmin, D. (2017). Fine-grained concrete of composite binder. *IOP Conference Series: Materials Science and Engineering*, Vol. 262, 012025. DOI: 10.1088/1757-899X/262/1/012025.
- Fedosov, S. V., Akulova, M. B., and Slizneva, T. E. (2017). Research of regularity of a structure formation in the cement stone mixed by the mechanoactivated water with the polyvinyl acetate admixture. *Academia. Architecture and Construction*, No. 2, pp. 117–122.
- Feng, S., Xiao, H., and Geng, J. (2020). Bond strength between concrete substrate and repair mortar: Effect of fibre stiffness and substrate surface roughness. *Cement and Concrete Composites*, Vol. 114, 103746. DOI: 10.1016/j.cemconcomp.2020.103746.
- Ibragimov, R. A. and Korolev, E. V. (2022). Influence of electromagnetic field on characteristics of crushed materials. *Magazine of Civil Engineering*, No. 114 (6), 11408. DOI: 10.34910/MCE.114.8.
- Ibragimov, R. A., Korolev, E. V., Deberdeev, T. R., and Leksin, V. V. (2019). Efficient complex activation of Portland cement through processing it in the vortex layer machine. *Structural Concrete*, Vol. 20, Issue 2, pp. 851–859. DOI: 10.1002/suco.201800008.
- Kalyadin, A. Yu., Nalbandyan, G. V., Soloviev, V. G., Bogdanova, A. A., and Ushkov, V. A. (2019). Plasma modification of construction mortar components, an efficient method of increasing their performance. *Vestnik MGSU (Monthly Journal on Construction and Architecture)*, Vol. 14, Issue 5, pp. 548–558. DOI: 10.22227/1997-0935.2019.5.548-558.
- Khamatova, A., Khozin, V., Khohryakov, O., and Yakovlev, G. (2017). Quick setting composition based on steelmaking metallurgical slag. In: *10th International Conference on Environmental Engineering*, April 27–28, 2017, Vilnius, Lithuania. DOI: 10.3846/enviro.2017.026
- Khozin, V. G., Khokhryakov, O. V., and Kozlov, R. V. (2021). The environmental rating of «carbonate» cements is low water demand and concrete based on them. *Izvestija KGASU*, No. 2 (56), pp. 60–66. DOI: 10.52409/20731523_2021_2_60.
- Khuzin, A. and Ibragimov, R. (2021). Processes of structure formation and paste matrix hydration with multilayer carbon nanotubes additives. *Journal of Building Engineering*, Vol. 35, 102030. DOI: 10.1016/j.jobe.2020.102030.
- Li, Z., Lao, J., Wang, L., Lim, N. S., Tan, K. H., and Qian, S. (2022). A review on substitution of natural sand with granite fines in sustainable concrete. *Construction and Building Materials*, Vol. 346, 128417. DOI: 10.1016/j.conbuildmat.2022.128417.
- Ma, C.-K., Mohd Apani, N., Sofrie, C. S. Y., Ng, J. H., Lo, W. H., Awang, A. Z., and Omar, W. (2017). Repair and rehabilitation of concrete structures using confinement: A review. *Construction and Building Materials*, Vol. 133, pp. 502–515. DOI: 10.1016/j.conbuildmat.2016.12.100.
- Rong, H., Dong, W., Yuan, W., Zhou, X. (2021). An improved ring test to assess cracking resistance of concrete under restrained shrinkage. *Theoretical and Applied Fracture Mechanics*, Vol. 113, 102976. DOI: 10.1016/j.tafmec.2021.102976.
- Ruslan, I., Ruslan, B., and Evgenij, K. (2022). The effect of metal and polypropylene fiber on technological and physical mechanical properties of activated cement compositions. *Case Studies in Construction Materials*, Vol. 16, e00882. DOI: 10.1016/j.cscm.2022.e00882.

Shen, D., Liu, X., Zeng, X., Zhao, X., and Jiang, G. (2020). Effect of polypropylene plastic fibers length on cracking resistance of high performance concrete at early age. *Construction and Building Materials*, Vol. 244, 117874. DOI: 10.1016/j.conbuildmat.2019.117874.

Shen, D., Liu, X., Li, Q., Sun, L., and Wang, W. (2019). Early-age behavior and cracking resistance of high-strength concrete reinforced with Dramix 3D steel fiber. *Construction and Building Materials*, Vol. 196, pp. 307–316. DOI: 10.1016/j.conbuildmat.2018.10.125.

Sun, J., Wang, Y., Liu, S., Dehghani, A., Xiang, X., Wei, J., and Wang X. (2021). Mechanical, chemical and hydrothermal activation for waste glass reinforced cement. *Construction and Building Materials*, Vol. 301, 124361. DOI: 10.1016/j.conbuildmat.2021.124361.

Teixeira, O. G., Geraldo, R. H., da Silva, F. G., Gonçalves, J. P., and Camarini, G. (2019). Mortar type influence on mechanical performance of repaired reinforced concrete beams. *Construction and Building Materials*, Vol. 217, pp. 372–383. DOI: 10.1016/j.conbuildmat.2019.05.035.

Wang, L., He, T., Zhou, Y., Tang, S., Tan, J., Liu, Z., and Su, J. (2021). The influence of fiber type and length on the cracking resistance, durability and pore structure of face slab concrete. *Construction and Building Materials*, Vol. 282, 122706. DOI: 10.1016/j.conbuildmat.2021.122706.

Yang, J., Wang, R., and Zhang, Y. (2020). Influence of dually mixing with latex powder and polypropylene fiber on toughness and shrinkage performance of overlay repair mortar. *Construction and Building Materials*, Vol. 261, 120521. DOI: 10.1016/j.conbuildmat.2020.120521.

РЕМОНТНЫЕ СТРОИТЕЛЬНЫЕ РАСТВОРЫ, ПОЛУЧЕННЫЕ ПЛАЗМЕННОЙ МОДИФИКАЦИЕЙ И ВИХРЕВОЙ АКТИВАЦИЕЙ

Валентин Анатольевич Ушков¹, Руслан Абдирашитович Ибрагимов^{*2}, Олег Львович Фиговский³, Светлана Васильевна Самченко¹

¹ Национальный исследовательский Московский государственный строительный университет
Ярославское ш., 26, 129337, Москва, Россия

² Казанский государственный архитектурно-строительный университет
Зеленая ул., 1, 420043, Казань, Россия

³ Международный нанотехнологический исследовательский центр «Polymate»
ул. Шимкина, 3а, 34750, Хайфа, Израиль

*E-mail: rusmag007@yandex.ru

Аннотация

Введение: Повышение срока службы железобетонных конструкций возможно использованием эффективных ремонтных составов, полученных активацией исходных компонентов. **Цель исследования:** разработка эффективных ремонтных составов, полученных активацией их исходных компонентов. **Методы:** для обработки исходных компонентов применяется низкотемпературная неравновесная плазма (НТНП) и электромагнитная активация в аппарате вихревого слоя. В работе используется полипропиленовая, стальная, стеклянная, базальтовая фибра и из структурированного ферромагнитного микропровода. Применялась электронная микроскопия, рентгенофазовый анализ. **Результаты:** Показано, что совместное применение рассмотренных выше способов модификации сырьевых компонентов позволяет повысить прочность указанных материалов более чем на 50 %, что связано с особенностью структурообразования разработанных составов. Так, воздействие НТНП вызывает увеличение количества портландита и снижение основных фаз цементного камня – С3S и β-С2S, а вихревая активация способствует увеличению общего количества кристаллических фаз. Частицы кварцевого порошка, обработанного в электромагнитной мельнице, имеют слоистую структуру, высокую степень шероховатости поверхности, большую, развитую сетку трещин, а также вкрапления в результате ударных воздействий. Указанное повышает физико-механические свойства получаемых ремонтных составов в среднем 20 %. В ремонтных составах, дополнительно обработанных плазменной модификацией, наблюдается скопление гидратных новообразований на зёрнах кварца.

Ключевые слова: активация, фибра, плазма, вихревой слой.

DETERMINING VISCOELASTIC CHARACTERISTICS OF THE ELEMENTS OF MULTI-LAYER STRUCTURES BASED ON ENERGY DISSIPATION ANALYSIS

Artem Tiraturyan*, Evgeniya Uglova, Vladimir Akulov

Don State Technical University
Gagarin square, 1, 344010, Rostov-on-Don, Russia

*Corresponding author: tiraturjan@list.ru

Abstract

Introduction: The deteriorating operating conditions of roads is one of the most important problems facing specialists in the road industry. It is mainly associated with a reduction in the rigidity of road pavements made as extended multi-layer structures. To identify the causes of rigidity reduction, non-destructive testing is used, which is based on solving the inverse coefficient problem of restoring the elastic constants based on the response on the surface. **Purpose of the study:** We aimed to provide a rationale for a new pavement condition indicator that would take into account the history of deformation and loading from a source on the surface, based on which it would be possible to solve the inverse problem of restoring the elastic and viscous characteristics of pavement layers. **Methods:** To do that, we performed mathematical modeling of the stress-strain state of a multi-layer medium based on the solution of a system of dynamic Lamé equations. Viscosity is taken into account by introducing tangents of the angles of wave energy losses in the materials of layers. **Results:** The results obtained in modeling for the first time made it possible to establish the relationship between changes in the modulus of elasticity as well as tangents of the angles of energy losses in pavement layers and the amount of energy dissipation in the structure. **Discussion:** It should be noted that it is possible to switch from the bowl of maximum dynamic deflections as the main pavement condition indicator to the analysis of hysteresis loops on the road structure surface, recorded at different distances from the point of load application and being an analogue of the full bowl of dynamic deflections showing the history of the test object loading.

Keywords

energy dissipation, multi-layer structure, modulus of elasticity, hysteresis loop, falling weight deflectometer.

Introduction

Multi-layer structures are widely used in construction. These are, first of all, roads, where the multi-layer structure is represented by road pavement consisting of the surface course, base course and subgrade perceiving the load from transport and natural factors. The most effective method of non-destructive testing, used to determine the mechanical characteristics of structural layers in road pavement, is the method of determining the modulus of elasticity of the layers, based on solving the inverse problem of restoring the required parameters by maximum vertical displacements (bowl of deflections) recorded experimentally under impact loading. Recent years have witnessed fundamentally new approaches to solving this class of problems: with the use of artificial neural networks (Han et al., 2021; Saltan et al., 2013; Vyas et al., 2021; Wang et al., 2021), genetic algorithms to adjust the theoretical and experimental fields of vertical displacements (Fwa et al., 1997; Le and Phan, 2021; Park et al., 2010; Tsai et al., 2004; Varma et al., 2013; Wang et al., 2019; Zhang et al., 2021), new approaches to dynamic deformation analysis (Bazi and Assi, 2022; Booshehrian and Khazanovich, 2018; Cao et al., 2020; Lee et al., 2018; Zhang et al., 2019; Zhao

et al., 2015), consideration for the wave nature of deformation (Al-Adhami and Gucunski, 2021; Chatti et al., 2017; Marchant and Papagiannakis, 2010; Quan et al., 2022; Zaabar et al., 2014).

The wide range of those approaches is due to the high complexity of the problem being solved, mainly related to its optimization part, which requires correspondence between the parameters calculated with the use of mathematical models and the parameters recorded in field experiments. In most cases, experimental equipment for field measurements is represented by falling weight deflectometers (FWD) — a single-axle trailer with an impact loading mechanism mounted on it and equipment in the form of a beam with geophone sensors or accelerometers to record vertical displacements (Vyas et al., 2021). Mathematical models used to solve the direct problem of the theory of elasticity or viscoelasticity, depending on the formulation, may differ significantly. For example, both viscoelastic models of a multi-layer half-space in an analytical formulation (Al-Adhami and Gucunski, 2021; Bazi and Assi, 2022) and finite-element models of multi-layer structures (Chatti et al., 2017; Marchant and Papagiannakis, 2010; Park et al., 2010; Zaabar et al., 2014) can

be used. As for methods to solve the optimization problem involving the adjustment of theoretical and experimental parameters, well-known gradient methods, such as the Newton method, which make it possible to minimize the standard deviation between the theoretical and experimental values, as well as methods based on genetic algorithms, are used.

In recent years, the search for a pavement condition indicator that would allow specialists to take into account the history of road structure loading and, therefore, evaluate the viscoelastic properties of the materials of layers as accurately as possible has become the main trend in the development of new methods and models to determine the mechanical parameters of structural layers in road pavements. It is obvious that the bowl of maximum deflections cannot serve as that indicator since it is a discrete characteristic, which does not show dynamic deformation processes occurring within 0.07–0.1 s in dynamic loading during full-scale experiments. Chatti et al. (2017) suggested using the amplitude-time characteristics of deformation as such an indicator. However, in that case, it is quite difficult to derive relationships linking the change in the corresponding rigidity characteristics with the change in the shape of the amplitude-time characteristic for each sensor and time delays between the peaks of the amplitude-time characteristics for each of them. Thus, this problem remains unsolved and extremely relevant since the quality of design solutions developed based on the results obtained during the experiments, and, therefore, the cost and durability of operated roads, depend on accuracy of those results.

We aimed to provide a rationale for a new pavement condition indicator that would take into account the history of deformation and loading from a source on the surface, based on which it would be possible to solve the inverse problem of restoring the elastic and viscous characteristics of pavement layers.

To do that, it is necessary to perform numerical modeling of the influence of elastic and viscoelastic characteristics of pavement layers on the proposed condition indicator and obtain corresponding relationships as well as carry out a trial calculation of elastic and viscous characteristics of pavement layers for an operated road section and assess the correspondence of the results obtained with its operating condition.

Methods

During the study, we used a mathematical model for the dynamic stress-strain state (SSS) of a multi-layer half-space. The SSS is determined based on solving a system of dynamic Lamé equations with the use of the Hankel integral transform. Various researchers already considered solutions to this class of problems (Babeshko et al., 1989; Iliopolov et al., 2002; Lyapin et al., 2020; Vorovich et al., 1999).

The mathematical model is based on solving a system of Lamé equations in the following form:

$$(\lambda + 2\mu) \operatorname{grad} \operatorname{div} \mathbf{u} - \mu \operatorname{rot} \operatorname{rot} \mathbf{u} = \rho \frac{\partial^2 \mathbf{u}}{\partial t^2}, \quad (1)$$

where:

λ, μ — the Lamé coefficients,

ρ — the material density,

\mathbf{u} — the matrix vector of displacements.

The equation is solved by decomposing the displacement field into potential and vortex components in the following form:

$$\mathbf{u} = \operatorname{grad} \phi + \operatorname{rot} \psi. \quad (2)$$

By applying this decomposition and the Fourier integral transform to the system of Lamé equations, after a series of transformations we can obtain a system of independent differential equations. The solution to the problem can be found as follows:

$$\mathbf{u}^{(j)}(\mathbf{r}) = \frac{1}{4\pi^2} \iint_{\Gamma_1 \Gamma_2} \mathbf{K}(\alpha, \beta, z, \omega) \times \bar{\mathbf{T}}(\alpha, \beta) \exp[-i\alpha x - i\beta y] d\alpha d\beta, \quad (3)$$

where:

$\mathbf{K}(\alpha, \beta, z, \omega)$ — the components of the kernel of the integral representation of displacements;

$\bar{\mathbf{T}}(\alpha, \beta)$ — the Fourier transform of load $\mathbf{T}(x, y)$;

Γ_j — the integration contour determined by the principle of limiting absorption.

The solution algorithm was earlier described in more detail by Tiraturyan et al. (Tiraturyan, 2017; Tiraturyan et al., 2021; Uglova and Tiraturyan, 2017).

When the mathematical model was being developed, the presence of dissipation in the medium was taken into account by introducing tangents of the angles of wave energy losses in the material $tg\gamma$, considered in this equation when determining reduced vibration frequencies. Therefore, taking into account the principle of correspondence between elastic and viscoelastic problems:

$$\theta_j^2 = \theta_j^{*2} = re\theta_j^2 + i \operatorname{Im} \theta_j^2 = \theta_j^2 (1 + itg\gamma). \quad (4)$$

In terms of the applicability of the SSS modeling results to solving the problem of non-destructive testing of the condition of individual road pavement layers, the main issue is the development of an effective criterion for their condition. The general solution to this problem can be written as follows:

$$\bar{u}(R_i, t) = K(E_j)P(t); \quad (5)$$

$$\bar{u}(R_i, t) - K(E_j)P(t) = 0, \quad (6)$$

where:

$K(E_j)$ — the function that describes the theoretical relationship between the vertical displacements within the bowl of deflections and the modulus of elasticity of the material;

$P(t)$ — the load applied.

$\bar{u}(R_i, t)$ — the bowl of dynamic deflections.

The most effective way is to determine the full bowl of dynamic deflections $\bar{u}(P, R_i, t)$, where $t \in [0, t_{max}]$. The characteristic can be constructed by superimposing the amplitude-time characteristics of deflections $\bar{u}(R_i, t)$ on the loading pulse excited by standard means of dynamic tests $P(t)$. In essence, this characteristic is an analogue of a dynamic hysteresis loop calculated or recorded at characteristic points on the surface of the structure.

On the one hand, the function $\bar{u}(P, R_i, t)$ fully describes the kinetics of changes in the bowl of deflections on the pavement surface over the entire period of observation over object deformation. On the other hand, it is a hysteresis loop, and it can be uniquely characterized by the shape and area, which is an analogue of the energy spent on pavement deformation, determined as follows:

$$W = \int_0^t P(t) \dot{u}(t) dt. \tag{7}$$

Below, we present the results of studying the patterns of changes in this value depending on the rigidity of the structural road pavement layers and their viscosity.

Results and discussion

By using the developed model, we performed a series of numerical experiments to study the influence of the viscosity characteristics and modulus of elasticity of pavement layers on the area of the dynamic hysteresis loop. The tangent of the angle of energy losses in road pavement layers was used as the main viscosity characteristic. During numerical modeling, the following road pavement structure types were adopted (Table 1):

Figs. 1–6 show the results of calculating the areas of the dynamic hysteresis loops.

When the tangent of the angle of energy losses in asphalt concrete layers changes in the range from 0

to 1, the amount of energy dissipation (according to the sensor installed in the center of load application) varies within 14–20%. Smaller changes are typical for pavement structures with thinner layers, and larger changes are typical for thicker packages of asphalt concrete layers. Another characteristic feature is that the tangent of the angle of energy losses in asphalt concrete layers has the greatest effect in the area closest to the impact point, namely at a distance not exceeding 60 cm. The tangent of the angle of energy losses in subgrade soil has an effect in the range of 2–3% of the amount of energy dissipation, however, it is difficult to assign any area within the bowl of deflections to it since it affects all points in the range from 0 to 2.1 m.

The moduli of elasticity, mainly those with respect to subgrade soil, have a greater influence on changes in energy dissipation. For instance, a 4–6-fold change in the modulus of elasticity of subgrade soil results in a similar 3.7–5.7-fold change in energy dissipation. In terms of the conducted numerical experiments on the variation of the moduli of elasticity, the main finding is that the modulus of elasticity of subgrade soil has the greatest influence on changes in the amount of energy dissipation within the entire bowl of deflections. The moduli of elasticity of the intermediate layers have a significant effect within the entire bowl of deflections, and this effect tends to fade at a distance of about 90 cm. The modulus of elasticity of asphalt concrete has the greatest effect in the area from 20 to 120 cm from the point of load application, and beyond that area, this effect tends to fade.

The results obtained during numerical modeling allow us to conclude that it is possible to solve an optimization equation of the following form:

$$\bar{u}(P, R_i, t) - K(E_j, tg\lambda_j)P(t) = 0, \tag{8}$$

where:

Table 1. Road pavement structures on test sections

Road pavement structure No. 1	Modulus of elasticity, MPa / (loss angle tangent)	Road pavement structure No. 2	Modulus of elasticity, MPa / (loss angle tangent)	Road pavement structure No. 3	Modulus of elasticity, MPa / (loss angle tangent)
Layer 1: asphalt concrete — 29 cm	500–12,000 MPa (0 - 1)	Layer 1: asphalt concrete — 20 cm	500–12,000 MPa (0 - 1)	Layer 1: asphalt concrete — 19 cm	500–12,000 MPa (0 - 1)
Layer 2: crushed stone / sand mixture reinforced with cement — 20 cm	200–3000 MPa (0 - 1)	Layer 2: crushed stone / sand mixture reinforced with cement — 30 cm	200–3000 MPa (0 - 1)	Layer 2: crushed stone / sand mixture reinforced with cement — 30 cm	200–3000 MPa (0 - 1)
Layer 3: crushed stone / sand mixture — 40 cm	100–900 MPa (0 - 1)	Layer 3: crushed stone / sand mixture — 20 cm	100–900 MPa (0 - 1)	Layer 3: soil	100–900 MPa (0 - 1)
Layer 4: soil	20–120 MPa (0 - 1)	Layer 4: soil	20–120 MPa (0 - 1)		

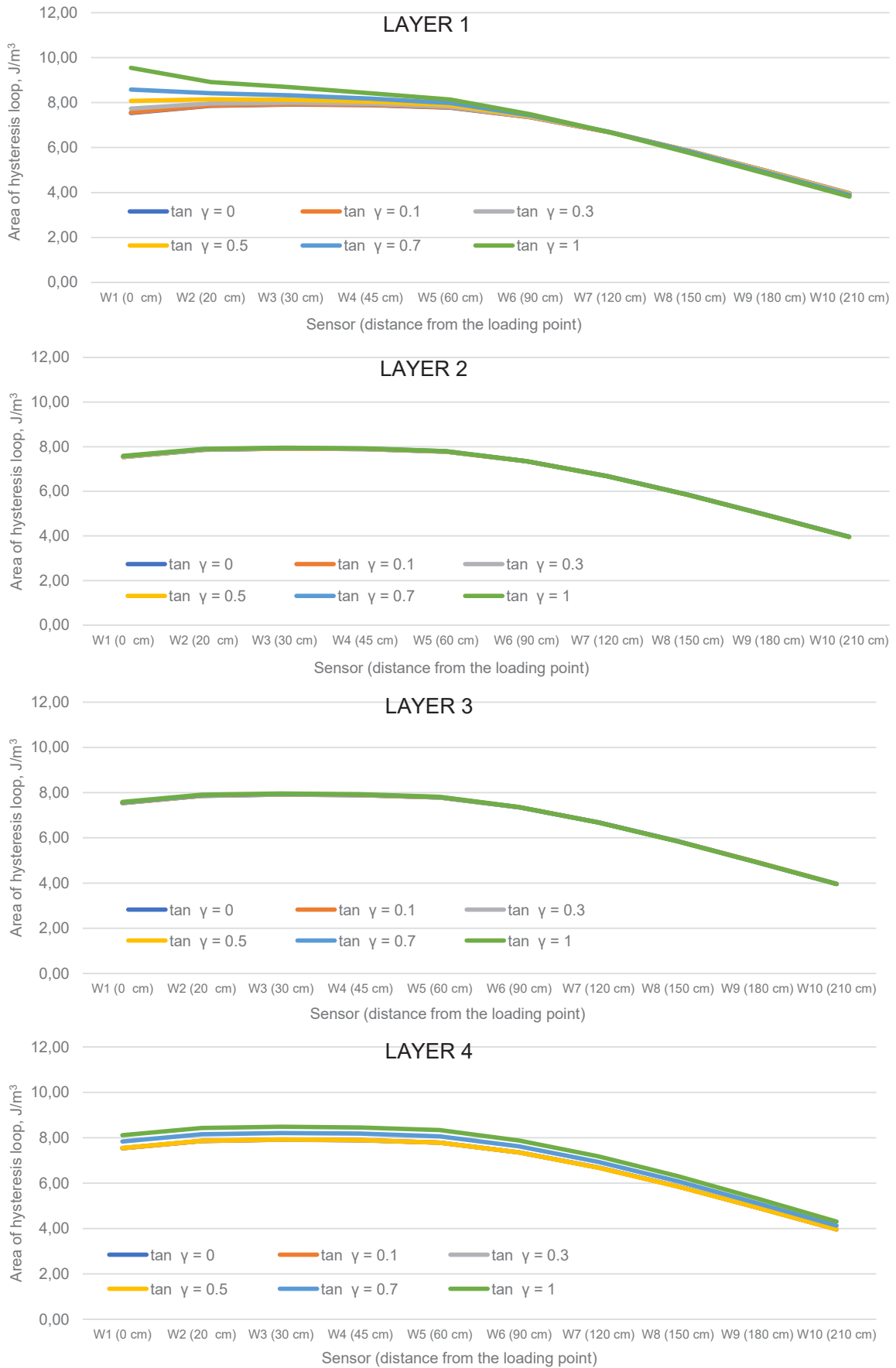


Fig. 1. Modeling the influence of the tangents of the angles of energy losses in pavement layers on the dissipation of impact energy for structure No. 1

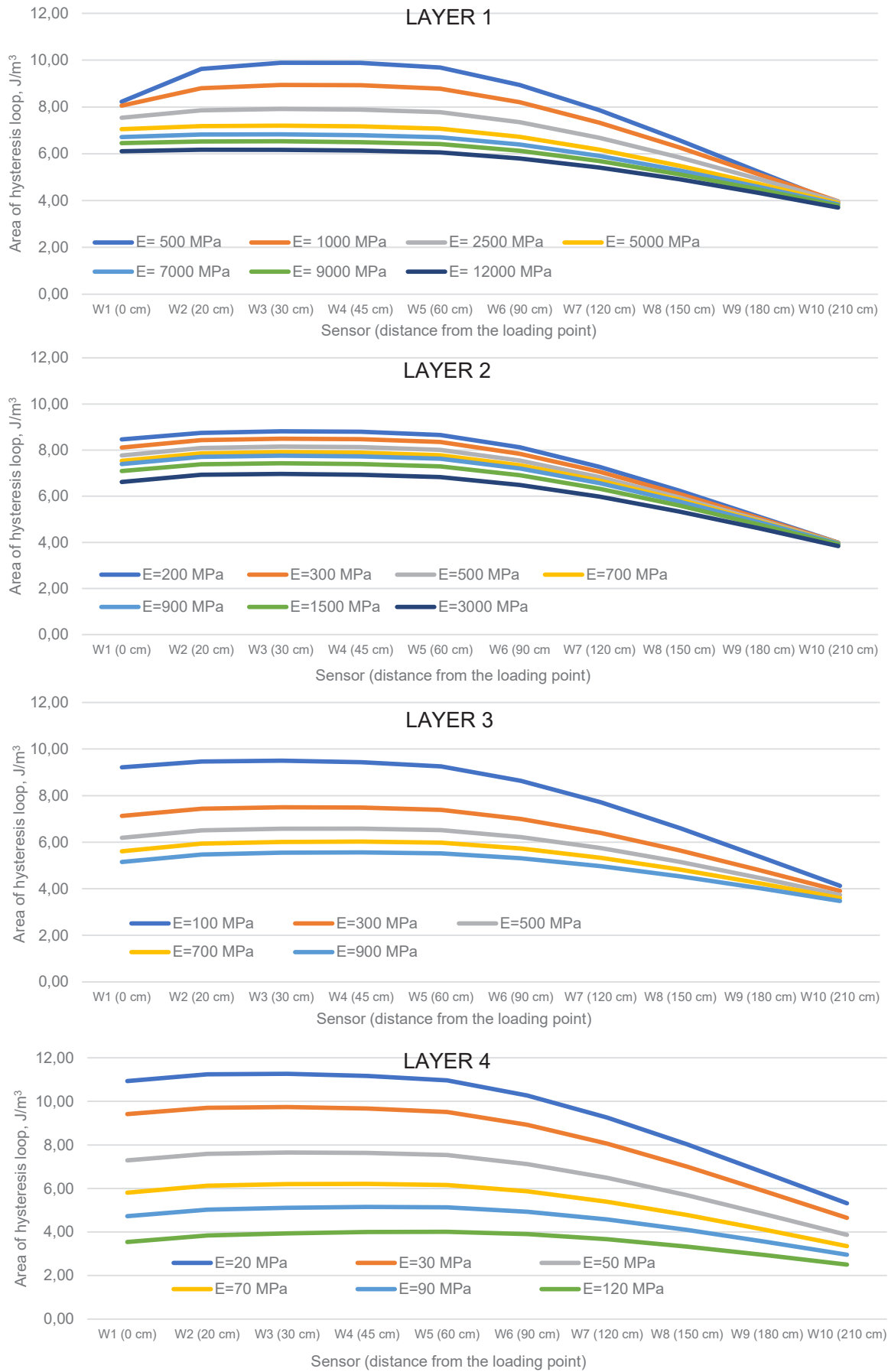


Fig. 2. Modeling the influence of the moduli of elasticity on the dissipation of impact energy for structure No. 1

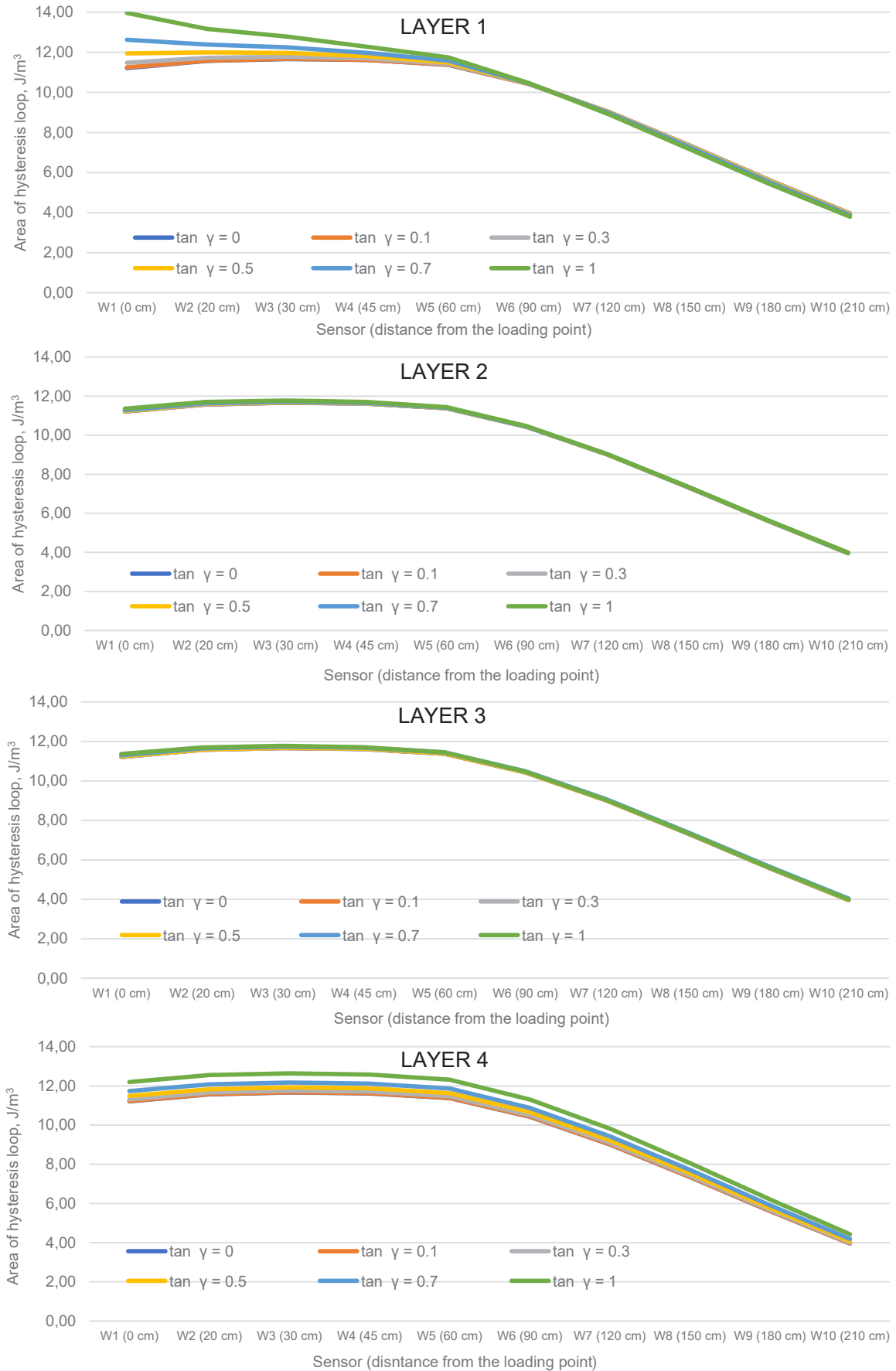


Fig. 3. Modeling the influence of the tangents of the angles of energy losses in pavement layers on the dissipation of impact energy for structure No. 2

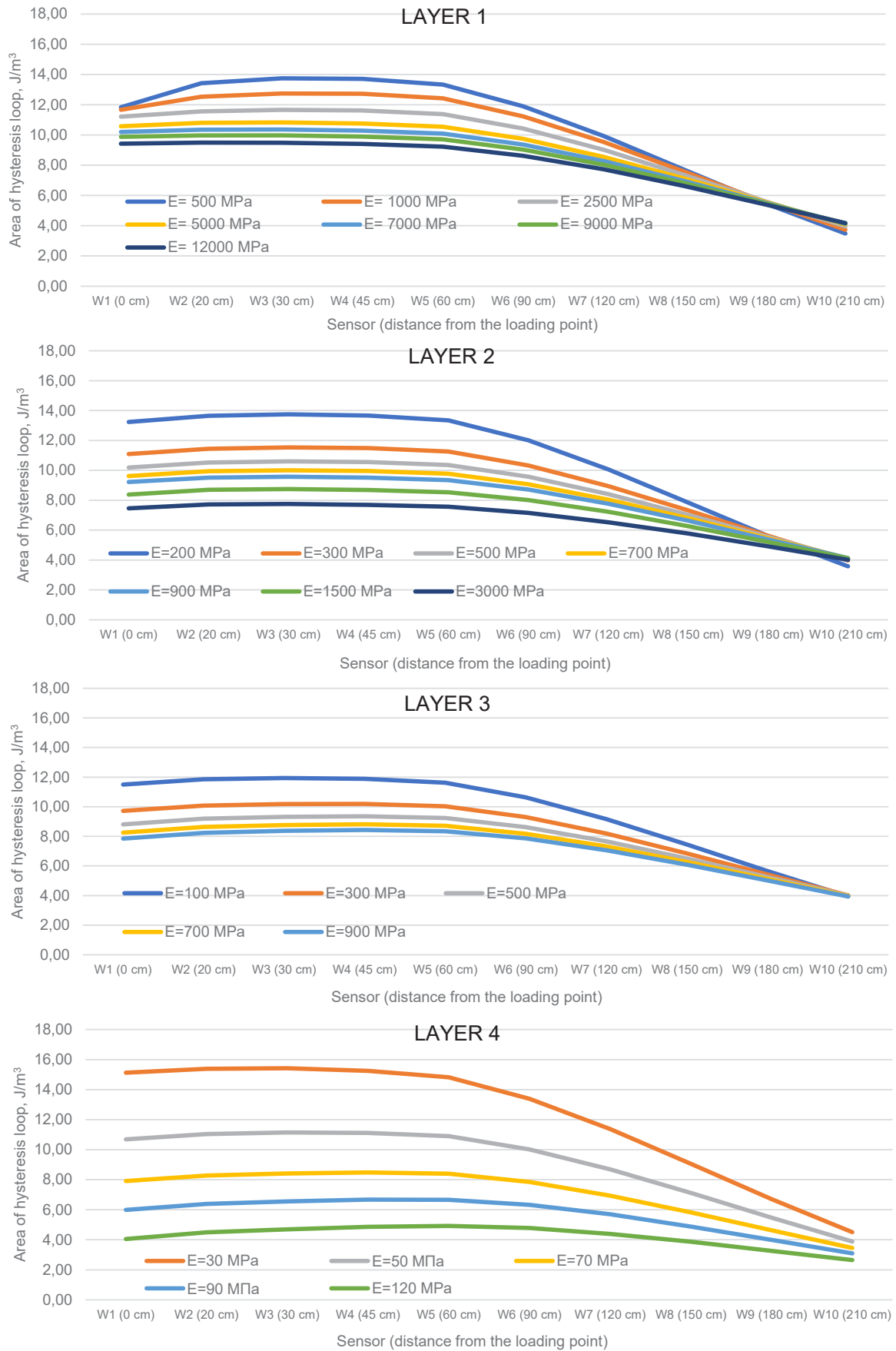


Fig. 4. Modeling the influence of the moduli of elasticity of pavement layers on the dissipation of impact energy for structure No. 2

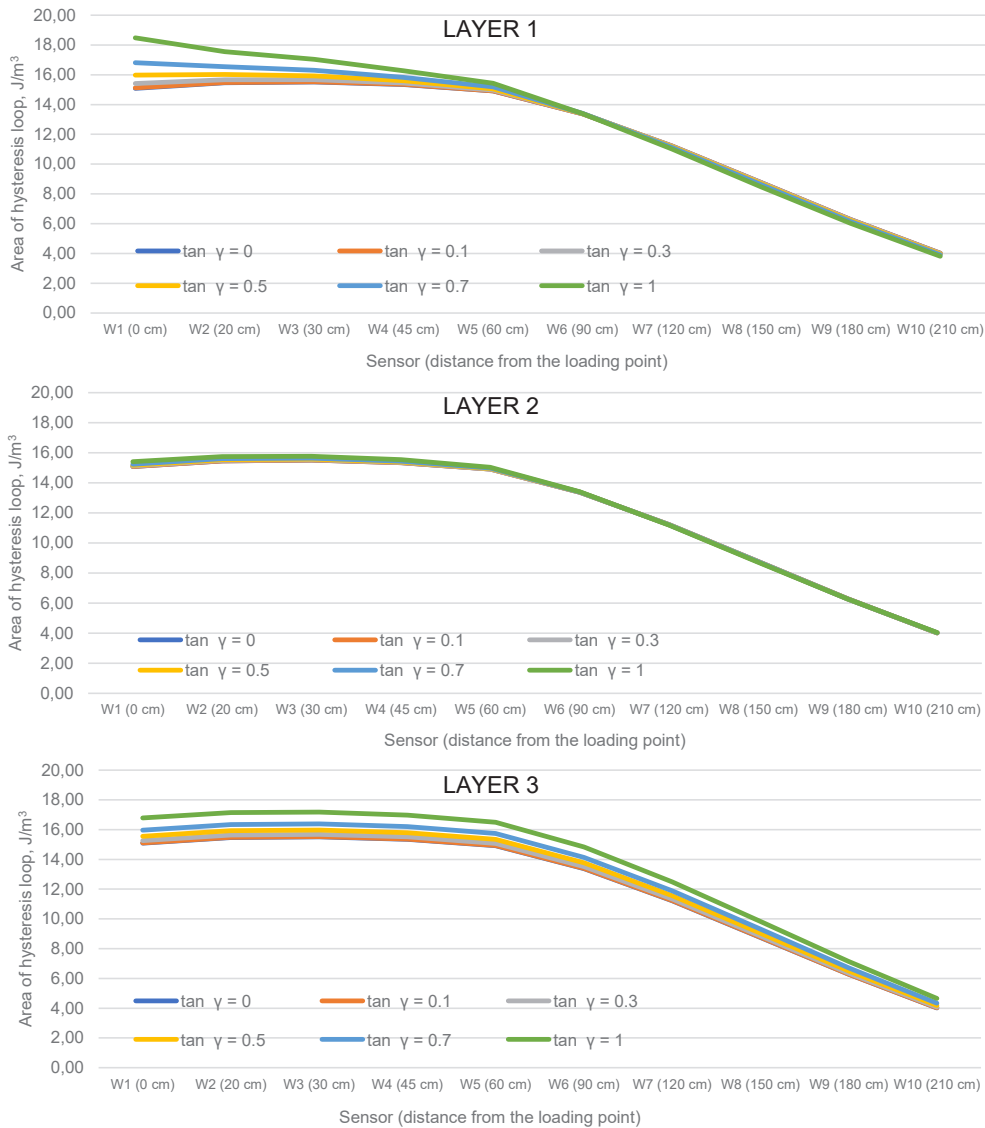


Fig. 5. Modeling the influence of the tangents of the angles of energy losses in pavement layers on the dissipation of impact energy for structure No. 3

$\bar{u}(P, R_i, t)$ — the complete experimental diagram of deformation on the pavement surface upon impact loading;

$K(E_j, tg\lambda_j)P(t)$ — the complete assumption diagram of deformation on the pavement surface, presented as the product of the function $K(E_j, \lambda_j)$ and the estimated pulse $P(t)$.

To test the proposed approach, we performed tests and then adjusted the obtained hysteresis loops on a section of a road with the following pavement structure (Table 2).

The hysteresis loops were experimentally recorded using an FWD PRIMAX 1500 equipped with a set of geophone sensors to record bowls of elastic deflections¹. It should be noted that in the examined area with two pavement layers recently

replaced, rutting and plastic deformations were observed near the pavement edges.

Fig. 7 shows the hysteresis loops recorded experimentally. In a similar manner, with the use of a mathematical model, we constructed estimated hysteresis loops for the design values of the modulus of elasticity of pavement layers (Fig. 8) and then adjusted them manually using the relationships obtained during the numerical experiment (Fig. 9). Figs. 7 and 9 show that the actual experimental and estimated bowls of deflections are characterized by sufficiently close loading and unloading trajectories. To quantify the correspondence between the estimated and experimental hysteresis loops, we present the calculated areas of the obtained hysteresis loops in the table 3.

Table 4 shows the final values of the adjusted moduli of elasticity and tangents of the angles of energy losses in the structural layers.

¹ Distance from the deflectometer sensor location to the point of load application: 0–0.20–0.30–0.45–0.60–0.90–1.20–1.50–1.80–2.10 m

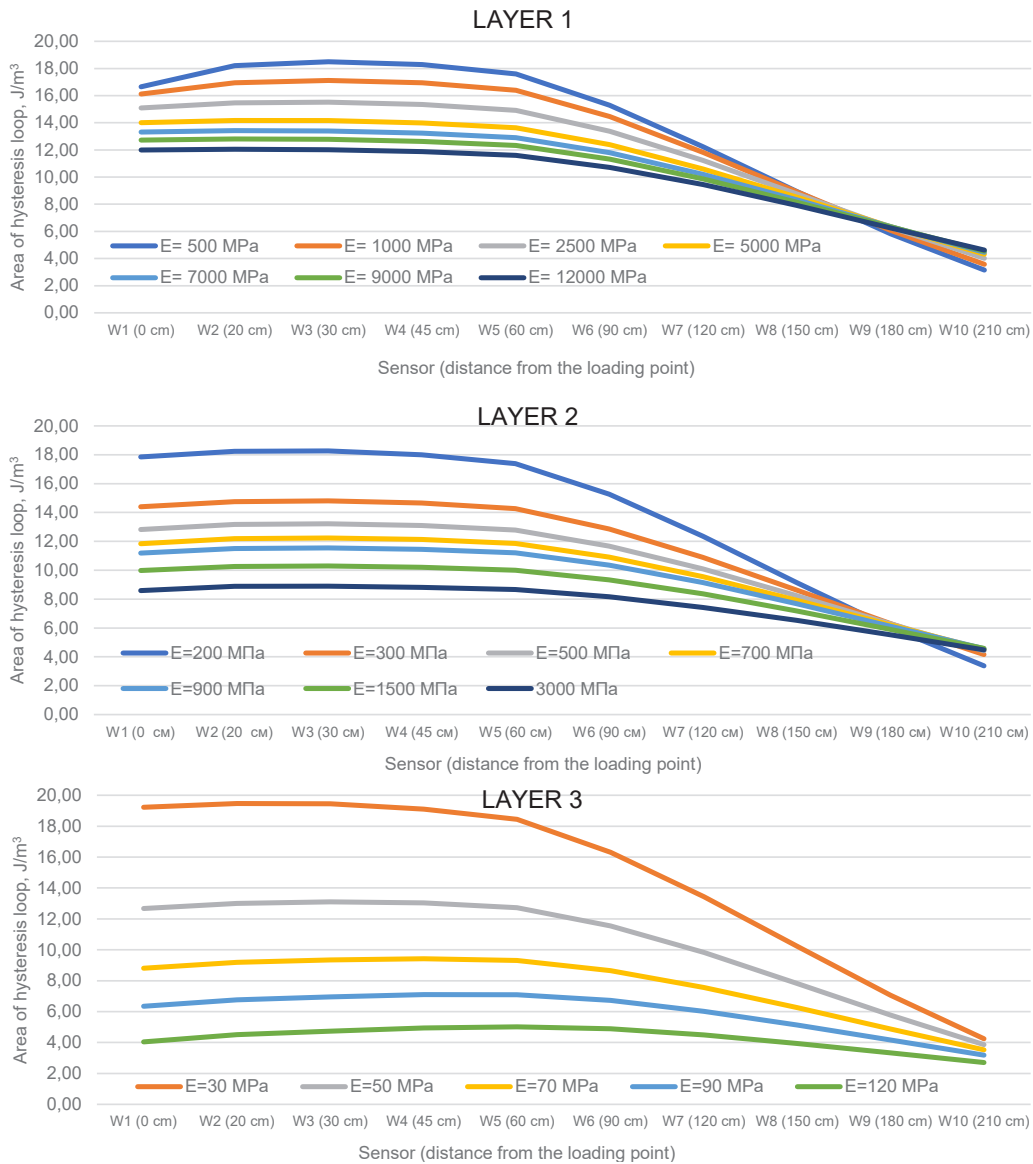


Fig. 6. Modeling the influence of the moduli of elasticity of pavement layers on the dissipation of impact energy for structure No. 3

The results obtained indicate a decrease in the modulus of elasticity of the base course made of the crushed stone / sand mixture. The moduli of elasticity of asphalt concrete and subgrade soil comply with the regulatory requirements. This confirms the fact that the weak intermediate

base course, with a periodically replaced asphalt concrete layer, resulted in rutting. Thus, when planning repair, it is necessary to include works on stabilizing the non-cohesive subgrade. The main advantage of the road pavement condition indicator proposed in this study is the possibility of restoring both elastic and viscous characteristics of the materials of structural layers in road pavements as well as ensuring correspondence between the estimated and experimental characteristics of response over the entire period of instrumental measurements.

Conclusions

- In this paper, we provided a rationale for the possibility of using hysteresis loops recorded at different distances from the point of load application as an effective road pavement condition indicator. Hysteresis loops serve as an analogue of the full

Table 2. Road pavement structures on test sections

Road pavement structure with a non-stabilized road bed	Layer thickness, cm	Design modulus of elasticity, MPa
Asphalt concrete	34	2500
Crushed stone / sand mixture	35	200
Soil – clay	–	47

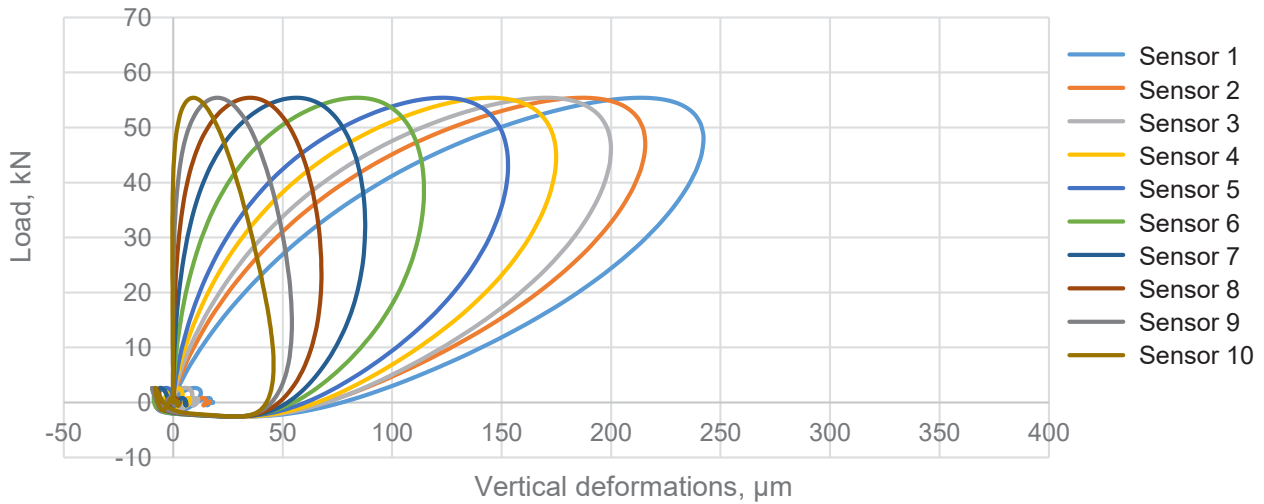


Fig. 7. Experimental dynamic hysteresis loops recorded on the test road section

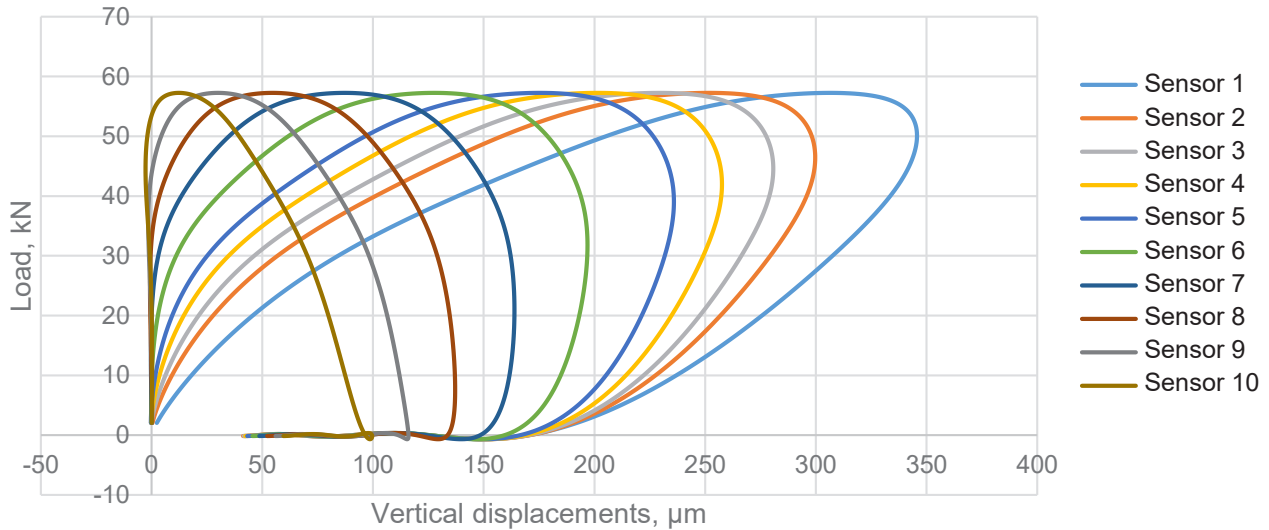


Fig. 8. Estimated dynamic hysteresis loops for the test road section before adjustment

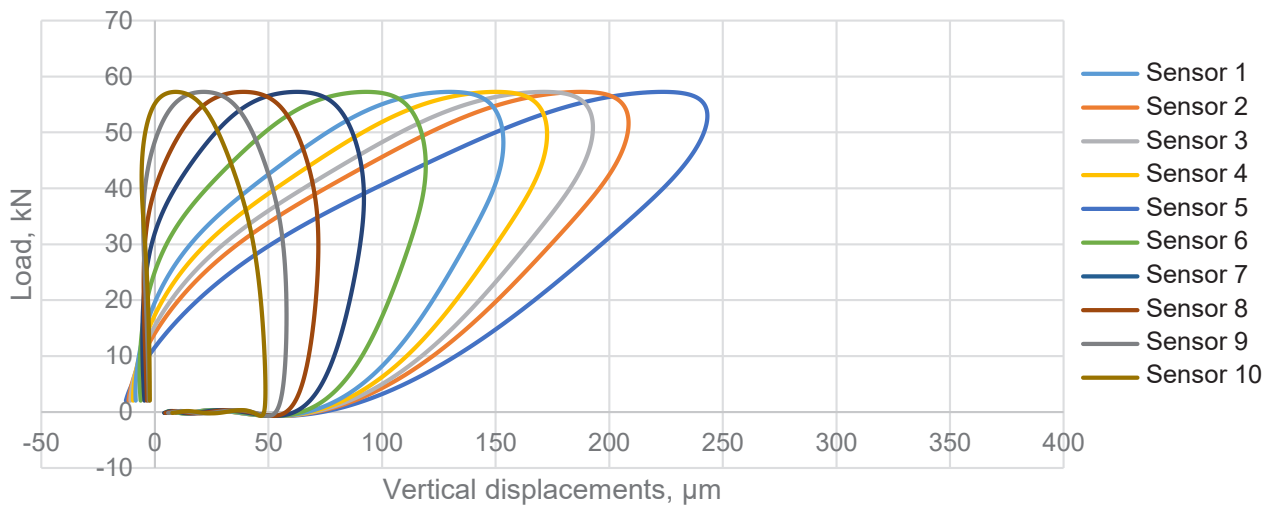


Fig. 9. Estimated dynamic hysteresis loops for the test road section after adjustment

Table 3. Results of comparing the resulting areas of the estimated and experimental hysteresis loops

Structure 1. Energy dissipation according to sensor, J/m ³										
Sensor	D1	D2	D3	D4	D5	D6	D7	D8	D9	D10
Experiment	7.28	6.78	6.60	6.09	5.60	4.70	3.95	3.23	2.59	2.02
Estimated values	7.05	6.68	6.48	6.19	5.87	5.00	4.01	3.31	2.81	2.20
Deviation	0.03	0.01	0.02	-0.02	-0.05	-0.06	-0.02	-0.02	-0.08	-0.09

Table 4. Final results of calculating the moduli of elasticity and loss angle tangents with account for the adjustment of the estimated bowls of deflections and hysteresis loops

Road pavement structure with a non-stabilized road bed	Modulus of elasticity, MPa	Loss angle tangent
Asphalt concrete	3860	0.7
Crushed stone / sand mixture	60	0.5
Soil – clay	152	1

bowl of deflections, combining the history of road pavement deformation and loading from a source on the surface.

- During numerical modeling, we established the following: the modulus of elasticity of subgrade soil has the greatest influence on the amount of deformation energy dissipation within the entire bowl of deflections; the viscous properties of asphalt concrete have the greatest effect on the amount of energy dissipation in the area closest to the impact point; and changes in the rigidity and viscous characteristics of the intermediate layers have the greatest influence on changes in energy dissipation in the middle zone of the bowl of deflections.

- In the test case, we showed the possibility of determining elastic and viscoelastic characteristics when using hysteresis loops recorded at different distances from the point of load application as the main road pavement condition indicator. The deviation of the estimated hysteresis loops from the experimental ones, obtained by varying the moduli of elasticity and tangents of the angles of energy losses in pavement layers, did not exceed 10%. Based on the calculations obtained, we determined the cause of defect formation on the test road section — the non-cohesive subgrade with the actual modulus of elasticity of 60 MPa against the design value of 200 MPa.

- The practical significance of the obtained research results is in improving the accuracy and reliability of the results of non-destructive testing of road pavement condition, which is manifested in the restoration of both elastic and viscous characteristics of the materials of road pavement layers. The results obtained can be used to assess the residual life of the road pavement as well its strength during operation.

Acknowledgment

The research was supported by a grant of the President of the Russian Federation for the state support of young Russian scientists with PhD (application MK-242.2022.4.).

References

- Al-Adhami, H. and Gucunski, N. (2021). Artificial neural network–based inversion for leaky Rayleigh wave dispersion curve from non-contact SASW testing of multi-layer pavements. *Transportation Infrastructure Geotechnology*, Vol. 8, Issue 1, pp. 1–11. DOI: 10.1007/s40515-020-00117-8.
- Babeshko, V. A. Glushkov, Ye. V., and Zinchenko, Zh. F. (1989). *Dynamics of inhomogeneous linear-elastic media*. Moscow: Nauka, 344 p.
- Bazi, G. and Assi, T. B. (2022). Asphalt concrete master curve using dynamic backcalculation. *International Journal of Pavement Engineering*, Vol. 23, Issue 1, pp. 95–106. DOI: 10.1080/10298436.2020.1733567.
- Booshehrian, A. and Khazanovich, L. (2018). Dynamic backcalculation for rigid pavements using generalized Vlasov model. In: Masad, E., Bhasin, A., Scarpas, T., Menapace, I., and Kumar, A. (eds.). *Advances in Materials and Pavement Performance Prediction*. London: CRC Press, pp. 461–464.
- Cao, D., Zhou, C., Zhao, Y., Fu, G., and Liu, W. (2020). Effectiveness of static and dynamic backcalculation approaches for asphalt pavement. *Canadian Journal of Civil Engineering*, Vol. 47, No. 7, pp. 846–855. DOI: 10.1139/cjce-2019-0052.
- Chatti, K., Kutay, M. E., Lajnef, N., Zaabar, I., Varma, S., and Lee, H. S. (2017). *Enhanced analysis of falling weight deflectometer data for use with mechanistic-empirical flexible pavement design and analysis and recommendations for improvements to falling weight deflectometers*. Publication No. FHWA-HRT-15-063. McLean, VA: Turner-Fairbank Highway Research Center, 297 p.
- Fwa, T. F., Tan, C. Y., and Chan, W. T. (1997). Backcalculation analysis of pavement-layer moduli using genetic algorithms. *Transportation Research Record*, Vol. 1570, Issue 1, pp. 134–142. DOI: 10.3141/1570-16.
- Han, C., Ma, T., Chen, S., and Fan, J. (2021). Application of a hybrid neural network structure for FWD backcalculation based on LTPP database. *International Journal of Pavement Engineering*, Vol. 23, Issue 9, pp. 3099–3112. DOI: 10.1080/10298436.2021.1883016.
- Iliopolov, S. K., Seleznev, M. G., and Uglova, E. V. (2002). *Dynamics of road structures*. Rostov-on-Don: Publishing House of Rostov State University of Civil Engineering, 258 p.
- Le, D.-V. and Phan, C. T. (2021). A study on Artificial Neural Networks–Genetic Algorithm model and its application on back-calculation of road pavement moduli. *2020 Applying New Technology in Green Buildings (ATiGB)*, pp. 53–59. DOI: 10.1109/ATiGB50996.2021.9423109.
- Lee, H. S., Von Quintus, H. L., and Steele, D. (2018). Effect of moving dynamic loads on pavement deflections and backcalculated modulus. No. 18-01768. In: *97th Annual Meeting of the Transportation Research Board*, January 7–11, 2018, Washington, DC, USA.
- Lyapin, A., Beskopylny, A., and Meskhi, B. (2020). Structural monitoring of underground structures in multi-layer media by dynamic methods. *Sensors*, Vol. 20, Issue 18, 5241. DOI: 10.3390/s20185241.
- Marchant, J. F. and Papagiannakis, A. T. (2010). A best-fit rigid pavement back-calculation method based on site-specific FEM analysis. In: Fratta, D. O., Puppala, A. J., and Muhunthan, B. (eds.). *GeoFlorida 2010: Advances in Analysis, Modeling & Design*. Reston, VA: American Society of Civil Engineers, pp. 2511–2520. DOI: 10.1061/41095(365)255.
- Park, S.-W., Park, H. M., and Hwang, J. J. (2010). Application of genetic algorithm and finite element method for backcalculating layer moduli of flexible pavements. *KSCCE Journal of Civil Engineering*, Vol. 14, Issue 2, pp. 183–190. DOI: 10.1007/s12205-010-0183-8.
- Quan, W., Ma, X., Si, C., Dong, Z., and Wang, T. (2022). Wave propagation approach for dynamic responses of transversely isotropic viscoelastic pavement under impact load. *Road Materials and Pavement Design*, Vol. 23, Issue 9, pp. 2076–2097. DOI: 10.1080/14680629.2021.1950817.
- Saltan, M., Uz, V. E., and Aktas B. (2013). Artificial neural networks–based backcalculation of the structural properties of a typical flexible pavement. *Neural Computing and Applications*, Vol. 23, Issue 6, pp. 1703–1710. DOI: 10.1007/s00521-012-1131-y.
- Tiraturyan, A. N. (2017). New approach to estimation of remaining life of flexible pavement. *Transport Construction*, No. 8, pp. 16–19.
- Tiraturyan, A. N., Uglova, E. V., Nikolenko, D. A., and Nikolenko, M. A. (2021). Model for determining the elastic moduli of road pavement layers. *Magazine of Civil Engineering*, Issue 103 (3), 10308. DOI: 10.34910/MCE.103.8.
- Tsai, B.-W., Kannekanti, V. N., and Harvey, J. T. (2004). Application of genetic algorithm in asphalt pavement design. *Transportation Research Record*, Vol. 1891, Issue 1, pp. 112–120. DOI: 10.3141/1891-14.
- Uglova, E. and Tiraturyan, A. (2017). Calculation of the damping factors of the flexible pavement structure courses according to the in-place testing data. *Procedia Engineering*, Vol. 187, pp. 742–748. DOI: 10.1016/j.proeng.2017.04.431.

- Varma, S., Kutay, M. E., and Levenberg, E. (2013). Viscoelastic genetic algorithm for inverse analysis of asphalt layer properties from falling weight deflections. *Transportation Research Record*, Vol. 2369, Issue 1, pp. 38–46. DOI: 10.3141/2369-05.
- Vorovich, I. I., Babeshko, V. A., and Pryakhina, O. D. (1999). *Dynamics of massive bodies and resonance phenomena in deformable media*. Moscow: Nauchny Mir, 246 p.
- Vyas, V., Singh, A. P., and Srivastava, A. (2021). Prediction of asphalt pavement condition using FWD deflection basin parameters and artificial neural networks. *Road Materials and Pavement Design*, Vol. 22, Issue 12, pp. 2748–2766. DOI: 10.1080/14680629.2020.1797855.
- Wang, H., Li, M., Szary, P., and Hu, X. (2019). Structural assessment of asphalt pavement condition using backcalculated modulus and field data. *Construction and Building Materials*, Vol. 211, pp. 943–951. DOI: 10.1016/j.conbuildmat.2019.03.250.
- Wang, H., Xie, P., Ji, R., and Gagnon, J. (2021). Prediction of airfield pavement responses from surface deflections: comparison between the traditional backcalculation approach and the ANN model. *Road Materials and Pavement Design*, Vol. 22, Issue 9, pp. 1930–1945. DOI: 10.1080/14680629.2020.1733638.
- Zaabar, I., Chatti, K., Lee, H. S., and Lajnef, N. (2014). Backcalculation of asphalt concrete modulus master curve from field-measured falling weight deflectometer data: using a new time domain viscoelastic dynamic solution and genetic algorithm. *Transportation Research Record*, Vol. 2457, Issue 1, pp. 80–92. DOI: <https://doi.org/10.3141/2457-09>.
- Zhang, X., Otto, F., and Oeser, M. (2021). Pavement moduli back-calculation using artificial neural network and genetic algorithms. *Construction and Building Materials*, Vol. 287, 123026. DOI: 10.1016/j.conbuildmat.2021.123026.
- Zhang, R., Ren, T., Khan, A., Teng, Y., and Zheng, J. (2019). Back-calculation of soil modulus from PFWD based on a viscoelastic model. *Advances in Civil Engineering*, Vol. 2019, 1316341. DOI: 10.1155/2019/1316341.
- Zhao, Y., Cao, D., and Chen, P. (2015). Dynamic backcalculation of asphalt pavement layer properties using spectral element method. *Road Materials and Pavement Design*, Vol. 16, Issue 4, pp. 870–888. DOI: 10.1080/14680629.2015.1056214.

ОПРЕДЕЛЕНИЕ ВЯЗКОУПРУГИХ ХАРАКТЕРИСТИК ЭЛЕМЕНТОВ МНОГОСЛОЙНЫХ КОНСТРУКЦИЙ НА ОСНОВЕ АНАЛИЗА ДИССИПАЦИИ ЭНЕРГИИ

Артем Николаевич Тиратурян*, Евгения Владимировна Углова, Владимир Владимирович Акулов

Донской государственный технический университет
пл. Гагарина, 1, 344002, Ростов-на-Дону, Россия

*E-mail: tiraturjan@list.ru

Аннотация

Введение: Ухудшение эксплуатационного состояния автомобильных дорог является одной из важнейших проблем, стоящих перед специалистами дорожной отрасли. В первую очередь его связывают со снижением жесткости дорожных одежд, представляющих собой многослойные протяженные конструкции. Для выявления причин снижения жесткости применяют неразрушающие методы контроля, в основе которых лежит решение обратной коэффициентной задачи восстановления упругих постоянных по замеренному на поверхности отклику. **Целью работы** является обоснование нового индикатора состояния дорожной одежды, учитывающего историю деформирования и нагружения поверхностным источником, на основе которого возможно решение обратной задачи восстановления упругих и вязких характеристик слоев дорожной одежды. Для достижения цели **использован метод** математического моделирования напряженно-деформированного состояния многослойной среды, базирующийся на решении системы динамических уравнений Ламе. Вязкость учитывается путем введения тангенсов углов потерь энергии волн в материалах слоев. **Результаты**, полученные в ходе моделирования, позволили впервые установить зависимости между изменением модулей упругости и тангенсов углов потерь энергии в слоях дорожной одежды и величиной диссипации энергии в ее структуре. При обсуждении полученных результатов отмечена возможность перехода от чаши максимальных динамических прогибов, как основного индикатора состояния дорожной одежды к анализу петель гистерезиса на поверхности дорожной конструкции, регистрируемых на различном удалении от точки приложения нагрузки и являющихся аналогом полной чаши динамических прогибов отражающей историю нагружения испытываемого объекта.

Ключевые слова: диссипация энергии, многослойная конструкция, модуль упругости, петля гистерезиса, установка ударного нагружения.

Guide for Authors

for submitting a manuscript for publication in the «Architecture and Engineering»

The journal is an electronic media and accepts the manuscripts via the online submission. Please register on the website of the journal <http://aej.spbgasu.ru/>, log in and press "Submit article" button or send it via email aejeditorialoffice@gmail.com.

Please ensure that the submitted work has neither been previously published nor has been currently submitted for publication in another journal.

Main topics of the journal:

1. Architecture
2. Civil Engineering
3. Geotechnical Engineering and Engineering Geology
4. Urban Planning
5. Technique and Technology of Land Transport in Construction

Title page

The title page should include:

The title of the article in bold (max. 90 characters with spaces, only conventional abbreviations should be used); The name(s) of the author(s); Author's(s') affiliation(s); The name of the corresponding author.

Abstract and keywords

Please provide an abstract of 100 to 250 words. The abstract should not contain any undefined abbreviations or unspecified references. Use the IMRAD structure in the abstract (introduction, methods, results, discussion).

Please provide 4 to 6 keywords which can be used for indexing purposes. The keywords should be mentioned in order of relevance.

Main text

It should have the following structure:

- 1) Introduction,
- 2) Scope, Objectives and Methodology (with subparagraphs),
- 3) Results and Discussion (may also include subparagraphs, but should not repeat the previous section or numerical data already presented),
- 4) Conclusions,
- 5) Acknowledgements (the section is not obligatory, but should be included in case of participation of people, grants, funds, etc. in preparation of the article. The names of funding organizations should be written in full).

General comments on formatting:

- Subtitles should be printed in Bold,
- Use MathType for equations,
- Tables should be inserted in separate paragraphs. The consecutive number and title of the table should be placed before it in separate paragraphs. The references to the tables should be placed in parentheses (Table 1),
- Use "Top and Bottom" wrapping for figures. Figure captions should be placed in the main text after the image. Figures should be referred to as (Fig. 1) in the text.

References

The journal uses Harvard (author, date) style for references:

- The recent research (Kent and Park, 1990)...
- V. Zhukov (1999) stated that...

Reference list

The list of references should only include works that are cited in the text and that have been published or accepted for publication. Personal communications and unpublished works should only be mentioned in the text. Do not use footnotes or endnotes as a substitute for a proper reference list. All references must be listed in full at the end of the paper in alphabetical order, irrespective of where they are cited in the text. Reference made to sources published in languages other than English or Russian should contain English translation of the original title together with a note of the used language.

Peer Review Process

Articles submitted to the journal undergo a double blind peer-review procedure, which means that the reviewer is not informed about the identity of the author of the article, and the author is not given information about the reviewer.

On average, the review process takes from one to five months.